IMPROVED DESIGN METHODS FOR

GROUND HEAT EXCHANGERS

By

RACHEL MARIE GRUNDMANN

Bachelor of Science in Mechanical Engineering

Oklahoma State University

Stillwater, Oklahoma

2013

Submitted to the Faculty of the
Graduate College of the
Oklahoma State University
in partial fulfillment of
the requirements for
the Degree of
MASTER OF SCIENCE
May, 2016

IMPROVED DESIGN METHODS FOR

GROUND HEAT EXCHANGERS

Thesis Approved:

Dr. Jeffrey D. Spitler

Thesis Adviser

Dr. Daniel E. Fisher

Dr. Richard A. Beier

ACKNOWLEDGEMENTS

First, I would like to thank my parents for encouraging me to get a graduate degree. I would certainly never have made it through without their continual support in all things.

My graduate advisor, Dr. Jeffrey D. Spitler, has my thanks for taking me on as a graduate student and giving me a consistent job throughout graduate school. With his help I have learned a lot about modeling geothermal systems, released and supported two versions of GLHEPro, and completed this thesis. I truly appreciated having you as my advisor and for reviewing this monster of a thesis.

My thanks to my fellow graduate students, some of whose work has been included in GLHEPro and this thesis. Especially, Matt, who had to put up with me the longest; and Sudha and Lu, for being good friends.

Finally, I would like to thank Brenda James, Gail Ezepek, Diane Compton, and Sharon Green for working with me to provide GLHEPro Technical Support. They are the key members at IGSHP and OSU who made everything go smoothly for my technical support work with GLHEPro.

Name: RACHEL MARIE GRUNDMANN

Date of Degree: MAY, 2016

Title of Study: IMPROVED DESIGN METHODS FOR GROUND HEAT EXCHANGERS

Major Field: MECHANICAL ENGINEERING

Abstract: As public awareness about energy conservation grows, so too does interest in alternative energy sources. Geothermal energy is an alternative energy source which consumers can access by installing a ground source heat pump (GSHP) system in the place of standard heating and cooling systems. A GSHP system can provide both heating and cooling and consists of one or more heat pumps, a ground heat exchanger (GHE), and circulating pumps. The GHE provides the heat source for heating and the heat sink for cooling. It is made up of a series of pipes installed in the ground in horizontal trenches or vertical bores. These pipes are filled with a working fluid that transfers heat to a building from the ground and vice versa. Specifying the appropriate size for the GHE is a key portion of the design for a GSHP system.

The purpose of this study is to improve the design methods for ground heat exchangers by adding to and improving the GLHEPro design tool. A series of new models have been added to the program including

- A finite line source model (FPFLS model) for modeling combinations of up to 30 inclined or vertical boreholes.
- A method for calculating short circuiting resistance in vertical and inclined boreholes.
- A method for modeling and sizing groundwater filled single U-tube boreholes.
- A new global ground temperature database.
- A Horizontal borehole model for straight trenches and horizontal slinky GHE

Improvements to the g-function interpolation methods were also applied.

It was found that these new models provided reasonable results and significant new features to GLHEPro V5.0. Several of the models implemented were previously validated: ground temperature model and the g-functions (temperature response functions) of the slinky model. A validation for the FPFLS model is included.

TABLE OF CONTENTS

Chapter Page

Chapter Page

LIST OF TABLES

Table Page

LIST OF FIGURES

Figure Page

Figure Page

Figure Page

CHAPTER I

INTRODUCTION

1.1 Overview

In today's society, energy efficient and environmentally friendly ways to reduce energy usage and dependence on fossil fuels are of great interest. This "green" movement is influencing designers to consider alternative energy sources, such as solar, wind, hydroelectric, and geothermal. It has also pushed building designs to be more energy efficient as a whole in order to meet the public's desire for more environmentally friendly designs. In buildings, heating and air conditioning equipment typically accounts for a large portion of the energy usage. Ground source heat pump systems offer an alternative method to provide air conditioning that is more efficient than traditional methods.

A ground source heat pump (GSHP) system consists of one or more heat pumps, a ground heat exchanger (GHE), and circulating pumps. The GHE is made up of a series of pipes placed in the ground which are connected to a heat pump(s) within the building. The GSHP system uses the ground as a heat source or sink for the heat pump throughout the year. The terms ground heat exchanger (GHE) and ground loop heat exchanger (GLHE) are largely interchangeable and refer just to the portion of the system installed in the ground. GLHEs can be installed in vertical or inclined boreholes or buried in horizontal trenches.

While GSHP systems are highly efficient they are also relatively costly compared to a more traditional air source heat pump. Traditional air source systems use relatively small coils that are typically contained in a single unit that can be placed outside the home or on the roof of businesses. Their coils are typically made of copper or aluminum and have additional cooling fins attached to increase the heat transfer area. Ground heat exchangers require much larger lengths of pipe, usually made from high density polyethylene (HDPE), to be installed into the ground. This requires trenches to be dug or boreholes drilled - both processes that become increasingly expensive as the length of the trench or bore increases. Thus the initial costs for a GSHP system are much higher than a traditional system.

In designing a GHE there are two primary design considerations; the hydraulic and thermal designs. The hydraulic design, which involves the selection of pipe, fittings, and pumps, determines the system pressure drop and energy consumption of the circulating pump(s). The thermal design of GHE systems focuses primarily on selecting the appropriate number of boreholes, borehole configuration, and borehole length for the specified building design and location. Generally the number of boreholes and borehole configuration can be constrained by the surface area available for borehole installation. Thus, one of the key factors in designing a GSHP system is to determine the necessary borehole length.

Sizing the GHE is important because the goal of a good design is to minimize the initial system cost and operating cost while still providing the heating and cooling required. Minimizing the initial cost is accomplished by minimizing the pipe length required. The length of the borehole is not the only factor to be considered in the design of a GSHP system; other factors are flow rate, pipe sizes, borehole size, borehole configuration, etc. Each of these variables affects the final cost or efficiency of the system. Designing the physical piping and selecting the necessary components is not especially hard. It is the thermal interaction of the GSHP with the ground that makes the design process difficult. There is no truly simple way to properly design a GHE so a

range of design methods have been developed to account for the thermal interactions; these methods are rules-of-thumb, derived analytical or hand calculation methods, and computer simulations.

Rules-of-thumb are simple relations that assume that the ground heat exchanger length is entirely a function of a building's peak loads (heating or cooling) or installed equipment capacity (Spitler and Cullin 2008). This can provide a reasonable sizing result if there is a strong relationship between peak and annual loads and if the ground properties are consistent with those assumed for the rule-of-thumb. This is commonly not the case as demonstrated by detailed simulations done by Spitler and Cullin (2008) for 3 different building types located at each of 14 locations in the United States. They found that the ratio of the required design length to peak heat extraction or rejection rates varied widely for different types of commercial/institutional buildings in the same location. These ratios are often the basis of rules-of-thumb for specifying the system design length. While rules-of-thumb are still given in some design guides (OSU and NRECA 1988), others warn against their use because rules-of-thumb are based on a specific design and installation conditions which may not be applicable in other cases (Kavanaugh and Rafferty 1997).

A more detailed design method is provided by manual, or hand calculation, methods. These methods include any of the various design methods that can be solved by hand or in a simple program. Many published manuals or installation guides fall into this category. These methods require many more calculations than rules-of-thumb and often actively consider ground and grout thermal conductivities and the borehole U-tube placement. For example, the "ASHRAE Blue Book Method" (Kavanaugh and Rafferty 1997; Kavanaugh and Rafferty 2014) provides methods to size vertical GSHP. The methods consist of a series of equations for vertical GSHP and tables and figures for sizing ground and surface water systems. Similarly, installation guides provide a manual method with more details on the installation process (OSU 1988).

While manual, or hand calculation, methods can provide a reasonable method for sizing GSHP systems, and are widely used, design programs can provide much better results. They also allow users to use more complex design methods without increasing the amount of time spent on the process. Some recent investigations have been made in validating and comparing a manual design method and the GLHEPro design program (Cullin et al. 2015) and found that the GLHEPro design tool provides a more accurate design for the system.

There are a variety of commercially available design tools and simulation tools to model and size GLHE borefields. Some software programs that will size GLHE systems are EED (Hellström and Sanner 1994), GCHPCalc or GshpCalc[1] (Kavanaugh 2010), Ground Loop Design (GLD) (Gaia Geothermal 2014), and GLHEPro (Spitler 2000). Other software can be used to model the GLHE as part of a full building simulation include EnergyPlus (Fisher et al. 2006), eQuest (Liu and Hellström 2006), and TRNSYS (University of Wisconsin Madison 2013).

The simulation based design program for GSHP considered in this thesis is GLHEPro V5.0 for Windows. Over the last 22 years much effort has gone into improving the methods used by GLHEPro. The purpose of this work is to improve the existing methods and to add new functionality to the program. The literature review in the following section gives an overview of the development of GLHEPro and some of the methods used within the program.

1.2 GLHEPro Background

GLHEPro, or GLHEPRO[2], is a GLHE design program that allows users to design a GHE system for a specific array of boreholes and a specific set of building or ground loads. The name of the program stands for Ground Loop Heat Exchanger Professional.

[1] The program was originally named GCHPCalc and later renamed as GshpCalc.
[2] Most of the publications use GLHEPRO but newer releases refer to the program as GLHEPro, which is deemed more appropriate because the acronym stands for Ground Loop Heat Exchanger Professional.

GLHEPro V1.02 was initially developed by Marshall and Spitler (1994) and distributed as an MS-DOS program by the International Ground Source Heat Pump Association. One of the reasons for its development was to provide a design program that operated in Customary US units (inches, feet, BTU, °F, etc.) for users in the United States. GLHEPro V1.02 was originally developed to serve the same purpose as a similar program which was developed in Metric units by Eskilson (1987b). The original code for GLHEPro was written in C with subprograms in FORTRAN as executables (.exe). A Microsoft Windows application was later written using Windows 3.1 API to provide an interface in response to requests from users (Manickam 1996). Both the DOS and Windows version allowed users to pick from a list of 185 borehole configurations arranged in lines, rectangles, squares, triangles, and circles. Some configurations allowed the boreholes to be inclined from vertical. The depth of the boreholes was scalable, but the ratio of the depth to the spacing between boreholes was held to be constant for each configuration (Marshall and Spitler 1994). Another improvement over other design programs of the time was that it did not require the loads to be applied directly on the GLHE. Monthly loads could be applied to the GLHE model through a simple heat pump model. The loads themselves had to be generated by another building modeling software (Marshall and Spitler 1994).

GLHEPro V2.0 was released in 1996 (Manickam 1996) and contained the g-functions for approximately 235 different borehole configurations (Manickam et al. 1996). This release was developed in Borland C++ as a Microsoft Windows Application (Bhargava 1998) and had six known updates released.

GLHEPro V3.0 was developed in Visual Basic 5.0 (Bhargava 1998) and officially released in 2000. It contained the g-functions for 307 different borehole configurations and allowed the spacing between boreholes to be set independently of the borehole depth (Mokashi et al. 2004). At this point, inclined boreholes were no longer offered as an option in the library of borehole configurations (OSU 2004). GLHEPro V3.0 was the first to use the main simulation methodology,

GLHESim, as a Dynamic Linked library or .dll file written in FORTRAN. Previous releases used the simulation code as an external FORTRAN executable (.exe).

GLHEPro V4.0 was officially released in 2007 (Young 2004; Cullin 2008). This version included all of the borehole configurations from V3.0 as well as allowing large rectangular borefields with up to 900 boreholes. It also allowed users to model double U-tube and concentric boreholes in addition to the standard single U-tube model (OSU 2007). It was developed in Visual Basic 6.0 and had nine known updates.

GLHEPro V4.1 was officially released in 2014. It had largely the same functionality as V4.0 but with the underlying programming language updated to VB.NET. The main simulation program, GLHESim, was ported to VB.NET so that a separate DLL would not be needed. There are seven known updates released for GLHEPro V4.1 at the time of publication for this document (OSU 2016a).

GLHEPro V5.0 is the most current version of GLHEPro and is the version which is described in this thesis. It was officially released in 2016. An additional FORTRAN DLL is included with the program to support the new g-function calculation methods discussed in Chapters II and VII of this thesis.

1.2.1 Subprograms

A series of subprograms have been included with GLHEPro at various points in its development. The following subprograms are the ones that provided significant improvements to the simulations or user options.

1.2.1.1 Borehole Sizing Routine

GLHEPro V1.0 sized the GLHE based on the applied loads and a set maximum or minimum design temperature for the outlet of the heat pump. The sizing operation was a simple iterative

optimization program designed to find the borehole depth required to meet the heat pump outlet temperature requirement (Marshall and Spitler 1994).

The search method used to size the system was the Regula Falsi method (Manickam 1996). This method was implemented because it required two initial guesses that did not need to be near the root but must bracket the root. The initial guesses bracketing the root were found with the standard Regula Falsi method and the final optimum with a Modified Regula Falsi algorithm. The Modified Regula Falsi algorithm increases computation speed by halving the value of the function at the unshifting bound of the search region every iteration.

1.2.1.2 Configuration Sizing Subprogram

To give designers more guidance in selecting the best configuration of boreholes for their system, a sizing subprogram that both sized the borehole depth and selected the configuration (i.e. arrangement of boreholes) was created and added to GLHEPRO V1.02 (Yeung 1996). The inputs to this subprogram are the maximum surface dimensions and the allowable range of borehole depths. The SELECT program would then select a series of borehole configurations based on the building loads. Each configuration would then be sized to find the optimum depth within the allowed range and then sized again to find the optimum spacing between boreholes for each configuration. This subprogram was not included in future releases.

1.2.1.3 Life Cycle Cost Sizing

The main purpose of design tools and sizing programs is to design a system that meets the needs at minimum cost with desirable efficiency. A subroutine to size a GLHE system based on minimizing life cycle cost was created for GLHEPRO V2.0. This simulation required designers to input the expected costs for drilling, piping, and components along with the number of boreholes and other system dimensions. It optimized the depth of the borehole with a golden section search based on the present worth of the initial installation costs and annual average

operating costs. The initial installation accounts for the cost of the heat pump, circulating pump, pipe, and borehole drilling. Annual operating costs were calculated from the heat pump and circulating pump power requirements (Yeung 1996). The downside to this subprogram was that it required many more inputs than the standard sizing routine. Because the first cost of the GHE makes up the majority of the life cycle cost, the optimal design is typically the same as or close to the minimum GHE size obtained by considering only the design temperature constraints. So while the results were given in the form of minimizing cost, they still had largely the same results on the overall system size as the standard sizing method used in GLHEPro.

1.2.1.4 Sizing Hybrid GSHP

In general, GSHP systems have the very best performance for locations where the heating and cooling loads on the ground are balanced. GSHP systems can work for systems with only heating loads but usually not for systems with only cooling loads. In particular, for larger systems with many boreholes, the imbalance in the loads can cause a gradual change in the local ground temperature that will work to reduce the system efficiency over time. Hybrid GSHP systems place a portion of the system loads on the GSHP and the remainder on the supplemental heat source or sink. The method applied by Cullin (2008) in GLHEPro V4.0 uses the existing sizing program to find the minimum borehole length required to remain between the applied maximum and minimum fluid temperature constraints. The remaining load is placed on a supplemental heat source or sink as needed. This heat sink (e.g. cooling tower) or heat source (e.g. boiler) is assumed to provide a constant sink/source for the applied loads.

1.2.1.5 Peak Load Analysis Tool

The design of GSHP is largely dependent on the loads applied to the system and is often sensitive to the peak loads and their durations. For this reason, the Peak Load Analysis Tool was provided with GLHEPro V4.0 onward. It is used to help identify the monthly heating and cooling loads for the year and the magnitude and duration of the monthly peak loads. This Microsoft Office Excel

spreadsheet used a combination of in-cell formulas and Visual Basic for Applications macros to graphically help users to determine the peak heating and cooling durations. The figures below are plots of the nondimensionalized peak temperatures. This is done by dividing the hourly temperature change by the maximum temperature for each hour of the peak load day. Therefore the target nondimensionalized temperature to be reached with the peak load duration is 1.0 (Cullin 2008). Two options were provided to allow the best approximation of the load. The first is "Average over duration" which selects the duration that has the highest average load. The second, "Maximum during duration", uses the absolute maximum load for each hour it is applied. So for Figure 1-1 the peak heating duration would be one hour of the maximum load over the duration and Figure 1-2 indicates that 3 hours of the averaged peak cooling loads should be applied for this case.

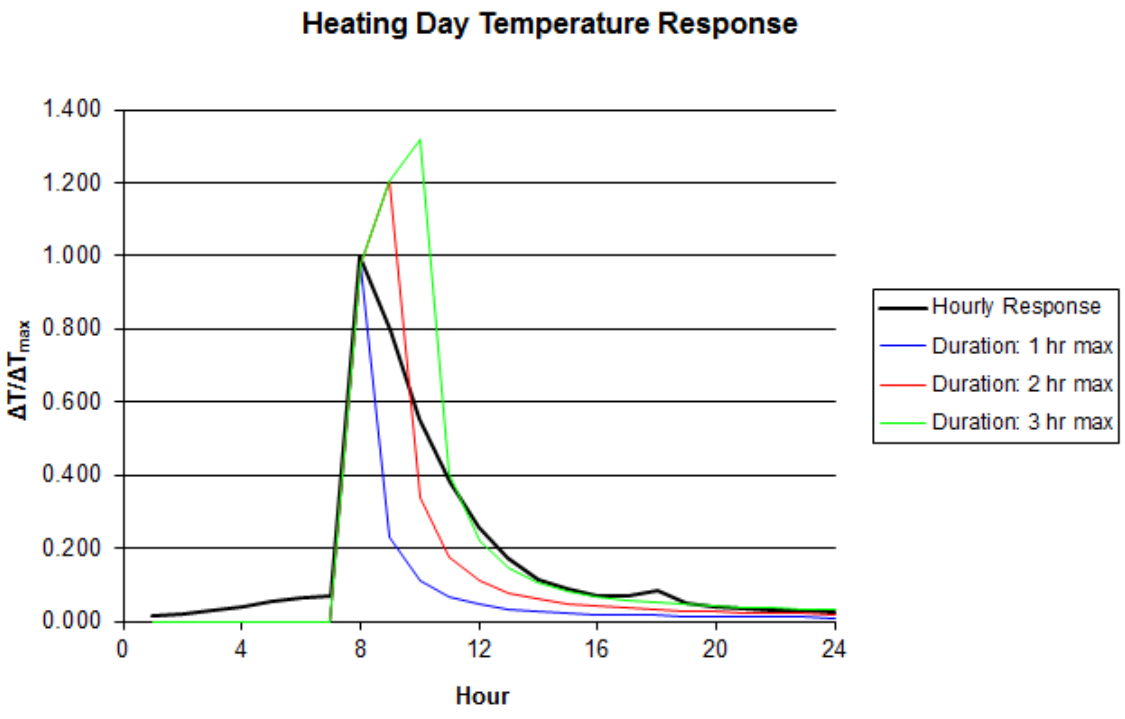

Figure 1-1: An example of Nondimensionalized peak heating temperature responses

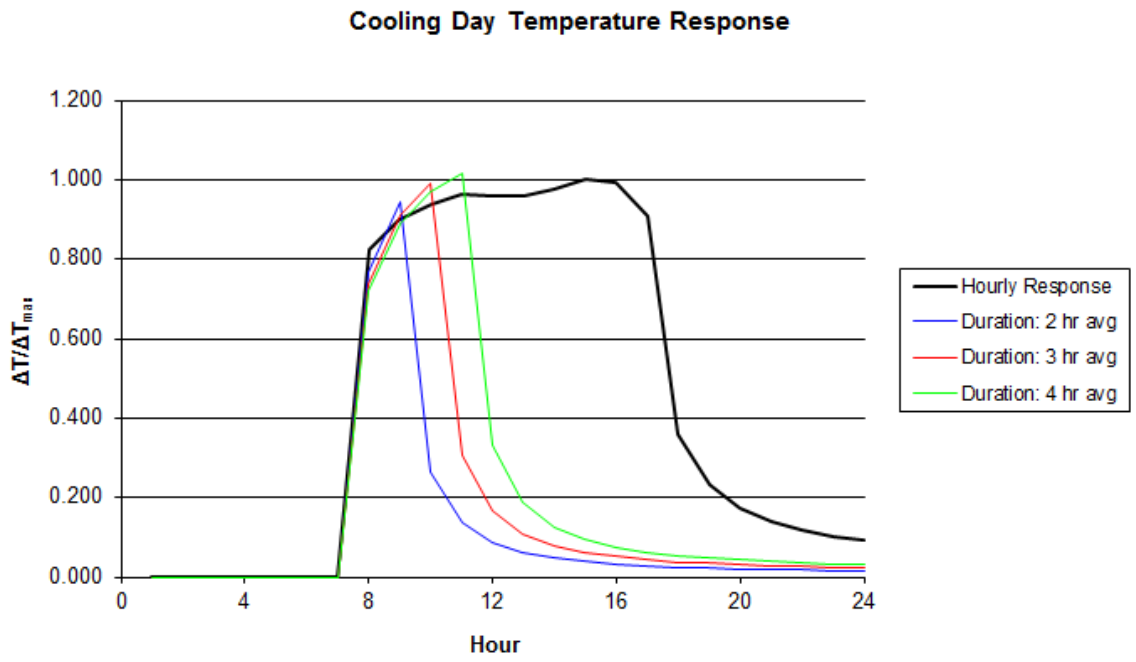

Figure 1-2: An example of Nondimensionalized peak cooling temperature responses

1.2.2 Handling Peak Loads

Ideally a simulation should be based on an hourly or smaller time step to provide the best possible model of the actual system. A monthly simulation, however, is sufficient for most systems and much less computationally intensive. The downside to using a monthly simulation is that it is difficult to account for the effects of extreme hourly or daily variations in the loads, which can be a key factor in the system sizing process.

Peak Loads were first included in the program V2.0 to provide a more accurate simulation of a real ground source heat pump system. Later the Peak Load Analysis Tool discussed in Section 1.2.1.5 was created to help users select the appropriate peak loads and load durations. The inclusion of peak loads allowed the system to be sized based on peak, or extreme, fluid temperatures entering the heat pump based on the applied hourly peak heating and cooling loads. This allowed users to specify the temperature operating range for the heat pump (Yeung 1996).

The peak heating and cooling loads could be applied for a set number of hours for a given month of the year.

The average monthly loads were then resolved into hourly loads and a pulse heat rejection rate calculated from the difference between the peak hourly load and the net hourly heat rejection. The pulse heat rejection was then used to get the temperature effect due to the peak load and the resulting temperature used to size the system length. The combination of average monthly loads and hourly peak loads is referred to as a hybrid timestep method (Cullin and Spitler 2011).

1.2.3 Borehole Thermal Resistance

The borehole thermal resistance was first identified as a quantifiable number by Palne Mogensen (1983). Claesson and Eskilson (1987b) list the borehole thermal resistance as one of the most important parameters to be considered in the design of ground heat exchangers. The best heat transfer between the system fluid and the ground is achieved by minimizing the borehole thermal resistance. GLHEPRO V2.0 was the first version to begin providing guidance on borehole thermal resistance in the FORTRAN subprogram BORERES.FOR (Yeung 1996). A borehole typically consists of two pipes surrounded by grout. The borehole resistance must account for both the resistance of the grout between a pipe and the borehole wall and the resistance between the two pipes. The simplest way to lay out the thermal resistance network is shown in Figure 1-3, where the diagram on the left shows the borehole thermal network and the one on the right a depiction of the borehole resistance.

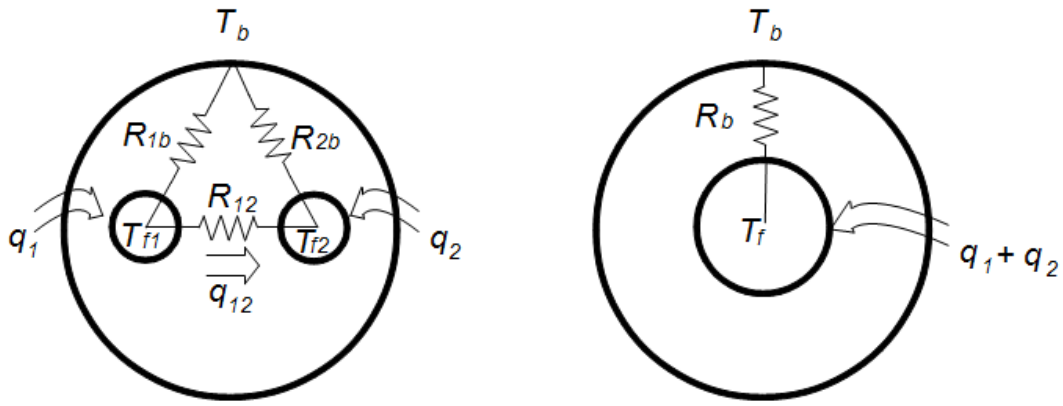

Figure 1-3: Single U-tube borehole resistance network and definition of borehole resistance R_b

The method used in GLHEPro V2.02 to approximate the borehole resistance used conduction shape factors and assumed that R_{1b} and R_{2b} could be approximated as the summation of the pipe conductive and internal convective resistances along with an effective grout resistance. The effective grout resistance was calculated using the grout thermal conductivity and the shape factor for a pair of eccentric cylinders of length L (Yeung 1996).

In GLHEPro V3.0, the shape factor methodology of Paul (1996) and Remund (1999) was implemented (Bhargava 1998). Their shape factor was created from a series of equation fits of experimentally validated numerical simulations. Three different configurations were considered, each with different spacing between the legs of the U-tube. The equation fit is a function of the ratio of the borehole diameter to the pipe outside diameter and two equation fit coefficients.

The Multipole method of Bennet, Claesson, and Hellström (1987) was later implemented to replace the shape factor method for calculating the borehole thermal resistance (Young 2004; Cullin 2008). The multipole method numerically models conductive heat flow between and within various pipes inside of two concentric homogeneous regions. The inner homogenous region is used to model the grout and the outer the ground. The method is very versatile as it allows any number of pipes to be placed asymmetrically within the borehole.

The multipole method makes use of a combination of line sources and multipoles. A modified version of the code provided in Bennet et al. (1987) was implemented in FORTRAN as a dynamic link library (DLL) and used in GLHEPro V4.0 (Young 2004). The modifications to the code were necessary to change the command line program into a DLL and to return the borehole resistance as a function of the ground, grout, and pipe conductivity, pipe size and placement, and internal convective resistance. The fluid temperature, average borehole wall temperature, and heat fluxes for each pipe as generated by the multipole method are intermediate variables in the resistance calculation (Young 2004). A more in-depth review of the multipole method is included in Section 4.2.1.1 as it relates to the short circuiting resistance calculations and more information on the line source method can be found in the model classifications section of Chapter II.

1.2.4 Thermal Analysis

The basis of the long-term GHE simulations in GLHEPro is the heat transfer methodology of Eskilson and Claesson (Eskilson 1987a). They modeled the heat extraction and rejection of a borehole by using a two dimensional finite difference method that couples the largely steady state heat transfer within the borehole to the transient process outside. They based this combination on the findings that it takes approximately two hours for the heat transfer within the borehole to reach steady state. More than 25 years are needed for a GLHE consisting of a single 100 meter deep borehole to reach steady state with the surrounding ground (Claesson and Eskilson 1987).

The 2D finite differences for each single borehole are then superimposed in space and time to give the response of a system of boreholes. To simplify matters, the thermal process is cylindrically symmetric around the borehole and the boreholes are often placed in a symmetric pattern. This symmetric borehole placement can only be used as a simplification if the boreholes considered are in parallel with the same fluid flow rate and inlet temperature. Basic heat extraction steps account for the temperature response of the boreholes due to interactions between

boreholes from a single heat pulse over a given duration. The response to these basic heat extraction steps are compiled into dimensionless g-functions that are a function of the natural logarithm of the dimensionless time, the borehole radius to depth ratio (r_b/H), and the borehole spacing to depth ratio (B/H).

$$g_s = \frac{2\pi k}{q_l} \Delta \bar{T}_w(t) \tag{1.1}$$

$$Logarithm\ of\ Dimensionless\ Time = \ln\left(\frac{t}{t_s}\right) \tag{1.2}$$

$$t_s = \frac{H^2}{9\alpha} \tag{1.3}$$

Where

q_l is the heat extraction/rejection per unit length of borehole [W/m]

k is the thermal conductivity of the ground [W m^{-1} K^{-1}]

H is the borehole length [m]

r_b is the borehole radius [m]

t is time [s]

t_s is the time scale [s], equation 1.3

α is the soil thermal diffusivity [$m^2 s^{-1}$]

Eskilson compiled g-functions for different configurations of boreholes, 50 of which were published as graphs in his doctoral thesis (Eskilson 1987a). Hellström (1991) later compiled the tabulated data set that is used in GLHEPro today. The figure below shows a series of g-functions for different configurations. Note that there are a couple of configurations shown in the figure

that have the same number of boreholes and that the configuration with the more densely packed borehole placement has a higher thermal response.

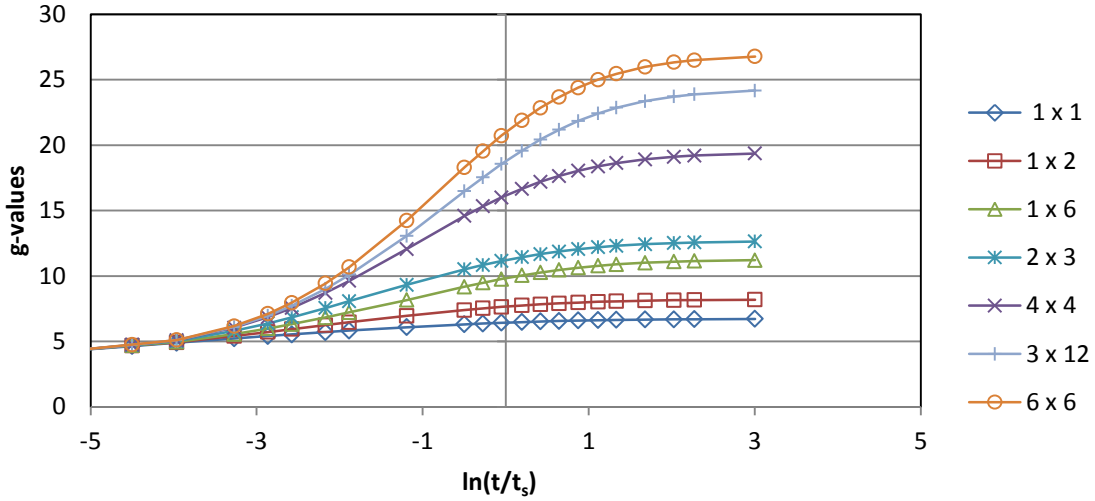

Figure 1-4: G-functions for various borehole configurations with 1 to 36 boreholes, r_b/H=0.0005, and B/H=0.1

There are a few limitations to this method. This model neglects the ground temperature gradient, the phase changes due to the freeze thaw cycle, and the groundwater flow and assumes that the borehole wall temperature is uniform (Claesson and Eskilson 1987b). The top of the borehole is assumed to be thermally insulated; the length of this insulated portion of the borehole is not deemed important, especially within the range of 1 to 5 meters (Claesson and Eskilson 1987b). The g-functions created by Eskilson and by other line and cylinder source models cannot accurately account for the initial temperature responses within the borehole and should not be applied to systems with short time steps without some other method to handle the response at short times. This is because these methods do not take the heat transfer between elements within the borehole into account. Eskilson defined the smallest time step at which his method could be applied as the point where:

$$t = \frac{5r_b}{\alpha} \tag{1.4}$$

Where

r_b is the borehole radius [m]

Other terms are defined in Equations 1.3

This value, t, is typically somewhere between three to six hours. In terms of dimensionless time this is where the natural logarithm of the dimensionless time is -8.5. For smaller time steps a short time step (STS) g-function method was implemented. The STS g-functions are dependent only on local borehole specifications and are calculated and appended to the g-functions of Eskilson for use in simulation.

The original method for calculating the STS g-functions was developed by Yavuzturk and Spitler (1999) using a numerical model with two-dimensional implicit finite volume discretization. Only half of the borehole was included in the model due to symmetry. The grid is laid out in polar coordinates with the U-tube pipes approximated as pie sectors with the same internal perimeter as the actual pipe.

The model was later modified by Xu and Spitler (2006) to account for variable convective resistance and thermal mass in the borehole. Their model is a one-dimensional model and provides short-term responses with acceptable accuracy but a much faster computation time. The grout thermal properties were carefully adjusted so that the borehole resistance values matched the values calculated by the Multipole method described in Section 1.2.3. For this to be done the borehole is simplified as was shown in Figure 1-3 for the borehole resistance calculations. The U-tube pipes are modeled as a single pipe surrounded by the grout and then the ground. The thermal mass of the fluid and grout are maintained by holding the cross-sectional area of the fluid constant and setting the outer diameter of the one-dimensional pipe to the square root of two times the actual outer pipe diameter.

GLHEPro treats the g-functions as dimensionless temperature responses within the main simulation program, GLHESim. These g-functions can then be superimposed to find the borehole wall temperature due to a series of applied loads.

$$T_{BHW} = T_{ground} + \sum_{i=1}^{n} \frac{Q_i - Q_{i-1}}{2\pi k_g} g\left(\frac{t_n - t_{i-1}}{t_s}, \frac{r_b}{H}\right) \quad (1.5)$$

Where

T_{BHW} = Temperature at the borehole wall [°C]

T_{ground} = Average undisturbed ground Temperature over the length of the borehole [°C]

Q_i = heat extraction/rejection to the ground per unit length of borehole [W/m]

k_g = ground thermal conductivity [W m^{-1} K^{-1}]

$g\left(\frac{t_n - t_{i-1}}{t_s}, \frac{r_b}{H}\right)$ = g-function, dimensionless temperature response, equation 1.1

Other terms are defined in Equations 1.3 and 1.4

Given the total borehole thermal resistance, the average fluid temperature can be calculated along with the average entering and exiting fluid temperatures (Spitler 2000).

$$T_f = T_{borehole} + Q_i R_b \quad (1.6)$$

$$T_{entering} = T_f + \frac{\dot{q}_{rejection,net}}{2\dot{m}c_p} \quad (1.7)$$

$$T_{exiting} = T_f - \frac{\dot{q}_{rejection,net}}{2\dot{m}c_p} \quad (1.8)$$

Where

T_f = Average fluid temperature [°C]

$T_{entering}$ = Temperature of fluid entering the borehole [°C]

$T_{exiting}$ = Temperature of fluid exiting the borehole [°C]

R_b = Thermal resistance of borehole [K/(W/m)]

$\dot{m}$ = fluid mass flow rate [kg/s]

c_p = specific heat of the working fluid [J/kg-K]

Other terms are defined in Equation 1.5

Some researchers have questioned the accuracy of the calculation method used to get the entering and exiting fluid temperature for the borehole (Marcotte and Pasquier 2008). This simple average temperature method assumes that the heat transfer rate along the length of the borehole is uniform, which is not always true (Beier 2011). Numerical solutions suggest that the average fluid temperature in the borehole is not actually the simple average of the entering and exiting fluid temperatures, but tends to be slightly closer to the entering fluid temperature with the temperature at the bottom of the borehole slightly closer to the exiting fluid temperature (Marcotte and Pasquier 2008). Rather than using a more detailed fluid temperature calculation, the effective borehole resistance that takes into account the short circuiting resistance can account for this temperature trend. The p-linear average method proposed by Marcotte and Pasquier (2008) has a similar degree of accuracy without accounting for short circuiting within the borehole thermal resistance. Javed and Spitler (2016) note that it is more consistent with current design methodologies to use the simple mean fluid temperature to get the effective borehole thermal resistance. For locations in North America, the effects of short circuiting are generally small but the option to account for them is discussed in more detail in Chapter IV.

1.2.5 Validations

The GLHEPro program has been validated against experimental data for both the temperatures returned by the model and the sized borehole depths. The data collected by Hern (2004) was used to generate the loads for a system of three vertical boreholes in parallel. The complete system installed at a test facility at Oklahoma State University in Stillwater, Oklahoma, consisted of four vertical and one horizontal borehole of which only three vertical bores were used. The purpose of the first validation was to compare the actual borehole entering and exiting fluid temperatures to the simulated values (Cullin 2008).

The results of the validation showed that GLHEPro V4.0 could reasonably approximate the end-of-month heat pump entering water temperature (EWT) in any of the 18 consecutive months considered. The largest errors occur during the months when the system transitions from heating to cooling dominated. This is because the simulation uses an average load for the month rather than accounting for a sudden shift from heating to cooling. The minimum and maximum heat pump EWT showed a much wider range of deviation. Some of this discrepancy is due to the approximation of the peak heating and cooling loads and their duration. The peak heating load does not actually occur at the end of the month as assumed by the simulation. Also the experimental data includes some periods where the system was shut down for various reasons; the simulation assumes continuous operation (Cullin and Spitler 2011). Despite the inaccuracies caused by assumptions in the model, it was found to be adequate for design purposes.

The second validation of GLHEPro V4.0.9 (Cullin et al. 2015) considered the Stillwater location and three others: Valencia Italy, Leicester UK, and Atlanta Georgia in the USA. The purpose of the validation was to compare the sizing results of the method in the ASHRAE Handbook and GLHEPro to experimental data. The ASHRAE design method is often referred to as the “Blue Book” method, as it was published by ASHRAE with a dark blue cover, by Kavanaugh and Rafferty (1997; Kavanaugh and Rafferty 2014).

Table 1-1: Over-/under-sizing errors for each design method

	Valencia	Leicester	Atlanta	Stillwater
Handbook (%)	103	60	-21	26
Design tool (%)	5	6	2	2

The results show that GLHEPro sizes the systems much more accurately than the handbook method. The Handbook method tends to over or under size the ground heat exchanger. Further investigations into this validation are considered in Chapter III.

1.3 Objectives

As discussed in the literature review section, the methods used in the GLHEPro design tool have evolved over the years to assist the user by adding borehole resistance calculations, peak load analysis, and a wider range of systems (e.g. double U-tube, concentric, more than 120 boreholes option, etc.). There are still many methods that can be improved and many additional functions that could greatly increase the versatility of the program. Some of these options are considered here.

Previous versions of GLHEPro were limited to vertical GSHP systems placed in predefined gridded configurations due to the use of tabulated or library g-functions. Allowing more freedom in the placement of boreholes within the system would enable designers to make better use of available space and more accurately model irregular borehole placement. The first objective is to develop and implement a method to calculate the g-functions for vertical, horizontal, and inclined boreholes. Furthermore, the implementation for vertical and inclined boreholes should allow the boreholes to be placed freely within a coordinate system so that borehole fields that cannot be defined as a series of rows and columns can be modeled. The model developed in Chapter II is referred to as the Free Placement Finite Line Source model or FPFLS model.

Some researchers have pointed out the limitations associated with the constant heat flux assumption that is used in the FPFLS model (Malayappan and Spitler 2013). The second objective is to demonstrate that the FPFLS model produces reasonable results for a range of GSHP systems. Thus, a validation of the FPFLS model is considered in Chapter III. Both the g-functions and GHE sizes determined from the calculated g-functions are considered in the validation. The g-functions calculated with the FPFLS method are compared to those generated with the methods of Claesson and Eskilson (1987a). Their g-functions are referred to as library g-functions because they are implemented within GLHEPro as a series of tabulated data. The GHE system sizes are validated against experimental data using GLHEPro V5.0 and both the library g-functions and the g-functions calculated with the FPFLS method. The experimental data was taken from the four GSHP systems considered in the paper by Cullin et al. (2015).

As noted by Claesson and Eskilson (1987b), the borehole thermal resistance is a very important part of the GHE model. Groundwater filled boreholes are used in Scandinavian countries and provide reduced borehole resistance due to natural convection in the borehole. There are currently no design programs that will calculate the convective resistances for groundwater filled boreholes, so implementing it in GLHEPro V5.0 will provide a significant contribution to design options (Javed and Spitler 2016). Short circuiting, where heat is transferred from the downward flow channel to the upward and vice versa, reduces the thermal efficiency of the GHE. It is often neglected in borehole models but can be important when boreholes are especially long or have very low flow rates. Deeper, or longer, boreholes are becoming much more common so it is becoming increasingly important to take short circuiting into consideration. Thus the third objective in Chapter IV is to allow users to model groundwater filled single U-tube boreholes and to account for short circuiting in the borehole thermal resistance calculations.

The models used in GLHEPro are all based on the usage of g-functions and library g-functions make up the majority of the g-function values used in GLHEPro. The current library was

generated with the methods of Eskilson (1987a) and provided by Hellström (1991). When they are used within the program they are often interpolated in order to get the correct values for the selected system dimensions. Improving the extrapolation and interpolation of these tabulated g-functions within a given configuration and between the long and short time step methods is the fourth objective covered in Chapter V. This will help to reduce errors in the simulation due to improper calculation of g-functions.

Chapter VI describes a new method to select undisturbed ground temperatures. The ground temperature model developed by Xing (2014) is included in this section. This model allows users to select undisturbed ground temperature profiles for locations around the world that are generated by a much more detailed model than the average annual air temperature model used in previous versions of GLHEPro.

Adding a series of horizontal GHE options was one of the goals of GLHEPro V5.0. A review of existing Slinky GHE models and the methodology and implementation of the selected model are given in Chapter VII. The Slinky GHE model based on the methodology of Xiong et al. (2013) was selected. This section also includes sample results for the various horizontal models that have been added to GLHEPro V5.0; namely the straight pipe and slinky pipe horizontal GHE models.

Finally, Chapter VIII covers the conclusions and recommendations for further research and development of GLHEPro.

CHAPTER II

FREE PLACEMENT FINITE LINE SOURCE METHODOLOGY

2.1 Introduction

A validation of the GLHEPro and the Superposition Borehole Model (SBM) g-functions, devised by Claesson and Eskilson (1987a), was completed by Cullin et al. (2015). Their results showed that GLHEPro and the SBM g-functions provided results that were not only reasonable, but also considerably better than the "Handbook" method detailed in the ASHRAE GSHP design guide (Kavanaugh and Rafferty 1997; Kavanaugh and Rafferty 2014). The current library of SBM g-functions used within GLHEPro is limited to 307 vertical borefield configurations. While this is a large number of options, it still limits users to arrays of boreholes in 'U', 'L', or rectangular shapes. The superposition borehole model used to derive the library of g-functions in GLHEPro could possibly be implemented to calculate the g-functions for user specified borefields. However, the calculation time for this numerical method can take several hours (with an AMD Phenom II X6 processor and 8GB RAM) which is unacceptable for sizing simulations in GLHEPro which may have to calculate the g-functions several times to size a single GHE (Cimmino and Bernier 2014).

2.2 Model Classifications

Alternatively, there are many different methods that can be used to generate g-functions and they can all be grouped into various classifications. Cimmino and Bernier (2014) identified three different boundary conditions that are commonly used in the calculation of g-functions.

- Type I has an equal and uniform heat flux or extraction for each borehole. It allows the temperatures along the boreholes to vary
- Type II has uniform heat flux or extraction for each borehole. The average temperature along each borehole length is equal for all boreholes
- Type III has an equal and uniform borehole wall temperature for all boreholes in the system

Claesson and Eskilson's (1987a) superposition borehole method was defined as having Type III boundary condition with uniform borehole wall temperatures for all boreholes. The Type III boundary conditions are thought to be the best approximation for a real system, but none precisely match the actual situation. A real situation would be closer to a uniform entering fluid temperature for each borehole. These classifications are dependent on the boundary conditions applied to the GSHP model and not specifically on the base borehole model. So the line source model could be modeled with any type of borehole condition. The most common analytical borehole models are described below.

2.2.1 Point Source and Infinite Line Source

The point source model consists of a point that continually rejects heat through conduction to an infinite homogeneous medium. Point source models have been presented by Fourier (1878), Kelvin (Thomson 1880, 1884), and Ingersoll et al. (1948).

The infinite line source method models the borehole as a line heat source that continuously generates and rejects heat through pure conduction heat transfer. The development of the infinite

line source method is often mistakenly credited to Lord Kelvin (Thomson 1880, 1884). This misconception is likely based on a comment made by Ingersoll and Plass (1984) that stated "The following [is an] elaboration of the Kelvin heat source theory"; in fact it was an elaboration of Fourier's methods rather than Kelvin's. A review of Kelvin's work will find a compendium of solutions based on Fourier's point-source solution but no mention of the line source model (Spitler and Gehlin 2015).

Fourier's point source solution, reprinted by Kelvin, was later used to develop the infinite line source model as an infinite series (Whitehead 1927) and later as an integral (Ingersoll and Plass 1948; Carslaw and Jaeger 1959, 161-2). The infinite line source can be derived by integrating Fourier's point source solution as shown in Appendix A.

When used to model U-tube boreholes, the infinite line source method places the line source at the center of the borehole and obtains the average borehole wall temperature. The fluid temperature is obtained assuming that the heat transfer within the borehole is quasi-steady state based on Morgensen's (1983) assumptions. This assumption allows all of the internal heat transfer in the borehole to be modeled as a simple borehole thermal resistance (Spitler and Gehlin 2015). An issue with this model is that it treats the borehole as an infinite line and therefore does not consider end effects.

2.2.2 Infinite Cylinder Source

Instead of modeling the borehole as a line, a cylinder can be used. The infinite cylinder source, often just referred to as the cylinder source model, assumes that the borehole consists of a cylindrical volume of infinite length. The contents of the borehole cylinder can be modeled in several different ways: as empty with all heat rejected from the cylinder wall, as a perfect conductor with specific thermal capacitance, and as a homogeneous material with thermal properties disparate from those of the ground (Carslaw and Jaeger 1959).

2.2.3 Finite Line Source

The finite line source builds upon the infinite line source model by imposing end effects and a boundary condition to model the ground surface. The ground surface is modeled by mirroring the borehole line source about the boundary as a line sink. This Method of Images creates a constant temperature boundary condition to model the surface of the ground. This is especially important for GHE modeling when the design period is greater than a year which is when the accuracy of the model becomes more important (Spitler and Bernier 2016). Because the finite line source model is based on the integral of the point source model, when the integral is evaluated numerically it resolves into a series of point sources.

2.2.4 Numerical Models

There are various numerical methods that use the finite difference method, finite element method, and finite volume method that can be used to model geothermal boreholes. These methods can be used to generate g-functions but are not typically used directly for design purposes (Spitler and Bernier 2016). The superposition borehole model of Eskilson and Claesson (1987a) is a numerical model that uses the finite difference method. It is often used as a basis of comparison for analytical models. This model is described in more detail in Section 1.2.4.

2.3 Review of Finite Line Source Models

There are many different ways to solve the finite line source model using integrals, double integrals, or fast Fourier transforms (FFT). Various authors have applied improvements and boundary conditions to the finite line source model in order to calculate the system temperature response or g-functions. Models that calculate only the system temperature response can typically be modified to provide g-functions instead.

Cui, Yang, and Fang (2006) developed an analytical finite line source mode for inclined boreholes to investigate the possibility of reducing the land required to install a GSHP system.

They used a 3D heat conduction model and superposition to model multiple boreholes. For ease of calculation they used the temperature at the middle of the borehole at the wall as the borehole temperature. This assumption results in a higher temperature than calculated using the mean or integrated temperature but the associated errors were presumed to be acceptable and result in a conservative system design. Their results show that inclined borehole systems can have 10-35% lower temperature rise on the borehole wall than strictly vertical systems. This method would be classified as a type BC-I with uniform heat flux (Cimmino and Bernier 2014).

Lamarche and Beauchamp (2007) devised an analytical solution for modeling GSHP systems with emphasis on long-term performance. Some simplifications are applied to make the model amenable for longer simulations. Important phenomena that are considered are axial effects and thermal interaction between boreholes. They use a finite line source model with the mean borehole temperature to get the g-functions. The double integral is broken up into the main and mirror line sources, resolved into a single integral, and solved for using Matlab® (MathWorks 2016). The resulting g-functions were found to have a good agreement with Eskilson's g-functions (1987a).

Marcotte and Pasquier (2009) presented an analytical finite line source method for generating the change in ground temperature due to temperature interactions between boreholes. The finite line sources are defined such that they can be placed each with their own length, inclination from vertical (dip), direction of inclination, and borehole burial depth. Each borehole is assumed to have a constant heat flux so this model qualifies as a type BC-I model as defined by Cimmino and Bernier (2014). Marcotte and Pasquier argue that the average borehole wall temperature and fluid temperature are the only temperatures required for geothermal design and that the uniform heat flux assumption provides an excellent approximation. They suggest that their FLS model could be reduced to a single value, such as a g-function, or solved with a Fast Fourier Transfer in MatLab® (MathWorks 2016).

In a method very similar to that of Marcotte and Pasquier (2009), Lamarche (2011) proposed a finite line source model for inclined boreholes based on the methods of Cui et al (2006). His model assumes that the top of the borehole sits at the ground surface. The heat flux along the borehole is assumed to be uniform so this model would also be classified as BC-I (Cimmino and Bernier 2014). Once again the double integral used to get the g-function value was solved with the Matlab® software (MathWorks 2016).

Claesson and Javed (2011) developed a method to get the short and long term responses for vertical GLHE systems. The short term response used an analytical solution that models the U-tube as a single equivalent-diameter pipe with average fluid temperatures. The thermal network for the system accounts for the fluid's thermal capacity and the resistance of the pipe and grout. The problem is solved with a Laplace transform followed by inversion to get the fluid temperatures in the time domain. The long term response is found using a finite line source model that is resolved down to a single integral. Interactions between boreholes are found by superimposing the responses of the boreholes in the system. This model can be classified as having Type I boundary conditions due to their uniform heat flux assumption (Cimmino and Bernier 2014). This model was implemented in a non-commercial version of GLHEPro by Malayappan (2012).

Cimmino and Bernier (2014) devised the classification scheme detailed in Section 2.2. They concluded that the BC-III classification finite line source model provided the best match with Eskilson's numerical method (1987a). The BC-II and BC-III classifications broke each borehole up into 12 segments in order to maintain the boundary constraints while the BC-I classification was modeled as a single segment. Each of the methods they considered used a numerical Fast Fourier Transform (FFT) to evaluate the finite line source models for each boundary classification. They evaluated the FLS/BC-III g-functions against Eskilson's g-functions for 312 borehole configuration with up to 144 boreholes and found the error between the two methods to

be within ±5% for 92% of the time. The calculations for type BC-III took 13 times longer on average than for type BC-II. As the number of borehole in the system increased so did the computation time.

By far the simplest method for generating g-functions is the BC-I type with the constant heat flux boundary condition. If this method could be implemented such that the g-function error remained within ±5% of Eskilson's g-functions then it should provide a simple and computationally efficient method for calculating g-functions. In general this method has been shown to have reasonable accuracy but tends to overestimate the g-functions for closely packed borehole fields (Malayappan and Spitler 2013). The magnitude of the overestimation is a function of the number of boreholes, the borehole spacing, the borehole depth, and the simulation duration. Thus by limiting the number of boreholes that may be used with the method, the error in the g-functions and the system sizing can be constrained to remain within ±5%. Malayappan and Spitler (2013) recommended that the g-functions for fields of up to 64 boreholes with fewer than 40% of the boreholes located in the interior of the configuration would meet this criterion.

The method implemented in this thesis is based upon the methodology of Marcotte and Pasquier (2009) and allows for boreholes placed with irregular spacing in the horizontal plane and borehole inclination from vertical. As noted in the title of this section the model implemented will be referred to as the Free Placement Finite Line Source (FPFLS) model. The model is to be implemented for use in borefield design and is validated against experimental data for a series of vertical ground loop heat exchangers (GLHE) in Chapter III. The constraints required to keep the error within the range of ±5% is considered during the validation of the FPFLS model in Chapter III.

2.4 Methodology

The model selected is that of Marcotte and Pasquier (2009) which presented an analytical finite line source method for generating the change in ground temperature due to temperature interactions between boreholes. The temperature perturbations are then compiled into g-functions by using Eskilson's (1987a) definition of a g-function. This finite line source method makes use of a double integral which can be resolved from a line into a series of points in a point source model (Ingersoll 1948-1954) where a single point in a homogeneous medium causes a change in temperature at a set distance after time *t*. It assumes that the heat flow along the borehole is uniform and that the surface temperature about the circumference of the borehole is substantially constant (Marcotte and Pasquier 2009). As noted in the introduction, the resulting GLHE sizing and simulation method will be referred to as the FPFLS method throughout the rest of this thesis.

The average borehole wall temperature difference at a given time *t* can be calculated as

$$\Delta\bar{T}_w(t) = \sum_{i=1}^{N} \frac{H_i}{H_T} \sum_{j=1}^{N} \Delta T_{j\to i}(t) \tag{2.1}$$

Where

H_i is the length of the current borehole being considered [m]

H_T is the total borehole length [m]

N is the total number of boreholes

$\Delta T_{j\to i}(t)$ is the mean variation in the borehole wall temperature of borehole *i* due to the interaction with the heat extracted or rejected from borehole *j*. Equation 2.2 gives the calculation method for $\Delta T_{j\to i}(t)$ as

$$\Delta T_{j\to i}(t) = \frac{q_j}{4\pi k H_i}\left(\int_{u_1^i}^{u_2^i}\int_{u_1^j}^{u_2^j}\frac{erfc\left(\frac{d(u_i,u_j)}{2\sqrt{\alpha t}}\right)}{d(u_i,u_j)}du_i du_j - \int_{u_1^i}^{u_2^i}\int_{u_1^j}^{u_2^j}\frac{erfc\left(\frac{d(u_i,u_j')}{2\sqrt{\alpha t}}\right)}{d(u_i,u_j')}du_i du_j{}'\right) \quad (2.2)$$

Where

q_j is the heat extraction/rejection [W]

α is the ground thermal diffusivity [m^2s^{-1}]

k is the ground thermal conductivity [W m^{-1} K^{-1}]

t is time [s]

u_n is a point on a borehole n, where n=*i* or *j*

u'_n is a point on a mirror of borehole n, where n=*i* or *j*

$d(u_i, u_j)$ is the distance between points u_i and u_j [m]

$erfc(u)$ is the complementary error function, where $erfc(u) = \frac{2}{\sqrt{\pi}}\int_u^\infty e^{-s^2}ds$

Other terms are defined in Equation 2.1

The second double integral term is an image or mirror of borehole *j* reflected about the ground surface in order to simulate a semi-infinite homogeneous medium. The ground surface is assumed to be a constant temperature boundary condition which is applied using the method of images (Carslaw and Jaeger 1959); the boreholes defined below the ground surface are mirrored about the boundary to produce images above it with opposite heat flux. So a single borehole rejecting heat to the ground would be modeled as having a mirror image absorbing heat above.

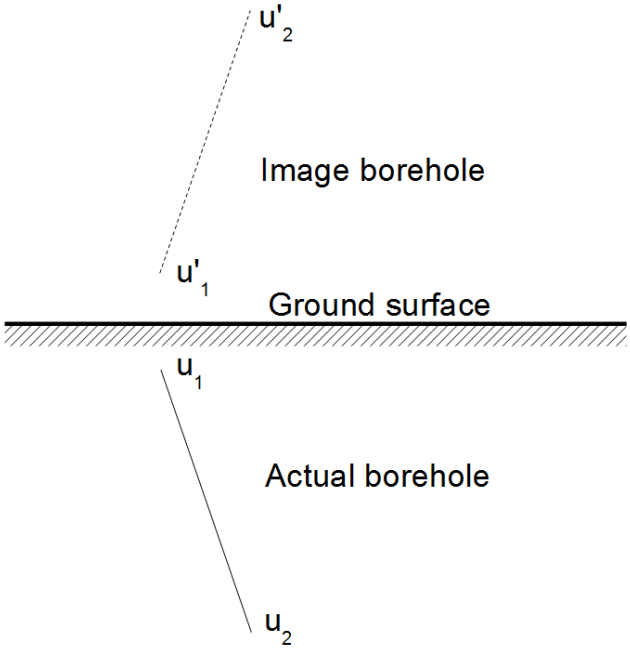

Figure 2-1: the method of images applied to each borehole

Each line is defined by a series of points set between user defined start and end points defined relative to a three dimensional Cartesian coordinate system. The values of $d(u_i,u_j')$ and $d(u_i,u_j)$ give the distance between these points as

$$d(u_i,u_j)=\left((x_i-x_j)^2+(y_i-y_j)^2+(z_i-z_j)^2\right)^{1/2} \tag{2.3}$$

$$d(u_i,u_j')=\left((x_i-x_j')^2+(y_i-y_j')^2+(z_i-(-z_j))^2\right)^{1/2} \tag{2.4}$$

Where

$u_n=(x_n,y_n,z_n)$ is a point on a borehole n, where n=*i* or *j*

$u'_n=(x'_n,y'_n,z'_n)$ is a point on a mirror of borehole n, where n=*i* or *j*

Equation 2.3 gives the distance to a point on pipe *j*, (u_j), from a point on pipe *i*, (u_i)

Equation 2.4 gives the distance to a point on the mirror of pipe *j*, (u_j').

The equation for $\Delta T_{j\to i}(t)$ can be further simplified, as shown in equation 2.5, because of the relationship between the points on the pipe *j* and its mirror image; that varies only in the value of z, or depth. H_i is included in the denominator to average the integral over its length.

$$\Delta T_{j\to i}(t) = \frac{q_j}{4\pi k H_i}\left(\int_{u_1^i}^{u_2^i}\int_{u_1^j}^{u_2^j}\frac{erfc\left(\frac{d(u_i,u_j)}{2\sqrt{\alpha t}}\right)}{d(u_i,u_j)} - \frac{erfc\left(\frac{d(u_i,u_j')}{2\sqrt{\alpha t}}\right)}{d(u_i,u_j')}dudu'\right) \tag{2.5}$$

Transitioning the temperature change to a g-function, g_s, is not difficult given that:

$$g_s = \frac{2\pi k}{q_l}\Delta\bar{T}_w(t) \tag{2.6}$$

Where

q_l is the heat extraction/rejection per unit length of borehole [W/m]

This is based on the definition of g-functions by Eskilson (1987a). Combining equations 2.1, 2.5, and 2.6 gives:

$$g_s = \frac{2\pi k}{q_l}\sum_{i=1}^{N}\frac{H_i}{H_T}\sum_{j=1}^{N}\frac{q_j}{4\pi k H_i}\left(\int_{u_1^i}^{u_2^i}\int_{u_1^j}^{u_2^j}\frac{erfc\left(\frac{d(u_i,u_j)}{2\sqrt{\alpha t}}\right)}{d(u_i,u_j)} - \frac{erfc\left(\frac{d(u_i,u_j')}{2\sqrt{\alpha t}}\right)}{d(u_i,u_j')}dudu'\right) \tag{2.7}$$

This can be simplified to:

$$g_s = \frac{1}{2}\frac{1}{H_T}\sum_{i=1}^{N}\sum_{j=1}^{N}\left(\int_{u_1^i}^{u_2^i}\int_{u_1^j}^{u_2^j}\frac{erfc\left(\frac{d(u_i,u_j)}{2\sqrt{\alpha t}}\right)}{d(u_i,u_j)} - \frac{erfc\left(\frac{d(u_i,u_j')}{2\sqrt{\alpha t}}\right)}{d(u_i,u_j')}dudu'\right) \tag{2.8}$$

The g-function values are stored in conjunction with dimensionless time factors. For comparison with Eskilson's g-functions these values have been set to a series of constants.

$$LN(T/Ts) = \ln\left(\frac{t}{t_s}\right) = \ln\left(\frac{9\alpha t}{{H_A}^2}\right) \tag{2.9}$$

Where

H_A is the average borehole length for the system [m]

t is the time [s]

t_s is the time scale [s], equation 1.3

α is the soil thermal diffusivity [m^2s^{-1}]

The finite line source (FLS) method and Eskilson's (1987a) numerical method are only applicable for times larger than:

$$t = \frac{5r_b^2}{\alpha} \tag{2.10}$$

Where

r_b is the borehole radius [m]

α is the soil thermal diffusivity [m^2s^{-1}]

At times shorter than this time, *t*, the accuracy of the FLS method is questionable. Thus any system response that occurred less than *t* seconds from the current time step may have an error associated with it. For very short time steps the detailed interactions near the borehole should be taken into account.

The short time step method of Xu and Spitler (2006) is used to generate the short time-step (STS) g-functions; it consists of a detailed numerical model that gets the nondimensionalized temperature response based on step pulse over a given period of time. More information on the STS method used in GLHEPro is given in Section 1.2.4.

2.5 Implementation

The method was implemented as a Dynamic Link Library (DLL) in FORTRAN. Inputs to the program are taken from a specially formatted text file and a series of g-functions and dimensionless times are returned in an output file. The input file is generated through a series of interfaces in GLHEPro which are detailed in the following sections. The vertical and inclined boreholes are defined through one set of forms and the horizontal systems through another more constrained system.

The double integrals shown in the final Equation 2.8 are solved by breaking the integral down into a series of 50 points for the line source currently being considered and 561 points for each of the other boreholes in the system. These points are then used with Simpson's 1/3 rule (Stewart 2003, p. 560) to get the response of one line source, composed of a series of points, to another. This is repeated until the responses between all of the boreholes have been calculated and summed according to the summation in Equation 2.8. The resulting g-function is then saved along with the corresponding dimensionless time and the process repeated until 27 g-function pairs (i.e. the g-function value and corresponding dimensionless time) have been saved to the output file.

This process is repeated each time GLHEPro requests the g-functions for a system that uses the FPFLS method. During a sizing routine this can occur multiple times, each time with slightly different inputs. In order to handle systems where the boreholes have been defined to have different borehole depths, the borehole field is sized by adding or subtracting a fixed length to each borehole or trench. This will preserve some of the initial variation in borehole or trench length.

2.5.1 Vertical and Inclined

For both vertical and inclined boreholes the borehole definitions are input as the Cartesian coordinates for the top of the borehole (Borehole Head), the inclination angle, the direction angle, and the borehole length. The borehole head is defined by a point in a 3D Cartesian coordinate system where *x* and *y* define the horizontal directions and *z* defines the vertical direction. On the z-axis the downward direction is assumed to be positive. The inclination angle is measured from vertical (i.e. the z-axis). The direction angle is measured clockwise from the positive y-axis, which is loosely defined as North. These inputs are then converted into a set of points that define the start and end point for each borehole. The interface in GLHEPro V5.0 used to input these values is shown in Figure 2-2.

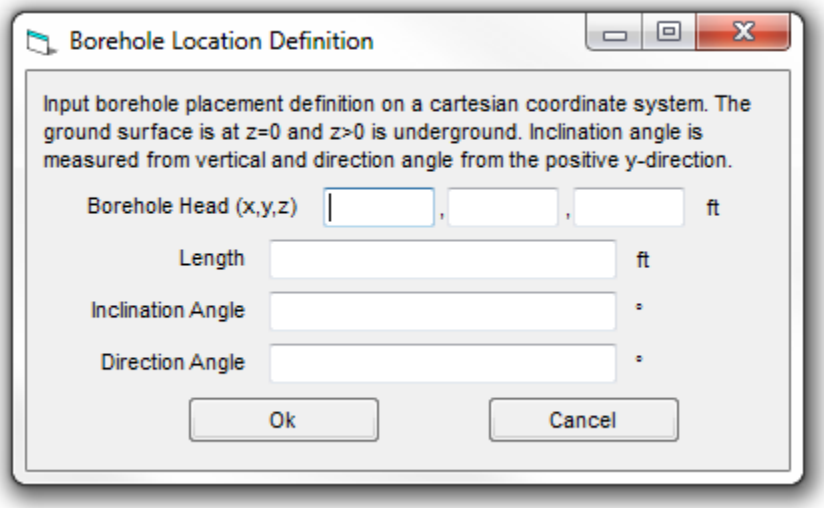

Figure 2-2: Input form for Borehole definition

The values for the borehole are then displayed in a table as shown in Figure 2-3 to allow the user to view the values for all of the boreholes in the system. To provide a more intuitive method for checking the layout of the loaded boreholes, the option to 'View' the system of boreholes is provided; selecting this option results in a form as shown in Figure 2-4 and 2-5 that displays the top, side and front view of the currently loaded borehole field.

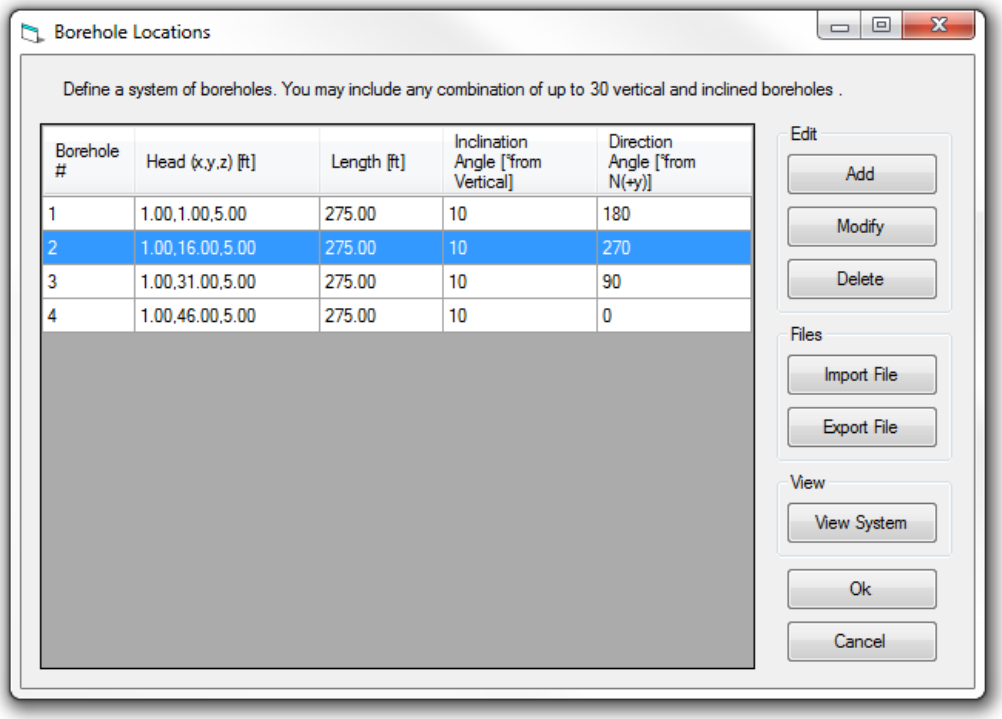

Figure 2-3: Table of borehole definitions for a circle of inclined boreholes using the FPFLS method

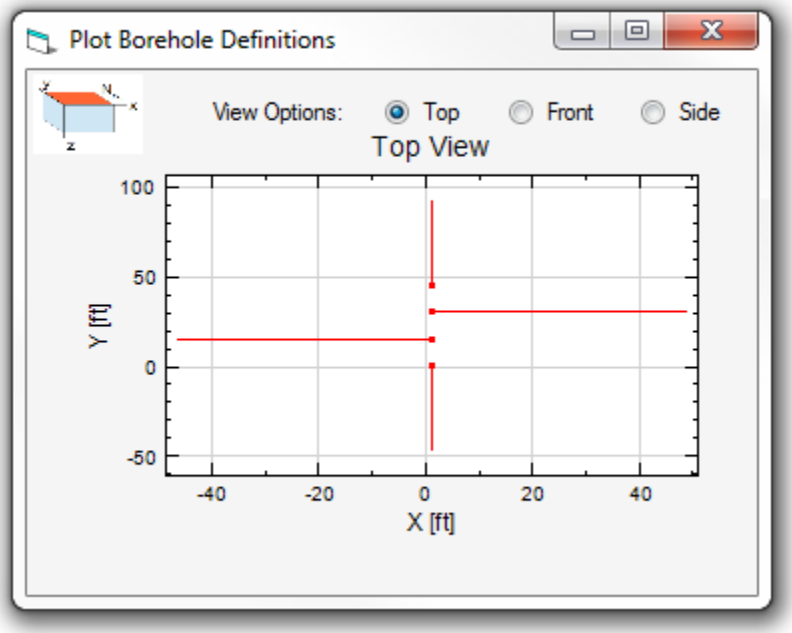

Figure 2-4: Top view of the boreholes defined in Figure 2-3 for the FPFLS method

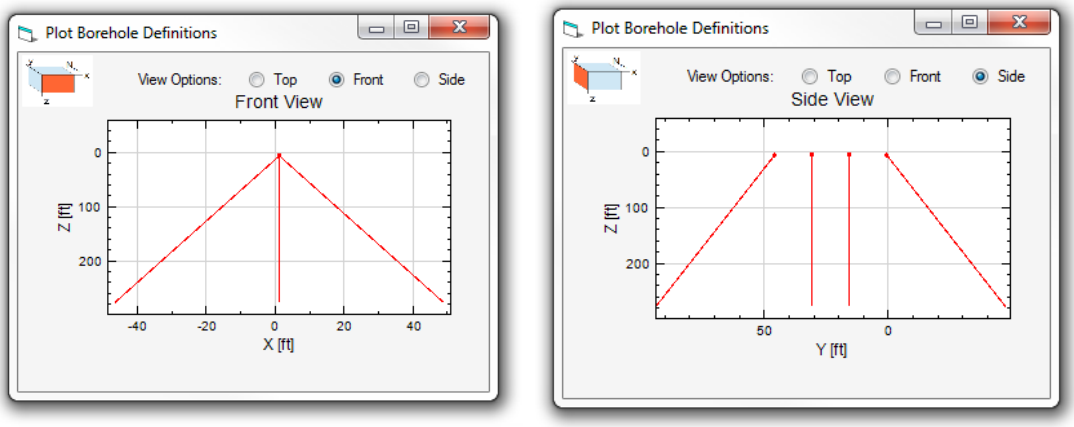

Figure 2-5: Front and Side view of the boreholes defined in Figure 2-3 for the FPFLS method

Systems with vertical and inclined boreholes can be modeled for single U-tube, double U-tube, and concentric boreholes. These options do not affect the calculation of the FPFLS method but they are important for the calculation of the short time step g-functions and the borehole thermal resistance.

The inputs required for calculating the borehole thermal resistance and g-functions for the vertical and inclined FPFLS method are shown in Figure 2-6. An in-depth discussion of each of these inputs can be found in the GLHEPro V5.0 User Manual (OSU 2016b). The inputs can be divided up into Borehole Specification, where the geometry of the borehole is defined; Borehole Fill, where the borehole is defined to be grouted or groundwater filled; Thermal Properties, including the volumetric heat capacities and thermal conductivities of the soil, grout and pipe; Fluid Properties; and Short Circuiting effects, which are optional (see Chapter IV).

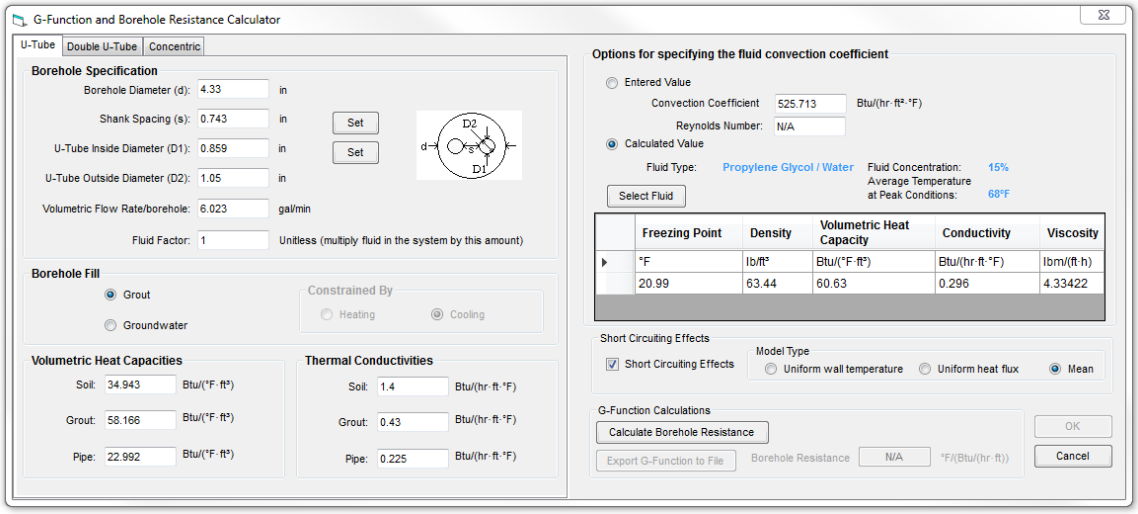

Figure 2-6: G-function and Borehole Resistance Calculator dialog for the FPFLS method in GLHEPro V5.0

2.5.2 Horizontal

There were two methods considered for implementing a horizontal system: the option to place horizontally bored boreholes or the option to approximate horizontal trenches. The horizontally bored boreholes could easily be modeled using the method implemented for the inclined systems by specifying an inclination angle of 90°, thus it was found to be more useful to provide a method to model horizontal trenches.

The horizontal option is implemented as essentially soil filled horizontal boreholes. The trenches are typically filled with the soil that was removed during their excavation. The model allows either a single or double U-tube option. This translates as either two tubes placed horizontally in a single trench (Figure 2-7) or four with a similar placement as shown in Figure 2-8. Using these limitations on the placement of tubes in the trench allows the short time step (STS) methods of Xu and Spitler (2006) to be extended into the horizontal model.

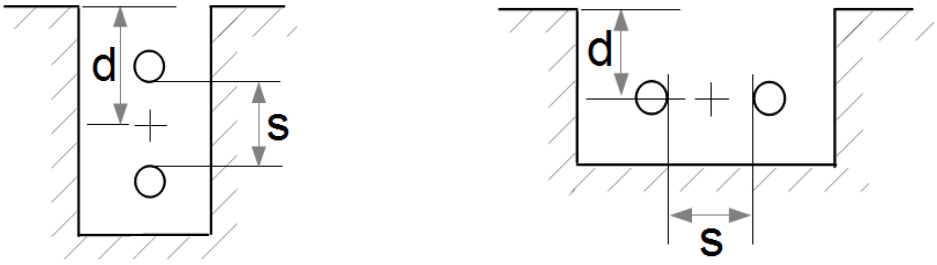

Figure 2-7: Single Horizontal configuration, two orientations that are handled the same

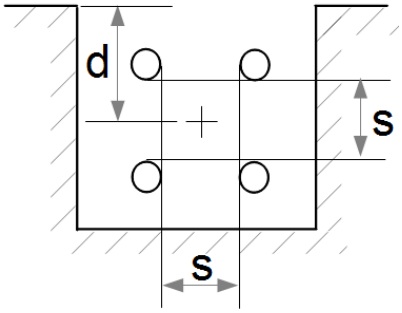

Figure 2-8: Double Horizontal configuration

Within GLHEPro V5.0 the horizontal GHE can be defined by specifying the trench length, number of trenches, distance between trenches, average burial depth of the system, tube diameters and spacing within the trench. Figure 2-7 and 2-8 show the possible tube configurations within the trench. Figure 2-9 shows the dialog which is used to load the inputs into the program; the left side of the form contains the inputs for the trench and tube definitions, the right side of the form contains the fluid, ground, and pipe properties and the Effective Resistance and g-function output option.

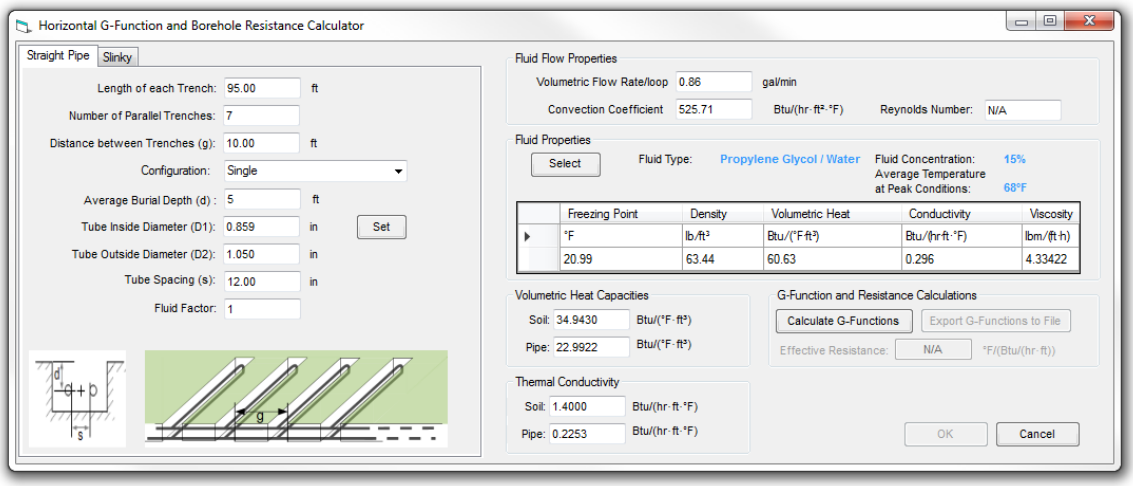

Figure 2-9: G-function and Borehole Resistance Calculator dialog for the Horizontal Straight Pipe model in GLHEPro V5.0

The "Effective Resistance" calculated for the straight horizontal pipes cannot be directly compared to the "borehole resistance" used for vertical systems. This is because it does not model the grout or have a defined borehole diameter. The borehole thermal resistance is calculated out to the circumference of the borehole for vertical and inclined systems. Horizontal systems do not have an actual borehole diameter so the resistance is calculated out to an effective radius from the horizontal pipes. The effective radius is set based on the assumption of 'B' spacing in the borehole (Paul 1996). The orientation of the tubes within the borehole or trench is not specified within the STS method as depicted by Figure 2.7. The FLS method treats the GLHE as a line and a borehole radius with its corresponding resistance and is thus independent of the internal borehole geometry.

No experimental validations were completed for the straight horizontal model. The sizing results for a straight horizontal GHE for the ASHRAE building in Atlanta, Georgia, are compared to the horizontal slinky sizing results in Section 7.5. The results were found to be reasonable but very dependent on the ground temperature selected.

2.6 Conclusions

The FPFLS method implemented gives designers a convenient method for generating the g-functions for systems with boreholes that are not installed in a grid and have varying depths or inclinations to vertical. This provides an enormous amount of flexibility when compared to using tabulated values.

The finite line source model is used often in ground heat exchanger design; not just in the design of the boreholes but also to solve for the borehole thermal resistance and ground temperature from the data collected during thermal response tests (Sanner et al. 2005).

Adding inclination to the borehole design is a fairly simple way to reduce the required borehole depth. Marcotte and Pasquier (2009) claimed that just slight inclination could reduce the total borehole length by 20%. This is due to the reduced interaction between boreholes.

There have been some studies that suggest that the constant heat flux method used introduces a greater sizing error during design than the more accurate constant borehole wall temperature assumption (Malayappan and Spitler 2013). The effects of these errors on the g-functions and sizing results of the FPFLS model are investigated in Chapter III and limitations placed upon the FPFLS method to keep the error within ±5%.

The FPFLS method assumes that the fluid flow rate through each borehole is the same. One item that should be considered for future work on the FPFLS model is to take into account flow rates that vary from borehole to borehole. This will occur for GHE that have boreholes with different depths if no active measures are taken to control the flows.

CHAPTER III

EXPERIMENTAL AND INTERMODEL VALIDATION OF FPFLS MODEL

3.1 Introduction

This chapter includes an experimental and intermodel validation of the Free Placement Finite Line Source (FPFLS) model described in Chapter II. The first section directly compares the g-functions of the baseline 'Library' g-functions based on the methods of Claesson and Eskilson (1987) and the FPFLS method for a variety of configurations. The second section considers the GHE sizing results using GLHEPro V5.0 and the two models (i.e. the Library g-functions and the FPFLS g-functions). Experimental data for four GSHP systems are used to define the inputs for the two g-function models. The borehole sizing results are compared to the actual system sizes to provide a basis for evaluation.

3.2 G-function Comparison

The g-function comparison that is considered here compares Eskilson's Library g-functions with those of the FPFLS method. During the comparison a series of interesting considerations were discovered. Some of these considerations must be taken into account to make a proper comparison with the FPFLS method and others are merely interesting.

Eskilson's g-functions are tabulated with respect to *B/H*, a ratio of the spacing between boreholes (*B*) to the length of the boreholes (*H*), and r_b/H, a ratio of the borehole diameter (r_b) to length. The value of the *B/H* ratio can be adjusted by shifting the value of *B* or *H*. It is interesting to note

that Eskilson varies the *B/H* ratio by increasing the spacing between boreholes. Presumably this was done so that the other ratio, r_b/H, might remain a constant value of 0.0005. When used in a simulation a correction factor is applied to correct the tabulated g-functions to the actual r_b/H values for the specific system. More information on the handling of the library g-functions is included in Chapter V. For the cases considered the borehole radius has been set to get an r_b/H value that matches Eskilson's tabulated values.

One input that is needed more for the FPFLS method than Eskilson's g-functions is the depth at which the top of the borehole is buried. Esklison used a depth of 4 or 5 meters between the ground surface and the top of the borehole for all of his example systems (Claesson and Eskilson 1987a). A single specific value is not given because they found that, for a fixed borehole length, the burial depth of the top of the borehole was not important. The actual g-functions used within GLHEPro were provided by Hellström[3] with no accompanying documentation so it is possible that a different depth was used.

Two different burial depths are considered in the simulations in order to show the effects that this has on the temperature response. Burial depths of 5 meters and 1 meter are considered. For all configurations the borehole length was set to 110 meters, the borehole radius to 55 millimeters, the thermal diffusivity of the soil to 1.62E-06 m^2/s, and the borehole spacing allowed to range from 2.2 to 55 meters.

A comparison of the g-functions for a series of different configurations of vertical boreholes is shown in Table 3-1. The percent error values in the table show the average, maximum, and minimum values for 8 sets of *B/H* values ranging from 0.02 to 0.5 for each borehole configuration listed. The range of time values considered in Table 3-1 ranges from about 2 days to approximately 100 years.

[3] Hellström attended the defense of this thesis and gave the burial depth used to calculate the g-functions by Claesson and Eskilson and in the g-functions in GLHEPro as 5 meters.

Table 3-1: Difference between Library g-functions and FPLS g-functions, % Error

	buried 5 m			buried 1 m		
Configuration	Average	Minimum	Maximum	Average	Minimum	Maximum
9 : 3 x 3	1.8	0.0	5.5	1.4	0.0	2.7
16 : 4 x 4	2.9	0.0	9.8	2.1	0.0	6.2
25 : 5 x 5	3.9	0.0	14.5	3.0	0.0	10.3
30 : 5 x 6	4.4	0.0	16.6	3.4	0.0	12.2
36 : 6 x 6	4.4	0.0	19.1	4.6	0.0	14.4

On average the percent error is less than 4.6% between the two methods. The minimum error for all cases considered typically occurred when the logarithm of the dimensionless time, ($ln(t/t_s)$), is equal to -3.96, which is approximately 6 months. The maximum percent difference typically occurs between B/H = 0.05 and 0.1 at the longest time step. The percent errors shown suggest that Hellström may have used a burial depth of 0 when generating the library g-functions that are used within GLHEPro.

Figure 3-1 shows a graphical representation of the g-function comparison for two cases. Note that the fit is better with a fewer number of boreholes, less dense borehole groupings, and smaller time values. This is in agreement with the results of a study by Malayappan and Spitler (2013) on the limitations of using the uniform heat flux assumption. As time goes on the interior boreholes tend to have a lower heat flux than the outer ones due to increasing temperature interaction between the boreholes (Malayappan and Spitler 2013). They gave no recommendations as to limitations on the error between g-function sets, focusing instead on sizing error.

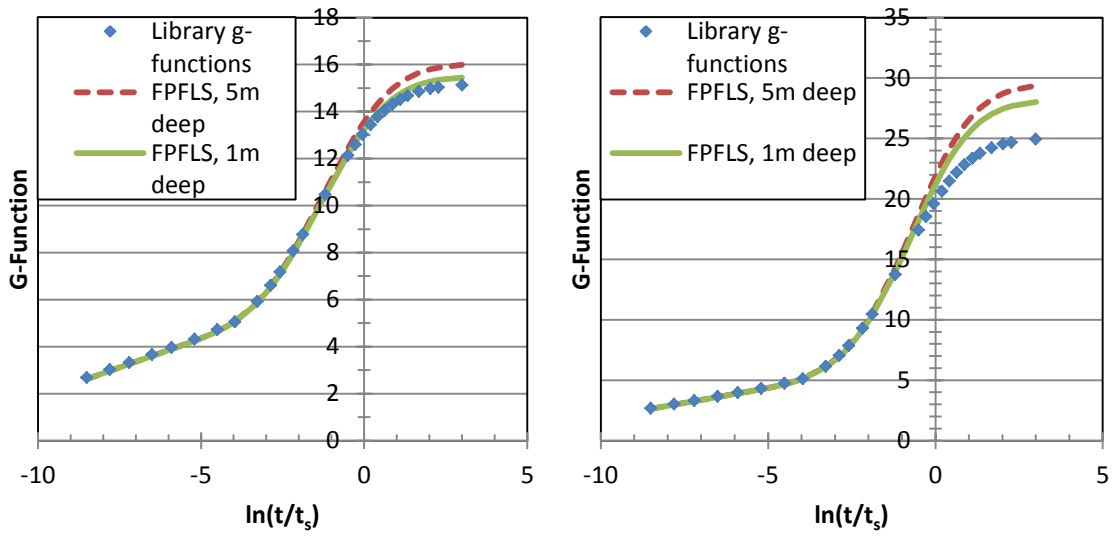

(a) (b)

Figure 3-1: Comparison of g-function for (a) 9:3x3 configuration and (b) 30:5x6 configuration with r_b/H=0.0005 and B/H=0.1

Figure 3-2 shows the results for a case with 9 boreholes, eight evenly spaced in a circle with one in the center. The outer boreholes in the circle are inclined outward at angle theta (θ) from vertical. Boreholes with the smaller, 1 meter burial depth show a better fit to Eskilson's g-functions as do boreholes with greater inclination. The increase in borehole inclination effectively increases the space between boreholes and reduces the borehole interactions that cause the discrepancy between the two methods.

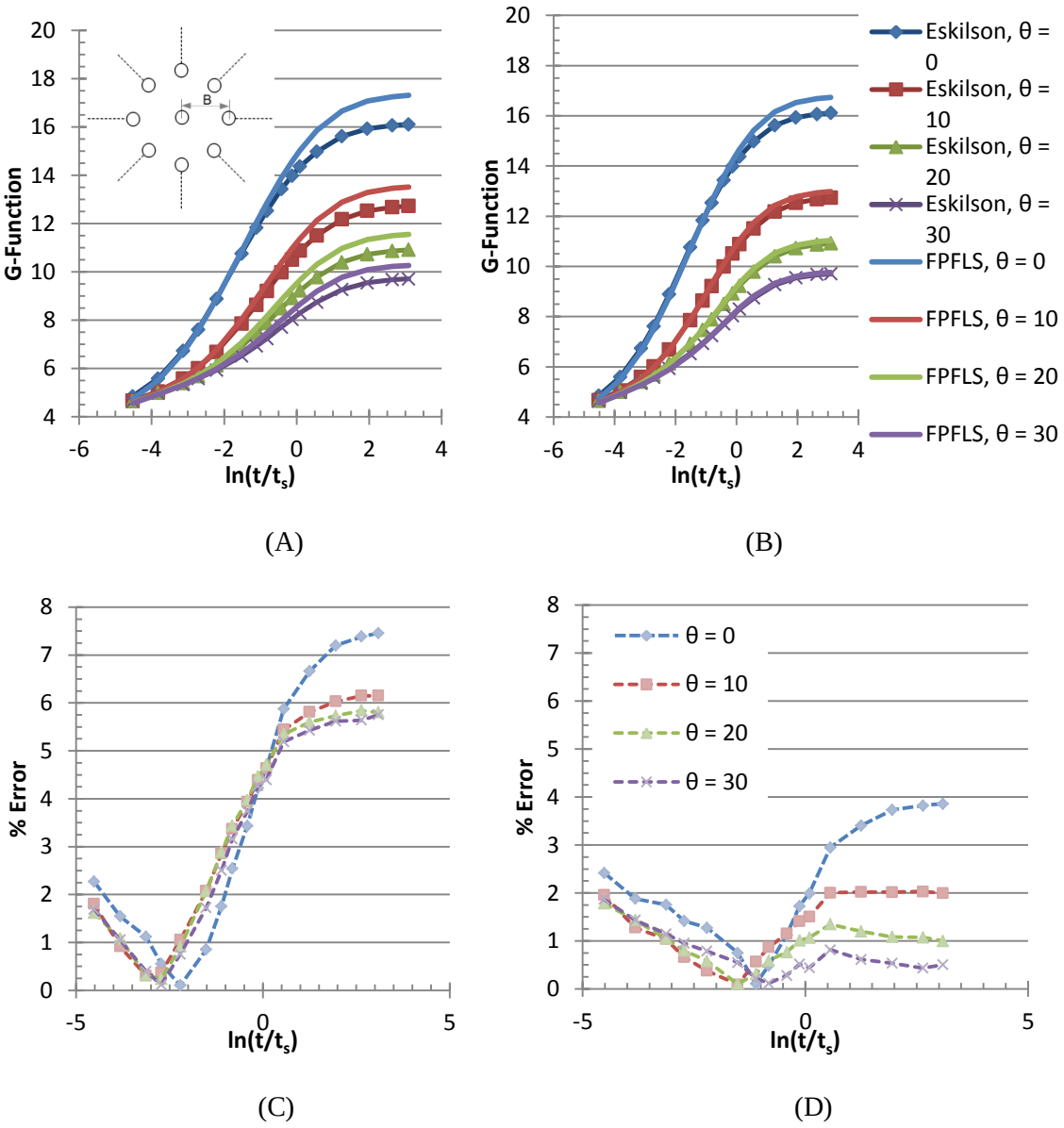

Figure 3-2: G-Functions for 8+1 boreholes in a circle with burial depth (A) 5 m and (B) 1 m and the associated Percent Error at depth (C) 5m and (D) 1m.

3.3 Sizing Comparison

The simulation-based design tool GLHEPro V5.0 was used to size the vertical GLHE for the four GSHP systems presented in this section using both the library g-functions generated by Eskilson (1987a) and those calculated with the FPFLS method. The sizing results from Cullin et al. (2015) are included for reference and to show that, while the inputs for each location specified in the

paper can be the same, the unspecified inputs as well as minor changes to the design program itself can cause a small but noticeable change in sizing results.

3.3.1 Locations

The sizing results of the four cases originally used by Cullin et al. (2015) will be compared when using the analytical FPFLS g-functions vs the library g-functions generated using Eskilson's methodology. Two of the cases are located in Europe, at Valencia, Spain, and Leicester, UK, and two in the United States, at Atlanta, Georgia, and Stillwater, Oklahoma. The loads used by Cullin et al. (2015) were used for each location where month 1 corresponds to January and so on.

The main system dimensions for each location are defined in Table 3-2 and further commentary on these values is considered in the following sections. Where the actual borehole placement is known to differ from the standard configuration an additional sizing simulation is completed to investigate the effects, if any, associated with simplifying the borehole placement into a standard grid. Also, in cases where there is vague or conflicting information between published sources, the values with the best supporting sources are used and the sizing errors associated with the inputs considered.

Each system of boreholes is installed some depth below the ground surface; this depth is rarely specified because it is not needed for most vertical GLHE models. A burial depth, or inactive borehole length, of 1 meter (3.28 feet) is assumed. The U-tubes are assumed to be placed in the borehole with even spacing between the U-tube legs and the borehole wall unless otherwise specified. This assumption matches the 'B' shank spacing definition given by Paul (1996).

Table 3-2: Summary of measured GHE data and Sizing specifications

Variables	Valencia[1]	Leicester[2]	Atlanta[3]	Stillwater[4]
Borehole depth, m (ft)	50 (164)	100 (328)	122 (400)	75 (246)
Borehole spacing, m (ft)	3 (10)	**5 (16)**	7.6 (25)	**6 (20)**
Borehole diameter, mm (in.)	150 (5.9)	126 (5.0)	**127 (5)**	114 (4.5)
U-tube inner diameter, mm (in.)	**26.2 (1.03)**	**26.2 (1.03)**	34.5 (1.36)	**21.8 (0.86)**
U-tube outer diameter, mm (in.)	**32 (1.26)**	**32 (1.26)**	42.5 (1.66)	26.7 (1.05)
Shank spacing, mm (in.)	**38 (1.50)**	**20.7 (0.81)**	18.5 (0.73)	20.3 (0.80)
Undisturbed Ground Temperature, °C (°F)	19.5 (67.1)	13.2 (55.8)	**20.3 (68.6)**	**17.3 (63.1)**
Total System flow rate, L/s (GPM)	0.76 (12)	30 (476)	9.5 (150)	0.63 (10)
Fluid Type*	Water	Propylene Glycol	Water	Water
Concentration, %	0%	20%	0%	0%
Mean Fluid Temperature, °C (°F)	20 (68)	17 (62.6)	20 (68)	20 (68)
Ground Thermal Conductivity, W/m-K (Btu/hr-ft-°F)	1.6 (0.92)	3.2 (1.8)	3.3 (1.88)	2.6 (1.5)
Grout Thermal Conductivity, W/m-K (Btu/hr-ft-°F)	1.6 (0.92)	**2.9 (1.2)**	1.7 (0.98)	**1.1 (0.64)**
Pipe Thermal Conductivity, W/m-K (Btu/hr-ft-°F)	0.42 (0.24)	0.42 (0.24)	0.42 (0.24)	0.39 (0.23)
Ground Volumetric Heat Capacity, kJ/m^3-K (Btu/ft^3-°F)	3000 (44.7)	3000 (44.7)	**2549 (38)**	2012 (30)
Grout Volumetric Heat Capacity, kJ/m^3-K (Btu/ft^3-°F)	3000 (44.7)	3000 (44.7)	**3901 (58.2)**	2012 (30)
Pipe Volumetric Heat Capacity, kJ/m^3-K (Btu/ft^3-°F)	2480 (37.0)	2480 (37.0)	**1542 (23)**	2480 (37)
Calculated BH Resistance, K·m/W (°F/(Btu/(hr ft)))	0.1234 (0.2137)	0.0835 (0.1447)	0.0918 (0.159)	**0.1600 (0.2770)**
Sizing duration, years	3	2	5	1
Sizing Temperature limits, °C (°F)				
Maximum HP EWT***, °C (°F)	30 (99.8)	23.52 (74.3)	30 (99.8)	32 (90)
Minimum HP EWT***, °C (°F)	11 (51.8)	2 (35.6)	10 (51.2)	10 (50)

*mixture with water (if applicable)
**Values in bold may differ between sources
***Heat Pump Entering Water (or fluid) Temperature

[1] Montagud et al. (2011), [2] Naicker and Rees (2011), [3] Cullin et al. (2014), Cullin (2014), & Vaughn (2014), [4] Hern (2004) & Gentry (2006)

3.3.1.1 Valencia, Spain

The experimental data for Valencia was taken from a study on the comparison of air-source systems to a GSHP system at the Universitat Politècnica de València (Montagud et al. 2011). The capacity of the water-to-water heat pump for the geothermal system is nominally 15.9kW cooling and 193kW heating. The GLHE system consists of 6 vertical boreholes in a regular rectangular 2 x 3 array.

The loads on the system are generated from approximately 250 m^2 (2691 ft^2) of space within the Department of Applied Thermodynamics at the Polytechnic University of Valencia. The space consists of 11 rooms and a hallway; of the rooms, 9 are offices and one is a computer classroom (Montagud et al. 2011). The loads and peak load durations used in Cullin et al. (2015) and shown in Table 3-3 are used for the comparison simulations.

Table 3-3: Simulation Based Design Tool GHE loads for Valencia.

Month	Total heating, kWh (kBtu)	Total cooling, kWh (kBtu)	Peak heating, kW (kBtu/h)	Peak cooling, kW (kBtu/h)
1	1640 (5595)	0 (0)	12.3 (41.8)	0 (0)
2	1628 (5556)	0 (0)	12.4 (42.3)	0 (0)
3	1372 (4682)	0 (0)	12.1 (41.1)	0 (0)
4	745 (2543)	0 (0)	11.6 (39.4)	0 (0)
5	0 (0)	1542 (5260)	0 (0)	17.1 (58.3)
6	0 (0)	2405 (8207)	0 (0)	17.4 (59.2)
7	0 (0)	3081 (10,513)	0 (0)	16.1 (54.9)
8	0 (0)	1759 (6001)	0 (0)	15.2 (52)
9	0 (0)	1578 (5383)	0 (0)	14.2 (48.5)
10	0 (0)	1123 (3833)	0 (0)	13.6 (46.5)
11	758 (2587)	0 (0)	9.8 (33.4)	0 (0)
12	1248 (4257)	0 (0)	11.3 (38.6)	0 (0)
Peak Load Duration, hrs			5	3

The system specifications used in the model are defined in Table 3-2. There is some uncertainty about a few values, specifically the U-tube diameter and spacing and the ground properties. One paper (Ruiz-Calvo et al. 2014) specifies a 25.4mm internal diameter and 70mm spacing, which is

taken to mean the center-to-center spacing of the two legs of the U-tube. The U-tube pipe size is assumed to be a nominal 32mm SDR11 pipe. Also two values were listed in one of the sources for the ground thermal conductivity and the volumetric heat capacity as either 1.43 W/m K and 2.25 MJ/m^3 K or 1.6 W/m K and 3 MJ/m^3 K respectively (Ruiz-Calvo et al. 2014). A summary of the uncertainties is shown in Table 3-4.

Table 3-4: Valencia sources of uncertainty

Variables	Range of values	
Shank spacing, mm (in.)	28.4-44.6	(1.12-1.76)
Ground Thermal Conductivity, W/m-K (Btu/hr-ft-°F)	1.43-1.6	(0.826-0.92)
Ground Volumetric Heat Capacity, kJ/m^3-K (Btu/ft^3-°F)	2250-3000	(33.5-44.7)

3.3.1.2 Leicester, United Kingdom

The largest system considered in this paper was monitored by researchers at De Montfort University in Leicester, UK (Naicker and Rees 2011). The system loads are provided by a 15,607m^2 (167,992 ft^2) educational building for which the GLHE system provides all of the necessary cooling and a portion of the heating (Naicker and Rees 2011). The experimental data used covers 2 years of operation starting in December 2009. The monthly loads shown in Table 3-5 used for the comparison are those presented in Cullin et al. (2015).

Table 3-5: Simulation Based Design Tool GHE loads for Leicester

Month	Total heating, kWh (kBtu)	Total cooling, kWh (kBtu)	Peak heating, kW (kBtu/h)	Peak cooling, kW (kBtu/h)
1	2618 (8932)	7989 (27, 259)	25.8 (88.1)	96.2 (328.3)
2	7391 (25, 218)	13,665 (46, 623)	40.6 (138.4)	49.5 (168.7)
3	4536 (15, 478)	15,106 (51, 543)	26.9 (91.6)	136.2 (464.7)
4	2226 (7596)	20,903 (71, 319)	27.4 (93.6)	166 (566.4)
5	1497 (5107)	11,052 (37, 709)	26.9 (91.6)	138.9 (474)
6	1870 (6379)	23,886 (81, 500)	58.8 (200.5)	196.3 (669.7)
7	2431 (8295)	13,764 (46, 961)	31.2 (106.4)	74.2 (253.2)
8	2821 (9626)	14,830 (50, 599)	13.4 (45.6)	101.9 (347.8)
9	2771 (9454)	9935 (33, 899)	22.4 (76.5)	92.1 (314.2)
10	5631 (19, 214)	14,356 (48, 981)	36.4 (124.2)	123.4 (421.1)
11	8146 (27, 795)	12,789 (43, 637)	39.5 (134.7)	40.5 (138.1)
12	3125 (10, 663)	9249 (31, 558)	33.5 (114.2)	38.6 (131.8)
Peak Load Duration, hrs			1	4

The system contains 56 boreholes in two arrays; one with 19 boreholes and the other with 37. The placement of the boreholes is not regular but can be adequately modeled with a regular 7x8 rectangular grid. The borehole spacing was not given in the Naicker and Rees (2011) paper so a borehole spacing of 10m (33ft) was used for the comparisons made by Cullin et al. (2015). Cullin makes no comments on why this particular spacing was selected (Cullin 2014; Cullin et al. 2015). The geothermal pipework layout later provided by Simon Rees showed the spacing to be better estimated as 5m (16ft) (Geothermal International 2009; Rees, personal communication 2015). Using this spacing while treating the two arrays as a single rectangular grid may cause oversizing because the spacing between the two arrays is not taken into account. The actual borehole locations are shown in Figure 3-3 in meters (Geothermal International 2009). The actual borehole locations can be used with the FPFLS method to investigate how much of an effect is made by approximating the borefield as a single rectangular field.

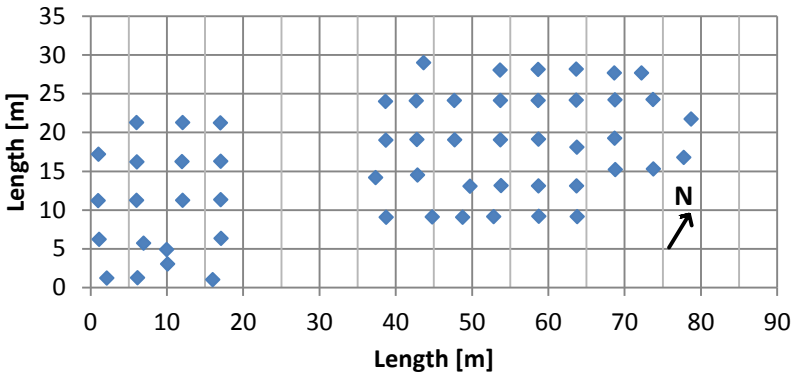

Figure 3-3: Actual borehole placement for Leicester location

The borehole spacing is the main source of uncertainty for this location; some other sources are the shank spacing and grout thermal conductivity. The U-tube dimensions are within tolerance of a nominal 32mm SDR11 pipe. The grout thermal conductivity is specified to be 2.0 W/m-K but only the top portion of the borehole is grouted. The available references do not give any measures on how much of the borehole is grouted and how much is backfilled. The phrasing used was "grouted near the top" (Naicker et al. 2011) which suggests that, at most, half of the borehole could be grouted. The overall grout thermal conductivity should be within the range of 2.6 to 3.1 W/m-K, assuming that the borehole is at best half grouted and at least a quarter grouted. The full range of thermal conductivities for the grout have been considered because it is not inconceivable that a designer might simply use the conductivity for the ground or grout instead of an average value for the length of the borehole. For the main case considered, a grout thermal conductivity of 2.9 W/m-K (1.2 Btu/hr-ft-°F) is used.

Table 3-6: Leicester sources of uncertainty

Variables	Range of values	
Borehole spacing, m (ft)	5-10	(16.4-32.8)
Shank spacing, mm (in.)	18.5- 20.67	(0.73-0.81)
Grout Thermal Conductivity, W/m-K (Btu/hr-ft-°F)	2-3.2	(1.2-1.8)

3.3.1.3 Atlanta, Georgia

The GSHP system considered in Atlanta, Georgia, is a part of the Living Laboratory (Vaughn 2014) in the ASHRAE Headquarters building. Information on the system operation is available by request through the ASHRAE website (ASHRAE 2015). The experimental data from March 2010 to December 2012 was used to generate the loads for the comparison. Periods where no data was collected, due to the GLHE or control system being non-operational or the data being lost for any reason, were replaced with estimated loads based on a cubic curve fit of the existing data and the daily average air temperature. The loads from Cullin et al. (2015) used in this comparison are shown in Table 3-7.

Table 3-7: Simulation Based Design Tool GHE loads for Atlanta

Month	Total heating, kWh (kBtu)	Total cooling, kWh (kBtu)	Peak heating, kW (kBtu/h)	Peak cooling, kW (kBtu/h)
1	1698 (5795)	0 (0)	8.8 (30)	0 (0)
2	1609 (5489)	0 (0)	7.5 (25.7)	0 (0)
3	1314 (4485)	2476 (8448)	51.3 (175.1)	29.9 (102)
4	72 (244)	6104 (20, 828)	20.7 (70.7)	60.1 (205.1)
5	4 (13)	12063 (41, 158)	0.7 (2.4)	77.1 (262.9)
6	6 (20)	15414 (52, 591)	1.2 (4.2)	87 (296.9)
7	7 (24)	15, 023 (51, 259)	1.1 (3.8)	219.8 (750)
8	8 (27)	13, 624 (46, 486)	1.2 (4.1)	89.7 (306.1)
9	31 (107)	7568 (25, 820)	5.7 (19.6)	66.6 (227.3)
10	1358 (4633)	3307 (11, 284)	48.5 (165.3)	54.5 (186.1)
11	4719 (16, 100)	653 (2227)	49.6 (169.3)	14.7 (50.3)
12	4351 (14, 846)	750 (2559)	46.6 (159)	13.4 (45.9)
Peak Load Duration, hrs			2	2

The system is composed of 12 boreholes in a 2x6 rectangular field located under the building's parking lot (Vaughn 2014). The system definitions are shown in Table 3-2. The values for the volumetric heat capacities used by Cullin et al. (2015) were not included in the paper or the Cullin thesis (2014) but could be recovered from the model input files and are included in Table

3-2. Alternative values were used by Laura Southard (2013) in a project report at Oklahoma State University; these values were used as part of the uncertainty analysis.

Table 3-8: Atlanta sources of uncertainty

Variables	Range of values	
Borehole diameter, mm (in.)	127-140	(5-5.5)
Undisturbed Ground Temperature, °C (°F)	19.5-20.3	(67.1-68.6)
Ground Volumetric Heat Capacity, kJ/m^3-K (Btu/ft^3-°F)	2549-2951	(38-44)
Grout Volumetric Heat Capacity, kJ/m^3-K (Btu/ft^3-°F)	2481-3901	(37-58)
Pipe Volumetric Heat Capacity, kJ/m^3-K (Btu/ft^3-°F)	1542-2480	(23-37)

The main source of uncertainty for this location is the ground temperature. There are two possible ground temperatures: 19.5°C (67.1 °F) and 20.3°C (68.6°F) which were calculated from the results of the thermal response test taken of the system in February 2008 (Ewbank 2008). The first temperature is the best estimate for the undisturbed ground temperature at the bottom of the borehole; it is the temperature of the fluid that was at the very bottom of the borehole at the beginning of the thermal response test. The second temperature is the calculated average ground temperature over the length of the borehole during the first full cycle of fluid through the GLHE. This temperature would be the best approximation for the average borehole wall temperature as it accounts for the ground's temperature gradient. The average ground temperature is used for the main simulation because it matches the ground temperature selection methodology recommended by Claesson and Eskilson (1987b) and matches the input required by GLHEPro. The undisturbed ground temperature at the bottom of the borehole is still considered when considering the error on the sizing results because it was reported as the undisturbed ground temperature in the original thermal response test (Ewbank 2008) and it is not unreasonable that a new designer might use this value instead of the average ground temperature.

3.3.1.4 Stillwater, Oklahoma

The original GLHE experiment at Oklahoma State University was implemented by Hern (2004) with four vertical boreholes and one horizontal loop in the GLHE. The same installation was later used by Gentry et al. (2006) but with only three vertical boreholes enabled in the GLHE in a 1x3 configuration. System loads were supplied by two cooling dominated test cells. Each test cell consists of a conditioned equipment and control room with a conditioned room above. Two identical water-to-water heat pumps with 10.6 kW (36.2 kBtu/h) of nominal capacity supply hot water and chilled water; for the period considered, only one heat pump is in use at a time (Gentry et al. 2006).

The data was collected at 1 minute intervals from March 2005 to August 2006 and collated into hourly temperature and heat extraction/rejection rates across the GLHE. The hourly heat extraction/rejection rates from the first year of operation were then used to define the monthly average loads and peak heating/cooling loads and durations. For periods when the system was off for maintenance, zero loads were applied. The loads presented in Cullin et al. (2015) for this location are shown in Table 3-9.

Table 3-9: Simulation Based Design Tool GHE loads for Stillwater from Cullin et al. 2015

Month	Total heating, kWh (kBtu)	Total cooling, kWh (kBtu)	Peak heating, kW (kBtu/h)	Peak cooling, kW (kBtu/h)
1	1698 (5795)	0 (0)	8.8 (30)	0 (0)
2	1609 (5489)	0 (0)	7.5 (25.7)	0 (0)
3	1959 (6683)	160 (545)	7.5 (25.5)	13.5 (46)
4	75 (255)	1320 (4503)	0.5 (1.7)	9 (30.6)
5	66 (225)	1701 (5802)	3.2 (10.8)	9.7 (32.9)
6	1 (4)	2704 (9227)	1 (3.2)	12.5 (42.8)
7	13 (44)	3271 (11161)	1.4 (4.8)	10.1 (34.6)
8	2 (8)	3775 (12881)	0.5 (1.8)	10.3 (35)
9	23 (77)	3366 (11486)	1.8 (6.1)	9.9 (33.7)
10	621 (2117)	1133 (3876)	4.8 (16.3)	9.4 (32.1)
11	452 (1542)	1009 (3441)	9 (30.6)	9.3 (31.8)
12	1504 (5132)	0 (0)	9.2 (31.4)	0 (0)
Peak Load Duration, hrs	-	-	2	2

The system dimensions and definitions are shown in Table 3-2. The main source of uncertainty is the borehole spacing which is reported to be 6.1 (20') or 9.1m (30') in Cullin et al. (2015). The 6.1m (20') spacing is better supported by Hern (2004) and Gentry et al. (2006). There is also some uncertainty in the grout thermal conductivity with values ranging from 1.06-1.19 W/m-K (0.61-0.69 Btu/hr-ft-°F) measured by Hern (2004) and 1.59 W/m-K (0.92 Btu/hr-ft-°F) listed in Cullin et al. (2015).

Table 3-10: Stillwater sources of uncertainty

Variables	Range of values	
Borehole spacing, m (ft)	6.1-9.1	(20-30)
Grout Thermal Conductivity, W/m-K (Btu/hr-ft-°F)	1.06-1.59	(.61-.92)

3.3.2 Results and Discussion

It was not the intent of this validation to match the sizing results presented by Cullin et al. (2015) but to use the best information for the locations provided to compare the sizing results with the FPFLS g-functions to the library g-functions.

Table 3-11 displays the sizing results of three models and the actual borehole size for each location. The sizing results from Cullin et al. (2014) are provided in the table for reference. The 'Cullin et al' results were calculated with GLHEPro V4.0.9 while the other two methods were modeled using GLHEPro V5.0.0. The Library g-functions model makes use of the standard borehole configurations and library g-functions available in GLHEPro to model each location. The specific configuration used for each location is given in Sections 3.3.1.1-3.3.1.4. The FPFLS model uses the methodology described in Chapter II for the g-function calculations during the sizing simulation.

Table 3-11: Sizing Comparison, constant undisturbed ground temperature

Borehole Depth, m (ft)	Valencia[1]	Leicester[2]	Atlanta[3]	Stillwater [4]
Actual	50 (164)	100 (328)	122 (400)	75 (246)
Sized, Cullin et al. (2015)[5]	52 (172)	106 (342)	125 (409)	76 (250)
Sized, Library g-functions	52 (170)	112 (366)	130 (427)	79 (258)
Sized, FPFLS	51 (167)	111 (365)	129 (424)	78 (257)
Percent Error, %	Valencia	Leicester	Atlanta	Stillwater
Sized, Cullin et al. (2015)[5]	5.0	6.0	2.0	2.0
Sized, Library g-functions	3.6	11.5	6.7	4.9
Sized, FPFLS	2.0	11.1	6.0	4.3

[1] Montagud et al. (2011), [2] Naicker and Rees (2011), [3] Cullin et al. (2014) & Vaughn (2014), [4] Hern (2004) & Gentry (2006), [5] Modeled with GLHEPro V4.0.9.

The sizing results indicate that the FPFLS method gets results similar to the library g-functions. The trend is fairly consistent, with each location being sized to have boreholes about 1 meter (0.5-1.5%) shorter with the FPFLS method than with the library g-functions. For all cases the percent

difference between the two methods is less than 2% with the FPFLS method tending to size shorter borehole lengths.

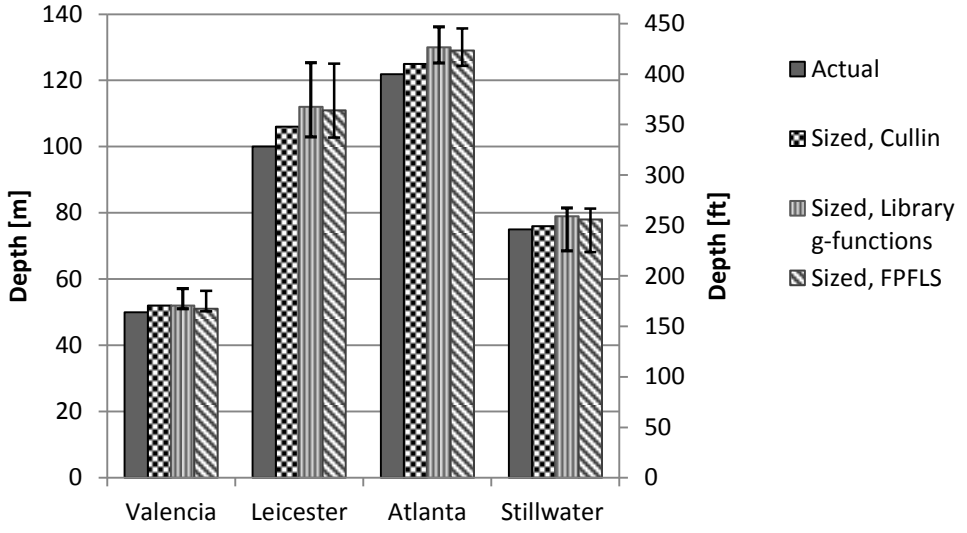

Figure 3-4: Sizing results for each location accounting for the effects of uncertainties

The effects of the uncertainties in the inputs for each location are shown by the error bars in Figure 3-4. Both models show a similar response to the applied uncertainties which goes to further support the applicability of the FPFLS system alongside the Library g-functions.

The simulation method used in GLHEPro and all the cases considered in this validation uses a hybrid time step that uses monthly loads with a peak load day added on to the end of each month (Cullin and Spitler 2011). The accuracy of this simulation method is approximately ±6% so any errors in the sizing results less than 6% may simply be the result of the time step approximation used.

Only two locations have a percent error greater than 6%: Leicester in the UK and Atlanta, Georgia. For Atlanta the 6-6.7% error is due to the effects of the ground temperature on the sizing results. The higher temperature used in the main comparison more accurately models the ground temperature over the length of the boreholes. The sizing error for Leicester is largely a

factor of the borehole spacing selected. The effects of the borehole spacing for this location are considered in more detail in Section 3.3.2.1 below.

3.3.2.1 Leicester, United Kingdom

The total percent error for Leicester, UK, is greater than the 5% sizing error recommended by Malayappan and Spitler (2013) and the 6% possible error due to the hybrid time step simulation method. However, the percent difference between the two methods is 0.7%, which does fall below the recommended limit. Figure 3-4 illustrates the range of sized borehole depths due to the uncertain values listed in Table 3-6. The relatively large uncertainty on the sized borehole depth is largely due to the range of borehole spacing.

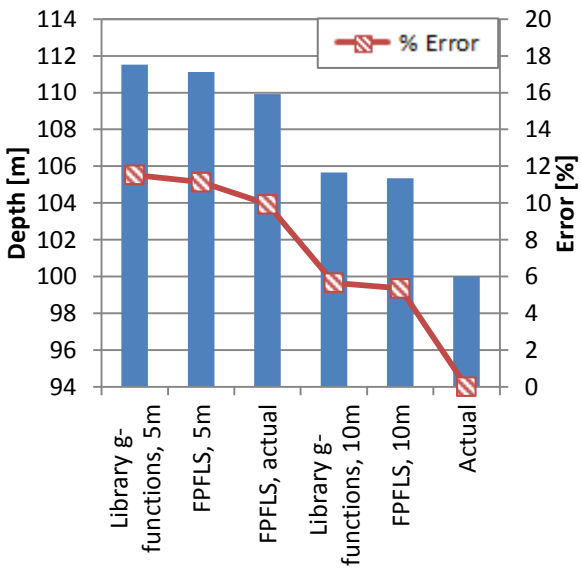

Figure 3-5: Effects of borehole spacing on sizing for Leicester

Figure 3-5 shows a graphical representation for the sized borehole depths for the Leicester location when considering the effects of borehole spacing. As discussed in Section 3.3.1.2, various simplifications are needed to model the non-uniform borehole layout used at the Leicester installation. Cases are considered using both the Library g-functions of Eskilson and the FPFLS

method with the boreholes arranged in a 7x8 grid with regular 5m or 10m spacing. The actual spacing between the boreholes as shown in Figure 3-3 was also used to size a system using the FPFLS method. Improving the placement of the boreholes in this case did improve the sizing of the system when compared to the 5 m spacing but an improvement decreasing each borehole length by 1 m is largely negligible when compared to the overall length of the system.

3.4 Conclusions

The g-function comparison suggests that to limit the percent error in the g-functions to around 5%, a limit should be applied to the number of boreholes that can be sized with the FPFLS method. The configurations for which the higher g-function errors were found have relatively tight borehole placement. Almost any other configuration with the same number of boreholes should have similar or smaller error when compared to the numerical g-functions.

The sizing comparison showed that the FPFLS method gives reasonable sizing results; the percent difference between the sizing results of library g-functions and the FPFLS g-functions is less than 2% with the FPFLS method tending to size shorter borehole lengths by about 1 m (0.5-1.5%).

It was decided to limit the number of boreholes to 30 in a given configuration. This places a limit on the expected error in the g-function values, the expected error in sizing, and on the simulation and sizing run time. Larger systems take more time to compute the g-functions and thus many times longer to size because each sizing iteration calculates the g-functions anew.

The sizing comparison also suggests that it is worthwhile to enforce the 30 boreholes limitation; the sizing error for Leicester with 56 boreholes is much greater than for the other locations. This is, however, also shown to be true when using Eskilson's g-functions in the sizing so it is

apparent that more than just the number of boreholes is a factor in the error associated with the g-function method used for sizing.

Some other factors that have been hypothesized will increase the error of the FPFLS method, and any method that assumes a uniform heat flux, are the balance of the heating and cooling loads and the sizing duration. The limitations placed on the system are conservative enough that the effects of these factors should be small. Malayappan and Spitler (2013) suggested that allowing 64 boreholes with spacing constraints would be reasonable; thus 30 boreholes with no spacing constraints should be more than reasonable.

CHAPTER IV

EFFECTIVE BOREHOLE THERMAL RESISTANCE AND SHORT CIRCUITING

4.1 Introduction

A significant portion of the ground heat exchanger effectiveness is determined by the borehole thermal resistance. The lower the borehole thermal resistance is, the better it can transfer heat to and from its surroundings.

The best method to determine the effective borehole thermal resistance is to perform a thermal response test (TRT). The TRT gives the local ground thermal conductivity and the effective borehole thermal resistance. Unfortunately, this may not be exceedingly useful at the design stage before the GHE has been installed. Also if a single test borehole is used for the TRT test, the calculated ground thermal conductivity and borehole thermal resistance are likely to vary between boreholes.

In order to perform a thermal response test a pilot borehole must be installed and connected to a test rig that can apply a specific heat load to the borehole. The temperature response of the system is measured at both the inlet and outlet of the GLHE. These temperatures can then be used to estimate the effective thermal conductivity and the effective borehole thermal resistance using either various line source methods (Mogensen 1983, Eklöf and Gehlin 1996, Beier and Smith 2002, Witte et al. 2002, Bandos et al. 2009) or a parameter estimation method (Austin et al. 2000).

While thermal response tests provide the best values for the ground thermal properties they are not always an option during the design process. For this reason it is important to be able to use an accurate borehole resistance calculation method. For many cases, values for the local borehole thermal resistance (R_b) are acceptable and users can calculate the resistance values for various grouted or backfilled borehole configurations with a 2-dimensional analysis.

Some of the more accurate models account for short circuiting, where some heat is transferred between the inlet pipe and the outlet pipe in the borehole instead of being transferred from the tubes to the surrounding grout and ground. This reduces the effectiveness of the borehole's heat transfer and could require a larger GHE size. The effects of short circuiting are often negligible but can have a significant impact on systems with very deep boreholes or low flow rates. For both of these cases the difference between the inlet and outlet temperature can be significant enough to induce heat transfer between the two flow channels. For the majority of installations in North America, short circuiting effects will be negligible.

The effective borehole thermal resistance (R_b^*) accounts for the short circuiting resistance in the borehole in addition to the standard conductive and convective resistances. The methods used in this chapter for calculating the effective borehole thermal resistance are versatile and fairly easy to implement because they build on the existing local resistance calculations and need only one additional value for the short circuiting resistance.

Methods to get the local borehole thermal resistance and short circuiting resistance depend on whether the borehole is grouted or groundwater filled. Methods for calculating the local borehole thermal resistance are discussed in the Section 4.2.1.

For North American installation, boreholes are typically grouted for the full borehole length. There are, however, cases where the boreholes are not grouted for the full length but rather grouted only near the top and the remainder backfilled or allowed to fill with groundwater. This

is sometimes seen in Scandinavian countries where vertical boreholes are drilled into the bedrock, cased to the surface, sealed, and allowed to fill with groundwater (Spitler et al. 2016). This changes the borehole resistance calculations because they must now account for the effects of natural convection in the groundwater filled borehole. The thermal borehole resistance for groundwater filled boreholes is typically lower than for grouted boreholes. A recent study by Spitler et al. (2016) collected data in order to form correlations for the effects of convection in the groundwater filled annulus of a single U-tube borehole. Their method will be considered Section 4.2.1.2.

4.2 Methodology

The borehole thermal resistance can be defined in two ways; as the local borehole thermal resistance value, R_b, or as the effective borehole thermal resistance, R_b^*. A series of different values are needed to calculate the effective borehole thermal resistance which takes short circuiting resistance into account. The key values that must be calculated are R_a, R_{12}, and R_b. The calculation methods for these values vary depending on the assumptions made for the system configuration and backfill method.

The pipe configurations considered are single U-tube, double U-tube, and concentric as shown in Figure 4-1. The grey hatching in the figure indicates the backfilled portion of the borehole. The methods allow for the borehole to be backfilled with grout or a material of similar consistency. For single U-tubes a groundwater filled option is also considered.

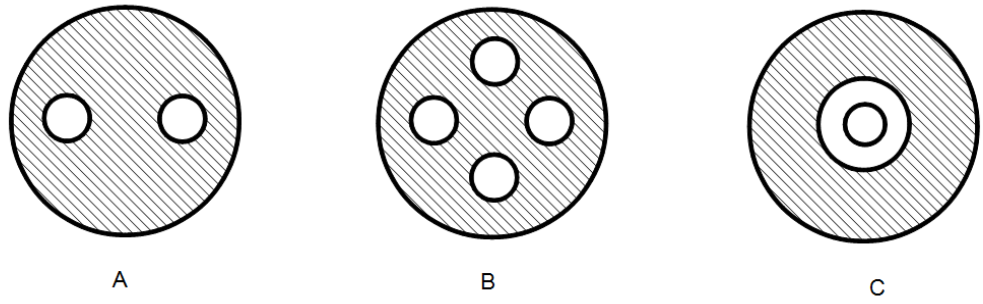

Figure 4-1: (A) Single, (B) double, and (C) concentric borehole configurations

4.2.1 Borehole Thermal Resistances

The local borehole thermal resistance R_b as defined by Hellström (1991, p.19) accounts for the convection at the pipe wall and the conduction through the pipe and borehole filling. Contact resistance between the various materials in the borehole can be neglected.

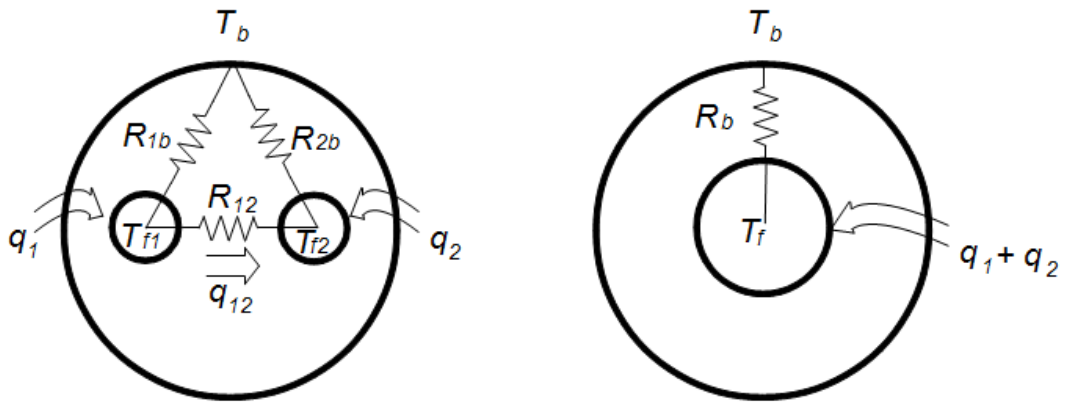

Figure 4-2: Single U-tube resistance network and simplification for a grouted borehole

Hellström (1991, §. 8.2.2) defines two main values that could be taken as the short circuiting resistance. These two values are R_a and R_{12}. The R_a value is the total resistance between the up and down flowing pipes in the borehole. This value can actually be measured experimentally with sufficient control. The resistance R_{12} however cannot be measured experimentally as it is

the theoretical network resistance between the up and down pipes assuming that heat only travels pipe to pipe and none is lost to the surroundings[4].

Hellström (1991 p. 79) defines R_a to be the equivalent resistance of the two parallel paths between the U-tube pipes.

$$\frac{1}{R_a} = \frac{1}{R_{1b} + R_{2b}} + \frac{1}{R_{12}} \tag{4.1}$$

Where R_{1b}, R_{2b}, and R_{12} are shown in Figure 4-2.

4.2.1.1 Grouted Boreholes, Multipole Method

The grouted borehole option is available for all of the borehole configurations shown in Figure 4-1. For single and double U-tube configurations the AMULTIPOLE function is used. This function uses the multipole method of Bennet et al. (1987). For concentric boreholes, the multipole method is not required and simple analytical methods suffice.

Single and Double U-Tube Boreholes

The multipole method developed by Bennet, Claesson, and Hellström (1987) computes the conductive heat flows to and between pipes within a set of concentric cylindrical regions. The inner concentric region models the borehole grout or backfill and the outer the surrounding soil. The two-dimensional heat transfer is modeled over a circular region perpendicular to the pipes with the boundary at the borehole wall of particular interest. It is at this boundary that the average borehole temperature is calculated.

The values for R_b and R_a for grouted boreholes are calculated using a modified version of the multipole code (Bennet et al. 1987). The modifications to the original code change the outputs of the program from system temperatures to resistance values. The GLHEPro program has used this

[4] Other values that Hellström also uses are R_{12}^{Δ} and R_{12}^{o}. Where R_{12}^{Δ} is the same as R_{12} used in this thesis.

method to calculate R_b for some time now (See Section 1.2.3) but it has only recently been modified to solve for R_a values.

R_b is calculated by setting the fluid in all U-tubes to the same positive temperature (T_f=10) and the ground or far field to a lower temperature (T_C=0). The 10th order multipole method is then applied to get the temperature effects on the ground at the borehole wall (*TPR* or T_{all}). Lower order multipole methods can provide reasonable results for many cases. Using the original 10th order multipole code, the borehole resistance can be calculated from the modeled fluid and borehole wall temperatures by adding the following equation:

$$R_b = \frac{T_f(1) - T_{all}}{\sum_{n=1}^{N_{pipes}} Q_n} \tag{4.2}$$

Where

R_b is the borehole thermal resistance, [°K m W^{-1}]

T_f is the average fluid temperature, [°C]

T_{all} is the borehole wall temperature due to the borehole temperature effects, [°C]

Q_n is the heat flux from the pipe, [W m^{-1}]

N_{pipes} is the number of pipes within the borehole

To get R_a from the fluid temperatures modeled by the multipole method, half of the pipes are set to $T_f(1)$=0.1 and the other half to $T_f(2)$=-0.1. The far field or undisturbed ground temperature is set to 0.

$$R_a = \frac{T_f(1) - T_f(2)}{\frac{N_{pipes}}{2}\, Q(1)} \tag{4.3}$$

Where

R_a is the equivalent resistance between the upwards and downwards flowing tubes, [°K m W^{-1}]

Other terms are defined in Equation 4.2

For a single and double U-tube the number of pipes, N_{pipes}, is 2 and 4 respectively. Figure 4-3(b) shows the layout of the pipes within the borehole and the sign of the temperatures applied for the R_a resistance calculations. For a single U-tube, only pipes 1 and 2 would be modeled as shown in Figure 4-3(a). Figure 4-3(c) shows the temperature assignments for a double U-tube with the U-tubes installed in series; this option is not currently available in GLHEPro V5.0. One of the inputs to the Multipole function is the Mode which indicates that either R_b (Mode=1) or R_a (Mode=2) should be calculated.

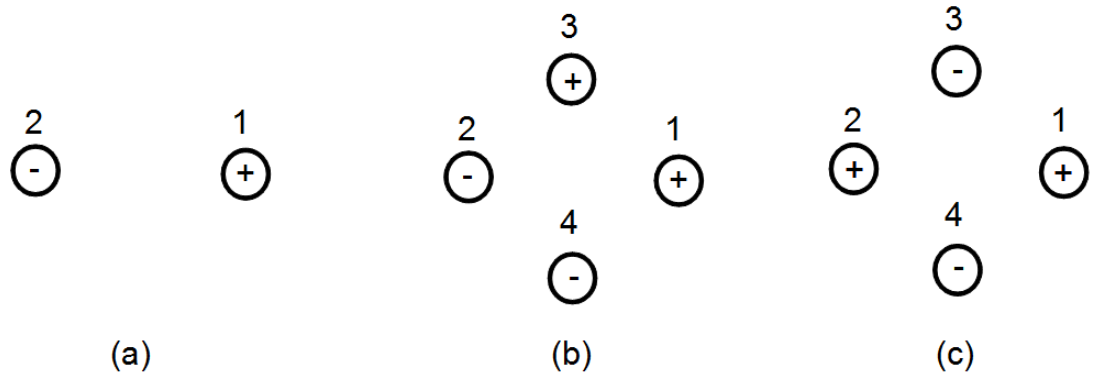

Figure 4-3: Pipe placement and sign of assigned temperature for R_a calculation (Mode=2)

Concentric Boreholes

For Concentric tubes the resistance calculations are fairly simple and the Multipole method is not required. Figure 4-4 shows a schematic for a concentric borehole and the associated resistance network. In the figure the T_{f1} indicates where the pipe flow occurs, the *a* or T_{f2} the annulus flow, and the *g* the grout. Because all the resistances are in series they can simply be summed up into the borehole resistance (R_b) and the short circuiting resistance (R_{12}) where R_{12} is equal to R_a.

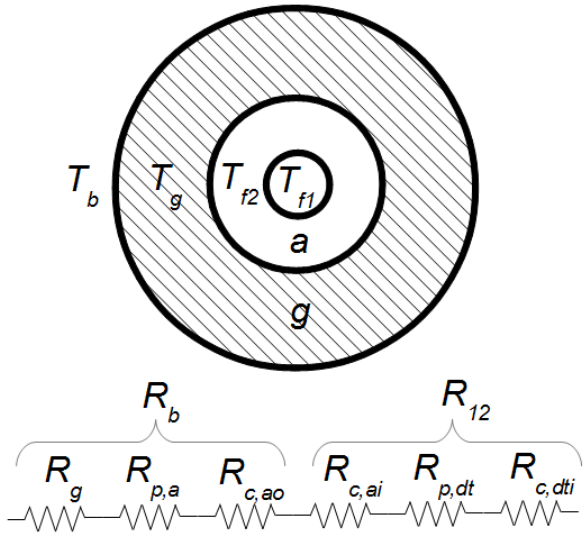

Figure 4-4: Concentric borehole and resistance network diagram

$$R_{12} = R_{c,dti} + R_{p,dt} + R_{c,ai} = \frac{1}{h_{ip}A_{ip}} + \frac{ln\left(\frac{OD_p}{ID_p}\right)}{2\pi k_p} + \frac{1}{h_{op}A_{op}} = R_a \qquad (4.4)$$

$$R_b = R_{c,ao} + R_{p,a} + R_g = \frac{1}{h_{oa}A_{ao}} + \frac{ln\left(\frac{OD_a}{ID_a}\right)}{2\pi k_p} + \frac{ln\left(\frac{2r_b}{OD_a}\right)}{2\pi k_g} \qquad (4.5)$$

Where

h is the convection coefficient [W m^{-2} K^{-1}]

A is the surface area per unit length [m]

k is the thermal conductivity [W m^{-1} K^{-1}]

OD is the outside diameter [m]

ID is the inside diameter [m]

The subscript *p* stands for pipe, *a* stands for annulus, *g* stands for grout, *c* stands for convection, *i* stands for inside, and *o* for outside. The convection coefficient for inside the inner pipe is calculated using the Nusselt number from Gnielinski's correlation (Cengel and Ghajar 2011). For both of the surfaces in the concentric annulus, h_{op} and h_{oa}, the convection coefficients can be calculated by:

$$h = \frac{Nu \cdot k}{d_h} \tag{4.6}$$

Where

Nu is the Nusselt number for the given surface, either Nu_{oo} or Nu_{ii}

k is the fluid thermal conductivity [W m^{-1} K^{-1}]

d_h is the hydraulic diameter, [m]

$$d_h = ID_{op} - OD_{ip} \tag{4.7}$$

Where

ID_{op} is the inner diameter of the outer pipe [m]

OD_{ip} is the outer diameter of the inner pipe [m]

For the annulus, Hellström (1991, p67-71) gives correlations for Nusselt numbers for the flows along the outer (Nu_{oo}) and inner (Nu_{ii}) surfaces of the annulus in the laminar region:

$$Nu_{ii} = 3.66 + 1.2(r^*)^{-0.8} \tag{4.8}$$

$$Nu_{oo} = 3.66 + 1.2(r^*)^{0.5} \tag{4.9}$$

Where

r^* is the ratio of the outside diameter of the inner pipe to the inside diameter of the outer pipe

For fully turbulent flow, Incropera and DeWitt (2002 p470) give that, for a first approximation, the inner and outer convection coefficients can be assumed to be equal. They suggest that the Dittus-Boelter equation be evaluated using the hydraulic diameter.

$$Nu_{ii} = 0.023Re^{0.8}Pr^{0.35} \tag{4.10}$$

$$Nu_{oo} = Nu_{ii} \tag{4.11}$$

Where

Re is the Reynolds number for the annulus flow calculated using the hydraulic diameter given in equation 4.7

Pr is the Prandtl number for the annulus flow

For this particular case the Prandtl number is raised to 0.35 rather than the 0.3 or 0.4 recommended for cooling or heating respectively. This is because a ground heat exchanger will not be used exclusively in heating or cooling.

4.2.1.2 Groundwater Filled Boreholes

The method for getting the borehole resistance for groundwater filled boreholes is similar in practice to that of grouted boreholes but is better approximated by a wye (Y) resistance circuit as shown in Figure 4-5 than the traditional delta circuit. This allows the convective resistance at the borehole wall to be considered as a single resistance value (R_{BHWc}). For symmetric boreholes the resistance from the circulating fluid in each pipe to the water in the annulus, R_{1p} and R_{2p}, are assumed to be equal. This gives:

$$R_{1p} = R_{2p} = R_{poc} + R_{pc} + R_{pic} \tag{4.12}$$

The borehole resistance, R_b, is then:

$$R_b = R_{BHWc} + \frac{R_{1p}}{2} = R_{BHWc} + \frac{R_{poc} + R_{pc} + R_{pic}}{2} \tag{4.13}$$

$$R_{12} = R_a = 2R_{1p} = 2\left(R_{poc} + R_{pc} + R_{pic}\right) \tag{4.14}$$

Where

R_{poc} is the convective resistance outside the U-tube pipe [K W^{-1} m]

R_{pc} is the conductive resistance through the pipe wall [K W^{-1} m]

R_{pic} is the convective resistance inside of the pipe [K W^{-1} m]

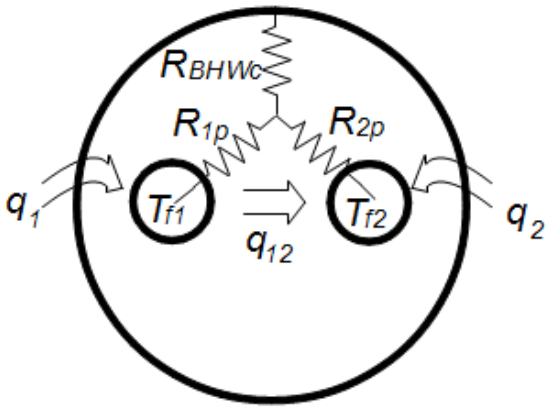

Figure 4-5: Wye resistance network for groundwater filled boreholes

The conductive pipe resistance, R_{pc}, is calculated by:

$$R_{pc} = \frac{\ln\left(\frac{r_{po}}{r_{pi}}\right)}{2\pi k_p} \tag{4.15}$$

Where

r_{po} is the outside pipe radius [m]

r_{pi} the inside pipe radius [m]

k_p the pipe's thermal conductivity [W m^{-1} K^{-1}]

The convection resistances are calculated from the convection coefficients *h* and the heat transfer areas for each surface.

$$R_{pic} = \frac{1}{2\pi r_{pi} h_{pic}} \tag{4.16}$$

$$R_{poc} = \frac{1}{2\pi r_{po} h_{poc}} \tag{4.17}$$

$$R_{BHWc} = \frac{1}{2\pi r_b h_{BHW}} \tag{4.18}$$

Where

h is the convection coefficient [W $m^{-2}K^{-1}$]

r_b is the borehole radius [m]

Other terms are defined in equations 4.13-4.15

The convection coefficient for the inner pipe is simply:

$$h_{pic} = \frac{Nu_{pi} \cdot k}{2 \cdot r_{pi}} \tag{4.19}$$

For both of the surfaces in the annulus, h_{poc} and h_{BHW}, the convection coefficients can be calculated by:

$$h = \frac{Nu \cdot k}{D_H} \tag{4.20}$$

Where

Nu is the Nusselt number for the given surface

k is the fluid thermal conductivity [W m^{-1} K^{-1}]

D_H is the hydraulic diameter [m]

The hydraulic diameter of the annulus is used as the length scale for the correlations.

$$D_H = \frac{4\pi\left(r_b^2 - N_P r_{po}^2\right)}{2\pi(r_b + N_P r_{po})} \tag{4.21}$$

Where

r_b is the borehole radius[m]

r_{po} is the outside radius of the inner pipe [m]

N_P is the number of pipes in the borehole

The Nusselt numbers are calculated with a series of correlations that were developed by Spitler et al. (2016) from data taken from a single, well instrumented groundwater filled borehole with a single U-tube. The data was collected over the course of several years. The resulting resistances were then validated against the measured thermal resistances for several locations in Norway and Sweden. These correlations are:

$$Nu_{po} = 0.30\left(Ra_{po}^*\right)^{0.25} \qquad 1.8E6 < Ra_{po}^* < 4.1E7 \tag{4.22}$$

$$Nu_{BHW} = 0.20(Ra^*_{BHW})^{0.25} \qquad 5.4E5 < Ra^*_{po} < 2.9E7 \tag{4.23}$$

The correlations for the Nusselt numbers were created so that they are only functions of the modified Rayleigh number, *Ra**.

$$Ra^*_{po} = \frac{g\beta q^{"}_{po} D_H^4}{k_w v_w \alpha_w} \tag{4.24}$$

$$Ra^*_{BHW} = \frac{g\beta q^{"}_{BHW} D_H^4}{k_w v_w \alpha_w} \tag{4.25}$$

Where

β is the volumetric thermal expansion coefficient for water [K^{-1}]

q'' is the heat transfer rate at the given surface [W m^{-2}]

k_w is the water conductivity [W m^{-1} K^{-1}]

v_w the waters kinematic viscosity [m^2 s^{-1}]

α_w is the thermal diffusivity of the water [m^2 s^{-1}]

v_w is the kinematic viscosity of the water [m^2 s^{-1}]

g is the gravitational constant, 9.81 [m s^{-2}]

Each surface has a unique heat extraction *q''*. The fluid thermal properties are evaluated at the film temperatures for the fluid near the respective surface. The film temperature can be calculated as the average of the surface temperature and the fluid temperature. For the outside of the U-tube pipes the heat extraction used is for both pipes. In general:

$$q" = \frac{q}{A_{surface}} \tag{4.26}$$

Where

$A_{surface}$ *is* the surface area of the surface of interest on an area per meter length of borehole basis [m^2 m^{-1}]

q is the heat rejection rate of the borehole [W m^{-1}]

The short circuiting resistance values for groundwater filled boreholes are very dependent on the heat flux of the system. For typical systems the heat flux, or heat transfer rate, is not constant and varies throughout the day and throughout the year. The heat transfer rate does have a large effect on the short circuiting so during sizing routines it will fluctuate along with the sized borehole depth if it were to be recalculated on a per time step basis. The current method implemented in GLHEPro V5.0 recalculates the effective borehole resistance each iteration during sizing but uses the heat flux that was specified in the initial calculation for the entire simulation; therefore, the heat flux to be used in the initial calculation must be carefully selected.

Selecting the heat transfer rate (W/m) within GLHEPro presents several options. The user can specify whether the system is heating or cooling constrained. The concept of the design being constrained as opposed to dominated is used because a system can be cooling dominated and still have the GHE size be based on the minimum entering fluid temperature to the heat pump or vice versa. Heating dominated systems are ones that extract more heat from the ground than they reject to the ground on an annual basis. The reverse is true for a cooling dominated system. A heating constrained system is typically sized such that it reaches the minimum temperature constraint specified for the system design.

An example of a cooling dominated and heating constrained system is the installation in Stillwater, Oklahoma, implemented by Hern (2004). Details on the installation can be found in Section 3.3.1.4 and Table 3-2. The sizing temperature constraints on the fluid temperature are from 10-32°C (50-90°F). Figure 4-6 shows the temperature responses for one year for the sized

system simulation. For this specific case the minimum temperature constraint is reached. This could be caused either by the effects of the ground temperature or the temperature limits applied during the sizing routine.

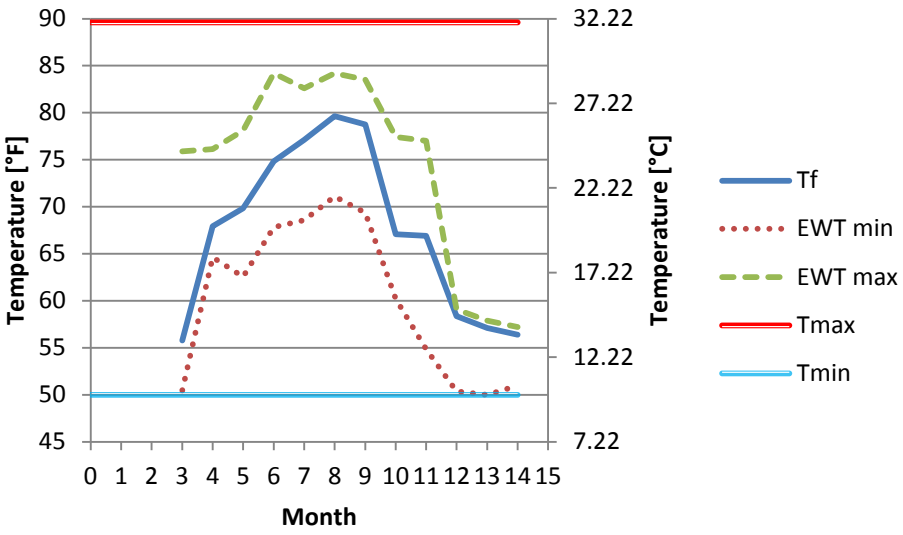

Figure 4-6: Example of a cooling dominated heating constrained system. (Hern 2004)

Once the heating/cooling constraint has been selected the peak load needed to calculate the short circuiting resistances for a groundwater filled single U-tube borehole must be found. The value used is the maximum peak load applied to the system. This value is found by calculating the total peak loads for each month and selecting the maximum value that corresponds to the selected heating/cooling constraint. The method for calculating the peak heat flux in W/m is:

$$q_{max} = \frac{1000}{H * NB} \max\left([pkLoad_{GLHE} + C_{HP} * pkLoad_{HP}]_{monthly}\right) \quad (4.27)$$

Where

H is the borehole depth [m]

NB is the number of boreholes

C_{HP} is the heat pump loads coefficient

pkLoadGLHE is the peak load on the GLHE [kW h^{-1}]

pkLoadHP the corresponding peak load on the heat pump [kW h^{-1}]

The heat pump loads coefficient (C_{HP}) is taken from the simple heat pump model used in GLHEPro. It is essentially the ratio of the heat rejection or extraction rate to or from the ground to the load met by the heat pump. GLHEPro models the heat pump using a simple correlation based on the heat pump properties and the entering fluid temperature to the heat pump (Spitler 2000).

4.2.2 Effective Borehole Resistance

The borehole resistance values, R_a and R_b, derived in Section 4.2.1 can now be used to get the effective borehole resistance. There are two main assumptions that can be made during the effective borehole thermal resistance calculations. Either the borehole wall temperature or the heat flux of the system is assumed to be uniform. For cases where the short circuiting is higher the uniform borehole wall temperature is held to be the better assumption (Spitler et al. 2016) but in many cases the two methods get similar results, thus the option to use the mean of the two methods has been included in GLHEPro V5.0 as an alternative option. If short circuiting is selected it will be automatically recalculated from saved R_a, R_b, and R_{12} values before each simulation and each sizing iteration in order to account for the effects of changing borehole depth.

4.2.2.1 Uniform Borehole Wall Temperature

Claesson and Hellström (2011) derive the effective borehole resistance from the general solution of a series of coupled equations for the axial fluid temperature balance of the borehole.

Assuming that borehole wall temperature is uniform the coupled equations can be solved with Laplace transforms resulting in:

$$R_b^* = R_b \eta * \coth(\eta) \tag{4.28}$$

$$\eta = \frac{H}{\rho_f c_f V_f} \frac{1}{2R_b} \sqrt{1 + 4\frac{R_b}{R_{12}}} \tag{4.29}$$

Where

η is the correction for the variation in the fluid temperature along the flow channels

H is the borehole depth [m]

ρ_f is the fluid density [kg/m^3]

c_f is the fluid specific heat capacity [kJ/K-kg]

V_f is the fluid volumetric flow rate [m^3/s]

For groundwater filled boreholes it is assumed that R_a is equal to R_{12}. For grouted boreholes the value of R_{12} cannot be calculated using the multipole method so it must be found by solving for the value in the delta resistance network as shown in Figure 4-2. This gives:

$$R_{12} = R_a \frac{R_{1b} + R_{2b}}{R_{1b} + R_{2b} - R_a} \tag{4.30}$$

This equation can be simplified for by making the assumption that $R_{1b}=R_{2b}$ and that $R_{1b}=2R_b$. This assumption is based on a simplification that is applied during the calculation of R_b when R_{12} is initially neglected and R_{1b} and R_{2b} are assumed to be equal and in parallel. So this gives:

$$\frac{1}{R_b} = \frac{1}{R_{1b}} + \frac{1}{R_{2b}} = \frac{2}{R_{1b}} \tag{4.31}$$

This changes the calculation of R_{12} to:

$$R_{12} = R_a \frac{4R_b}{4R_b - R_a} \tag{4.32}$$

As a result, it is possible for the value of R_{12} to be negative when $R_a > 4R_b$. This tends to occur as the spacing between the U-tube pipes increases past 2/3 of the maximum allowable spacing between the pipes, where the maximum allowable spacing is defined by the maximum amount of space available in the borehole. This negative resistance value causes no issues in calculations where the value of R_{12} is required. The negative R_{12} values can be explained by heat transfer between the tubes around the outside of the borehole. Within the calculations there are no issues because R_{12} must be between zero and $-4R_b$ to cause an error in equation 4.29; R_{12} has a vertical asymptote where $R_a = 4R_b$ due to the nature of equation 4.32 so it is very unlikely that it will ever cause an error.

4.2.2.2 Uniform Heat Flux

The uniform heat flux assumption also uses the series of coupled equations for the axial fluid temperature balance to solve for the effective borehole resistance (Claesson and Hellström 2011). Basic algebra and integration are sufficient to solve the system of equations such that:

$$R_b^* = R_b + \frac{1}{3R_a}\left(\frac{H}{\rho_f c_f V_f}\right)^2 \tag{4.33}$$

Where

ρ_f is the fluid density [kg/m^3]

c_f is the fluid specific heat capacity [kJ/K-kg]

V_f is the fluid volumetric flow rate [m^3/s]

Other terms are defined in Equation 4.29

Both the values of R_b and R_a can be found for the respective borehole filling as detailed in Section 4.2.1.

4.3 Results

For select cases the effects of applying the short circuiting resistance to a system are considered. The thermal resistance values considered are the local borehole thermal resistance (R_b), the effective borehole thermal resistance assuming a uniform borehole wall temperature ($R^*_{b,UWT}$) or a uniform heat flux ($R^*_{b,UHF}$), and the mean effective borehole thermal resistance ($R^*_{b,mean}$).

Two main factors in the calculation of the effective thermal resistance for grouted and groundwater filled boreholes are considered: the borehole length and the fluid mass flow rate in the borehole tubes. For each of these cases the effects of varying the flow rate in the borehole and the length of the borehole are considered. Systems with long boreholes or low flow rates are more likely to see significant short circuiting effects, to the extent that for typical North American installations the short circuiting effects are negligible. The base case used for these comparisons is shown in Table 4-1.

Table 4-1: Example system definition for short circuiting resistance results

Variables		
Configuration	Single U-tube	
Borehole depth, m (ft)	128	(419.9)
Borehole diameter, mm (in.)	110	(4.3)
U-tube inner diameter, mm (in.)	21.82	(0.9)
U-tube outer diameter, mm (in.)	26.67	(1.1)
Shank spacing, mm (in.)	18.87	(0.7)
Undisturbed Ground Temperature, °C (°F)	9.6	(49.3)
Total System flow rate, L/s (GPM)	0.38	(6.0)
Fluid Type*	Propylene Glycol	
Concentration, %	15	
Mean Fluid Temperature, °C (°F)	20	(68.0)
Ground Thermal Conductivity, W/m-K (Btu/hr-ft-°F)	2.42	(1.40)
Grout Thermal Conductivity, W/m-K (Btu/hr-ft-°F)	0.744	(0.43)
Pipe Thermal Conductivity, W/m-K (Btu/hr-ft-°F)	0.39	(0.23)
Ground Volumetric Heat Capacity, kJ/m^3-K (Btu/ft^3-°F)	2343	(34.94)
Grout Volumetric Heat Capacity, kJ/m^3-K (Btu/ft^3-°F)	3901	(58.17)
Pipe Volumetric Heat Capacity, kJ/m^3-K (Btu/ft^3-°F)	1542	(23.0)

The borehole in this example was sized for a system with a peak cooling load of 2 tons. Therefore general design recommendations suggest that the flow rate for this system should be greater than 5.25 GPM based on 2.5 GPM per ton of heating or cooling needed. A brief review of heat pump literature suggests that the allowable range of flow rates for a 2 ton heat pump is from approximately 1.2 to 6 GPM. A wider range of flow rates have been considered in order to consider all of the flow regimes from laminar to turbulent.

4.3.1 Short Circuiting in Grouted Boreholes

The first case is for a borehole with a fixed length or depth of 420 ft (128 m) and a flow rate that varies from 0.5 to 7 GPM. At least two data points were considered for each flow regime. Figure 4-7 shows the change in the resistance values as the flow rate within the borehole changes. Within the turbulent regime, which occurs when the flow rate is greater than 2 GPM for this case, the effective borehole resistance (R_b^*) is less than 14% different than the borehole resistance (R_b), with the maximum difference occuring just after the transition region.

There is a sudden change in the borehole resistance (R_b) around when the flow rate is 1 GPM; this is due to the transition between the laminar and turbulent reigmes. Gnielinski's method is used to get the Nusselt numbers in the turbulent region (Cengel and Ghajar 2011, page 489; OSU 2016b). In the transition region, linear interpolation between the constant laminar Nusselt Numbers and the lower limit of Gnielinski's correlation is used. This transition also has a slight affect on the effective resistance over the same region.

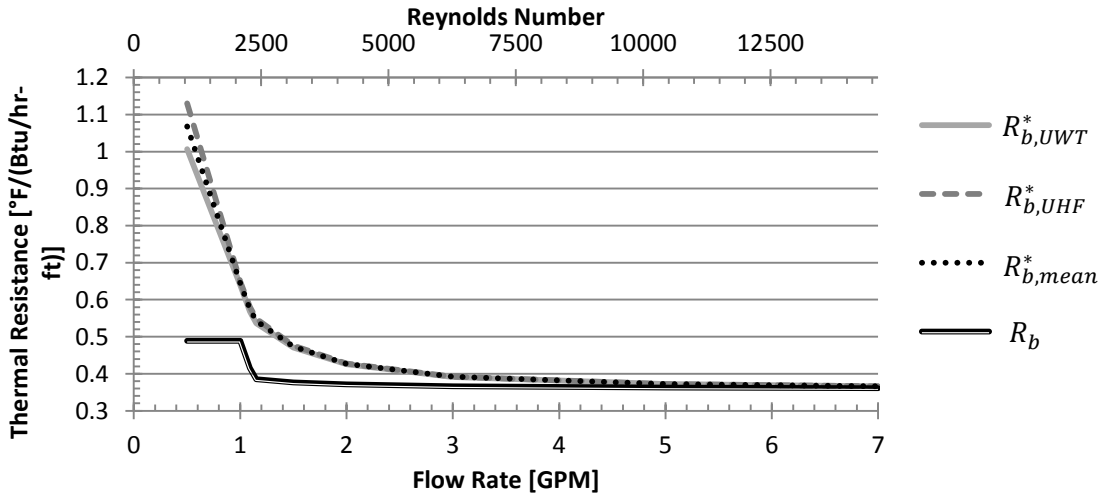

Figure 4-7: Comparison of the borehole resistance and effective borehole resistance with varying flow rate for a 420 ft deep grouted borehole

For a similar case with a fixed borehole depth of 1312 ft (400 m) the results are shown in Figure 4-8. This indicates that as the borehole depth increases the borehole thermal resistance (R_b) will remain the same but the effective borehole resistance (R_b^*) will increase. To further investigate

these effects, the resistances for a single borehole with a length ranging from 100 to 1000 feet (30 to 305 m) are considered in Figure 4-9.

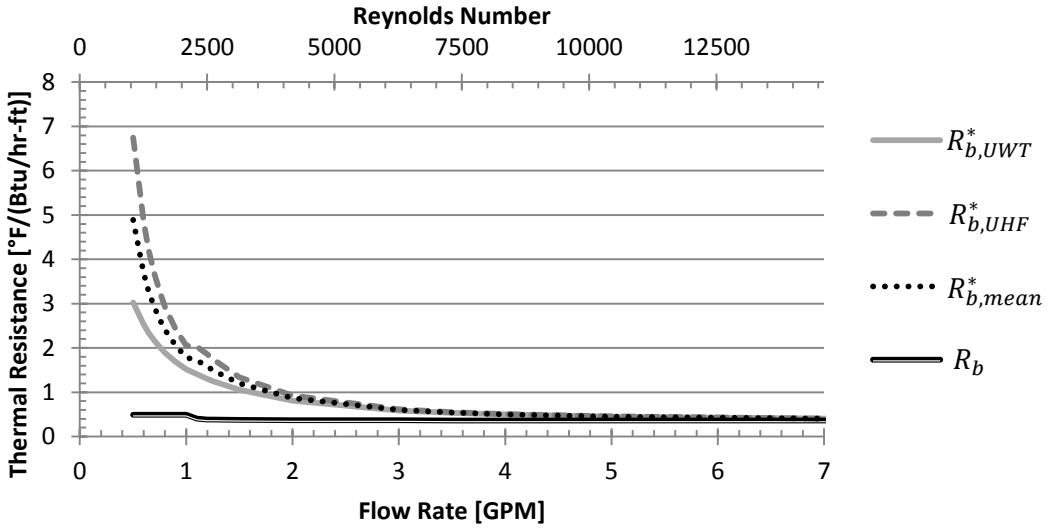

Figure 4-8: Comparison of the borehole resistance and effective borehole resistance with varying flow rate for a 1312 ft deep grouted single U-tube borehole

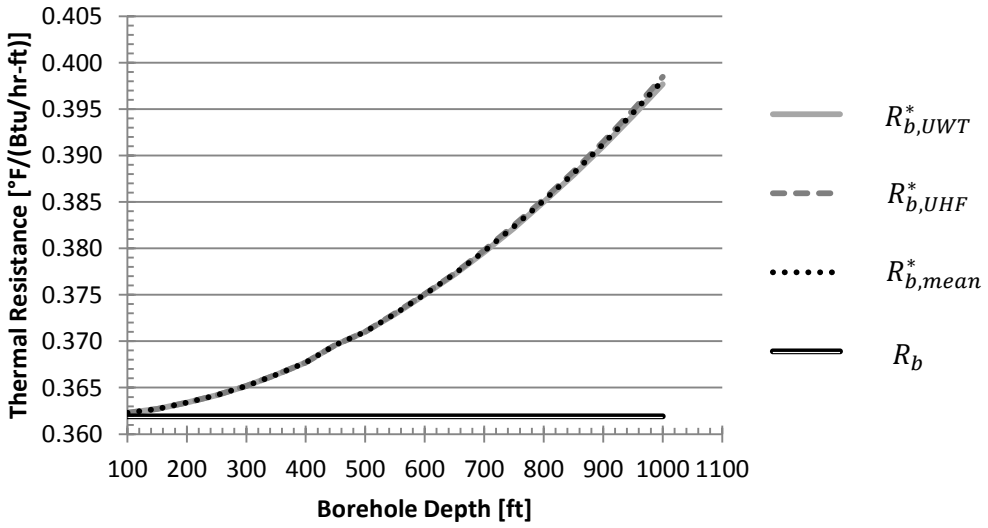

Figure 4-9: Comparison of the borehole resistance and effective borehole resistance with varying borehole depths and a flow rate of 6 GPM with a grouted single U-tube borehole

For Figure 4-9 the system flow rate is maintained at 6 GPM (0.38 L/s), keeping the flow firmly in the turbulent regime (Re=12577). This demonstrates that the short circuiting effects increase as the length or depth of the borehole increases, regardless of the flow regime. In this case the flow

rate is great enough that there is very little difference between the different effective resistance calculation methods; on the order of .2% difference maximum occurring at the longest borehole depth considered (1000 ft). The difference between R_b and R_b^* at this point is approximately 9.5 %.

A system that was actually sized to have a 1000 foot deep borehole would have different loads on the heat pump and a different system flow rate. A 5 ton unit rather than a 2 ton would be appropriate for a 1000 ft borehole and the system should operate between 2.9 to 14 GPM based on heat pump literature provided by manufacturers for units of this size. Using a flow rate of 12.3 GPM and a system depth of 1000 ft, the difference between R_b and R_b^* is 2.4%. This is significantly less than the 9.5% found previously with a system flow rate of 6 GPM.

A double U-tube borehole with the same variations in system flow rate and the same system dimensions as the 1312 ft (400m) deep single U-tube case gets a lower borehole thermal resistance as shown in Figure 4-10. The vertical axis is plotted in log scale to make the convergence of the resistance and effective resistance as the flow increases more apparent. The double U-tube assumes that the two U-tubes are installed in parallel, thus the flow rate through the tubes in the double U-tube is half of what is seen in the single U-tube for the same system flow rate.

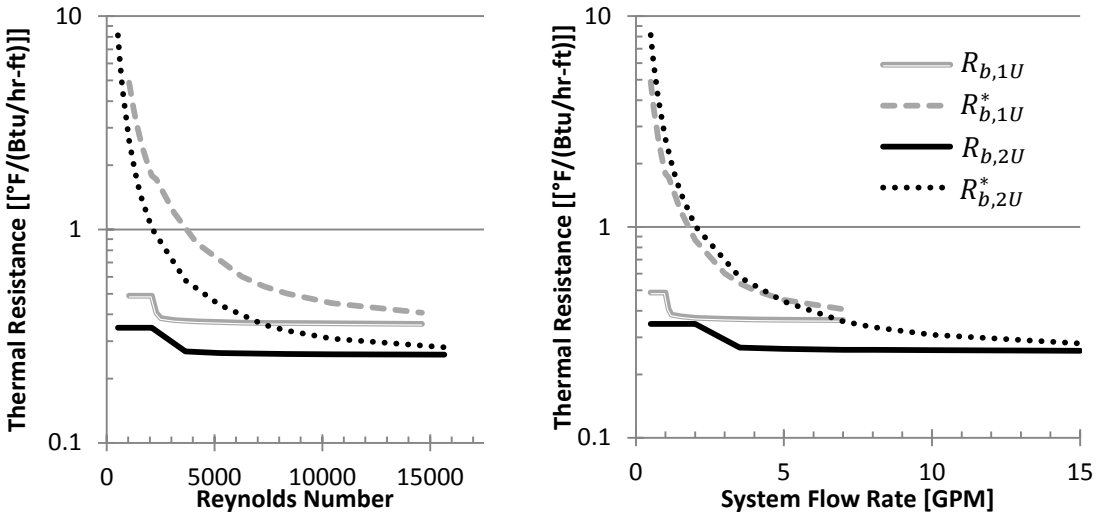

Figure 4-10: Comparison of R_b and R_b^*, mean for a Single U-tube (1U) and Double U-tube (2U) borehole

If instead the thermal resistance is plotted against the flow rate through the tubes, rather than the system, you get the values shown in Figure 4-11 for the single and double U-tubes.

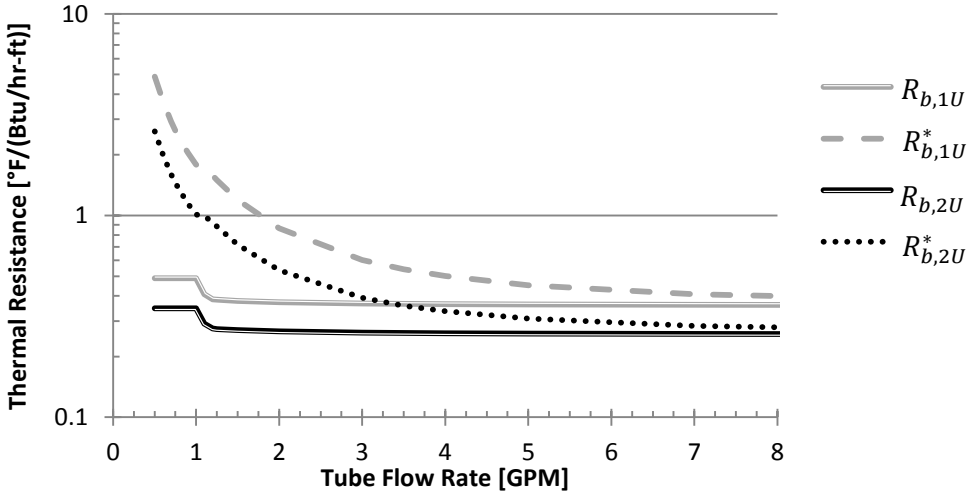

Figure 4-11: Comparison of R_b and R_b^*, mean for a Single U-tube (1U) and Double U-tube (2U) borehole

The concentric borehole case considered uses the same system fluid and thermal properties as shown in Table 4-1. The inner tube is a 2 inch SDR-11 pipe and the outer a 4 inch SDR-11 pipe. The concentric borehole shows a similar response to changing flow rate as the U-tube configurations but has two discontinuities: one where the inner pipe transitions from laminar to

turbulent and another where the annulus transitions. The first transition is visible in Figure 4-12 on the effective borehole resistance curves (R_b*) about where the system flow rate is 2.3 GPM. The second occurs between the flow rates of 7.5 and 8 GPM along the thermal resistance curve (R_b). As the system flow rate continues to increase the borehole thermal resistance and effective borehole resistance will converge.

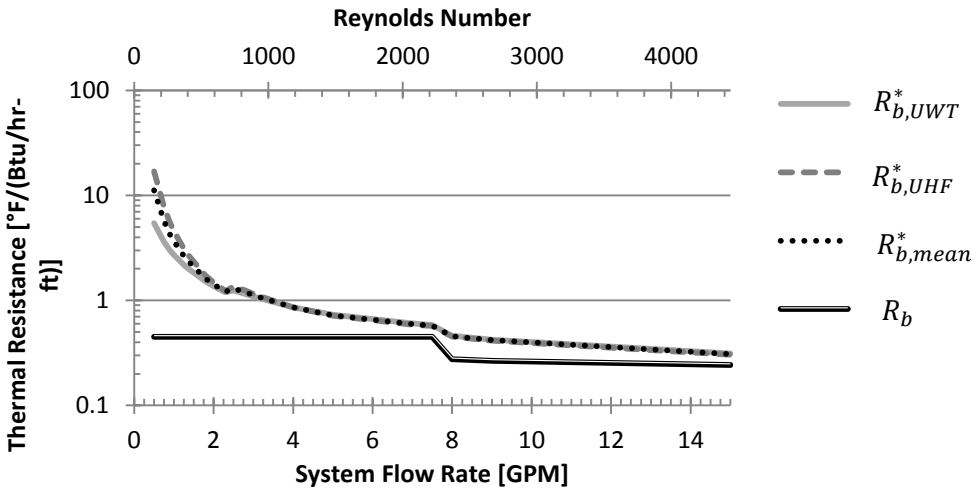

Figure 4-12: Comparison of the borehole resistance and effective borehole resistance with varying flow rate for a 1312 ft deep grouted concentric borehole

4.3.2 Short Circuiting in Groundwater Filled Boreholes

For groundwater filled boreholes the effective resistance is also a function of the loads on the system. A more complete system definition, including the loads on the heat pump, is included in Appendix B. As described in Section 4.2.1.2, to get the effective borehole resistance for a groundwater filled borehole the loads on the system must be defined as either heating or cooling constrained. There is no simple way of determining whether a system is heating constrained or cooling constrained without first attempting to simulate the system temperatures. The system shown in Table 4-1 and Appendix B is both heating dominated and heating constrained. Thus,

the maximum short circuiting will be caused by the heating loads placed on the GLHE and will occur when the system temperatures are at a minimum.

The effects of varying the system flow rate for a groundwater filled borehole are similar to that of a grouted borehole. Figure 4-13 shows that the difference between the borehole thermal resistance and the effective borehole resistance is most significant in the transient and laminar flow regions. A small but significant change in the effective borehole thermal resistance occurs as the flow through the tubes transitions from laminar to turbulent. At the lower edge of the turbulent flow regime (Flow rate ≈2 GPM), the percent difference between the borehole resistance (R_b) and the mean effective borehole resistance ($R^*_{b,mean}$) gets as high as 65%.

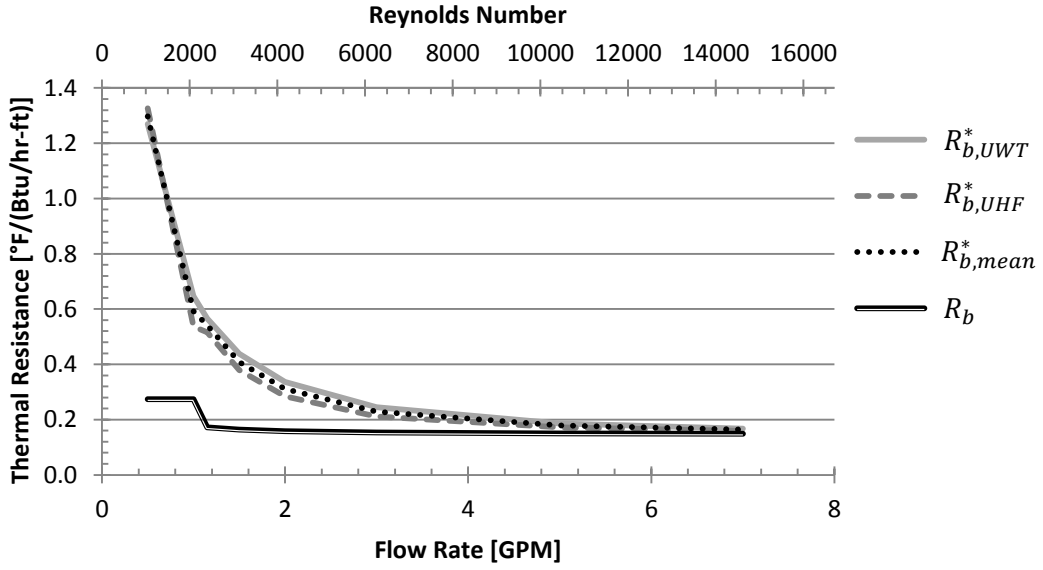

Figure 4-13: Comparison of the borehole resistance and effective borehole resistance with varying flow rate for a 420 ft deep groundwater filled borehole

Figure 4-14 shows the effects of varying the depth or length of the borehole while maintaining a system flow rate of 6 GPM (0.38 L/s). The difference between the two effective resistance calculation methods ($R^*_{b,UWT}$ and $R^*_{b,UHF}$) is approximately 15% with a 1000 ft deep borehole. The difference between the uniform borehole wall temperature and the uniform heat flux methods

is likely to continue increasing as the borehole length increases. This is due in part to the continued increase of the borehole thermal resistance (R_b) of the groundwater filled borehole.

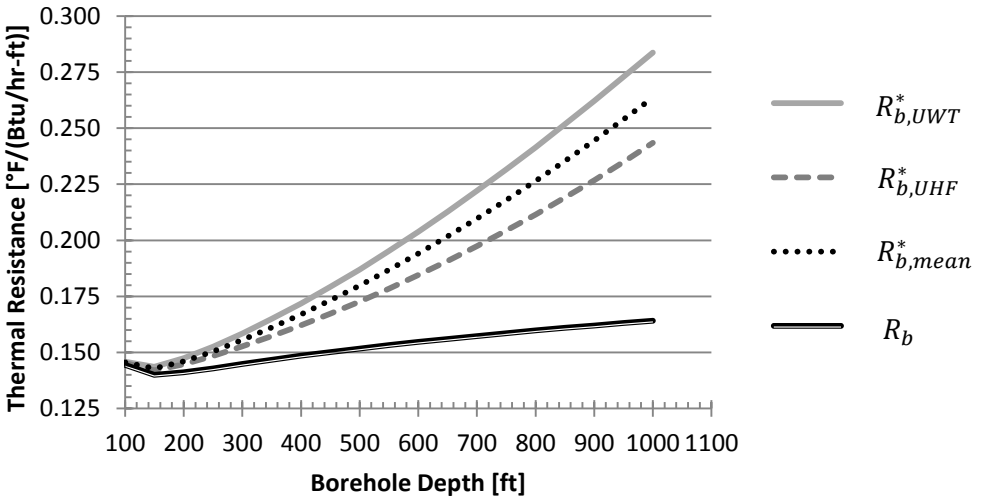

Figure 4-14: Comparison of the borehole resistance and effective borehole resistance with varying borehole depths and a flow rate of 6 GPM with a groundwater filled borehole

4.4 Conclusions

Ground heat exchangers with long boreholes or flow rates through the boreholes in or near the laminar flow range tend to show noticeable short circuiting effects. Ground heat exchangers for typical North American GSHP systems, however, are designed such that the short circuiting effects are negligible.

In general, groundwater filled boreholes tend to have a lower borehole resistance and to be more susceptible to short circuiting effects. Grouted and groundwater filled boreholes both follow similar trends with the short circuiting effects increasing as the flow rate decreases and as the borehole length increases.

For grouted boreholes, there is no significant difference between the uniform borehole wall temperature assumption and the uniform heat flux assumption, especially in the turbulent flow

regime. However for groundwater filled boreholes, in cases where there is significant short circuiting, the uniform borehole wall temperature approximation provides a significantly more accurate result (Spitler et al. 2016).

CHAPTER V

IMPROVED USE OF LIBRARY G-FUNCTIONS

5.1 Interpolation between library values of *B/H*

GLHEPro uses g-functions calculated using the methods of Eskilson and Claesson (Eskilson 1987a). Each g-function value has a corresponding dimensionless time value, $ln(t/t_s)$, that is used to reference when the g-function is applicable. The dimensionless time is discussed in more detail in Section 1.2.4. In order to make it possible to use the g-functions for design purposes they are stored inside the program in tables for each configuration. Each configuration contains a full set of g-function values for several borehole spacing to depth (*B/H*) ratios. This greatly reduces the simulation time but does introduce the possibility of interpolation error when the *B/H* ratio of the GHE does not exactly match one of the tabulated values. Figure 5-1 shows a plot of the tabulated g-function values for the 10 x 10 rectangular borehole configuration. The markers indicate the actual tabulated values.

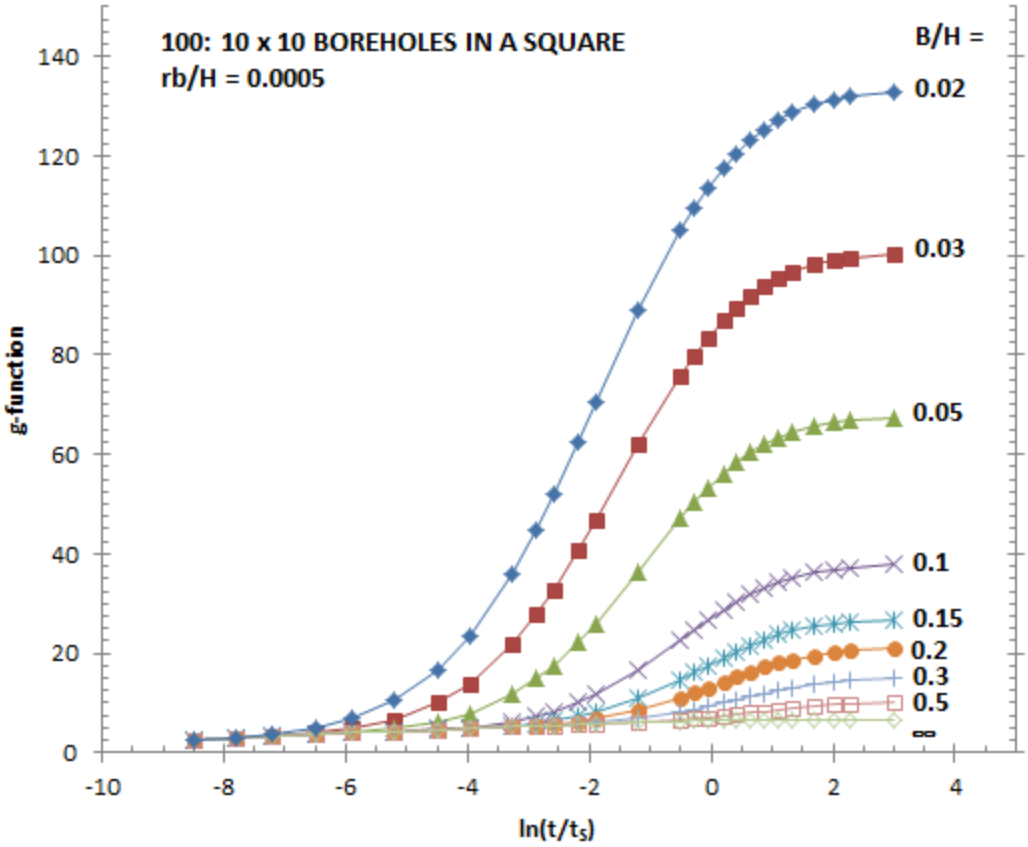

Figure 5-1: Eskilson's g-functions for a 10 x 10 borehole configuration with r_b/H=0.0005

5.1.1 Methodology

The g-function values for each configuration are tabulated with respect to the borehole spacing to active depth ratio, *B/H*. Typically systems have a *B/H* value between 0.05 and 0.1. All of the data sets have a borehole radius to depth ratio of 0.0005. GLHEPro uses logarithmic interpolation and extrapolation to get a set of g-functions for a given *B/H* value and then applies a simple correction for the actual system borehole radius to depth ratio. The equation used in GLHEPro V4.0 and older versions is:

$$g = g_1 + \frac{(g_2 - g_1)\left(\ln(B/H) - \ln\left(B/H_1\right)\right)}{\ln\left(B/H_2\right) - \ln\left(B/H_1\right)} \quad (5.1)$$

Where

g is the g-function value

B/H the borehole spacing to depth ratio corresponding to each g-function set

With the borehole radius correction applied the corrected g-function value is:

$$g_{corrected} = g - \ln\left(\frac{r_b}{0.0005\ H}\right) \quad (5.2)$$

Where

r_b is the borehole radius

H the active borehole depth

This corrected g-function is the final value that is used in all of the standard vertical borehole simulations within GLHEPro.

Malayappan and Spitler (2013) discovered that the method of interpolation used on the g-functions introduced an error to the simulation results due to the overestimation of the g-function values by as much as 4%. This 4% overestimation in the g-functions could lead to a 4% sizing error as may be inferred by the results in Figure 5-2 for a 10 x 10 borehole configuration. Figure 5-2 shows the sizing error between the Finite Line Source (FLS) procedure and the interpolated library g-functions. The "sag" between the non-interpolated points represents the sizing error due to interpolation.

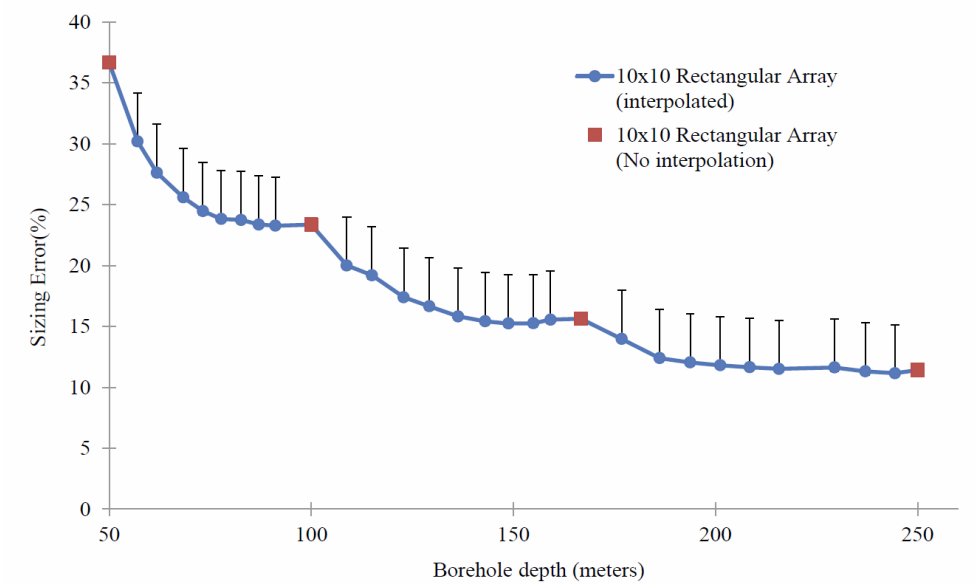

Figure 5-2: Sizing error due to interpolation, reprinted with permission from Malayappan and Spitler (2013)

Some investigation into the existing interpolation methods showed that there were issues with both the interpolation and extrapolation of the g-functions in GLHEPro. First the issues with interpolation will be considered.

The g-functions are tabulated for *B/H* values of 0.02, 0.03, 0.05, 0.1, 0.15, 0.2, 0.3, and 0.5 as shown in Figure 5-3. To check the accuracy of the current interpolation method it should be possible to replicate a given data set by interpolating between the neighboring curves. The results of this interpolation are shown in the following graph where the smooth curves represent the tabulated data and the dashed curves the values interpolated with Equation 5.1.

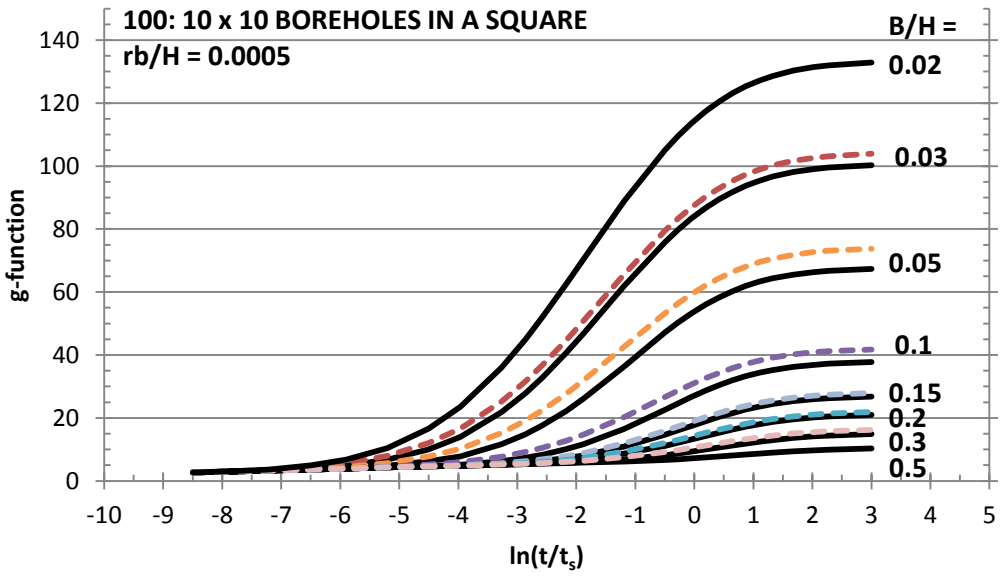

Figure 5-3: Tabulated and interpolated g-function values for a 10 x 10 borehole array using the original method of interpolation

An alternative interpolation method considered is to use the logarithmic value of both terms. This method is referred to as the "LogLog" method in the results and discussion. This method has been implemented in GLHEPro V5.0.

$$g = \exp\left(ln(g_1) + \frac{(ln(g_2)-ln(g_1))(ln(B/H)-ln(B/H_1))}{ln(B/H_2)-ln(B/H_1)}\right) \quad (5.3)$$

Where the terms are defined in Equations 5.1 and 5.2

5.1.2 Results and Discussion

Applying the logarithm to both terms in the interpolation results in a slight underestimation for the smaller *B/H* values and a slight overestimation of the larger *B/H* correlations as can be seen in Figure 5-4 below. For cases with *B/H* greater than 0.1 the interpolated curves lay on top of the tabulated data to the point that it is difficult to discern the difference between the two curves. This method shows visible improvement over the original method when considering the g-function plots, especially for the case where *B/H*=0.05.

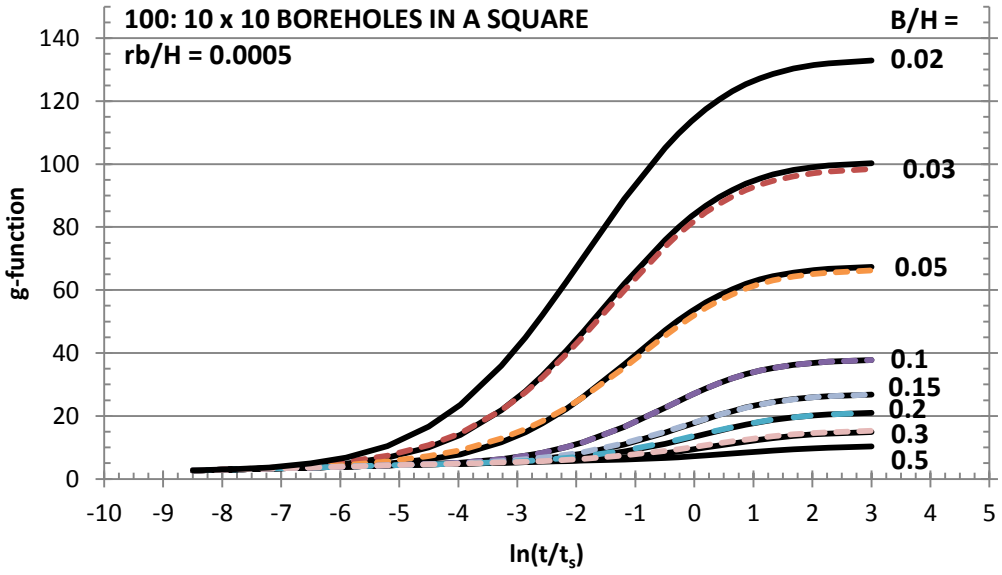

Figure 5-4: Tabulated and interpolated g-function values for a 10 x 10 borehole array using the "LogLog" method of interpolation

The root mean squared error (*RMSE*) on the percent error for all sets of g-functions in the 10 x 10, 5 x 6, and 2 x 5 borehole configurations were calculated as a means of directly comparing the two methods. Table 5-1 gives the results of the *RMSE* on the percent error for each data point in the configuration and the mean bias for the g-functions at two *B/H* values. The equations for the *RMSE* and mean bias are as follows.

$$RMSE(\%) = \sqrt{\frac{\sum_{i=1}^{n}\left(100*\frac{g_{interp,i}-g_i}{g_i}\right)^2}{n}} \tag{5.4}$$

$$Mean\ Bias = \frac{\sum_{i=1}^{n}(g_{interp,i}-g_i)}{n} \tag{5.5}$$

Where

g_{interp} is the interpolated g-function value

n is the total number of g-function values considered

Table 5-1: RMSE on % Error and Mean Bias for 3 configurations

Configuration	100: 10 x 10		30: 5 x 6		10: 2 x 5	
	Original	LogLog	Original	LogLog	Original	LogLog
RMSE of % Error for all *B/H* values	10.9	4.7	6.7	3.6	3.3	2.2
Mean Bias , *B/H* = 0.03	2.8	-1.1	0.8	-0.5	0.2	-0.1
Mean Bias, *B/H* = 0.3	0.7	0.4	0.5	0.2	0.2	0.1

The LogLog method approximately halves the *RMSE* for the larger borehole configurations. As the number of boreholes in the system decreases the improvement seen in the *RMSE* values also decreases. The larger and more tightly packed borehole configurations tend to have a larger temperature response over time and thus larger g-funtion values. Not only are the g-function values larger, they are also have a greater change in value for different *B/H* curves at a given dimensionless time value. The overall error decreases as the two data sets that are interpolated between come closer together. During actual use, the interpolation will be applied between neighboring *B/H* sets which should produce a reduction in the interpolation error. Attempts to predict the error reduction indicate that it is significant but inconsistent and dependent on more than just the spacing between the g-function curves.

The mean bias shows that the Original method consistently overestimates the g-function values and does so to a greater extent than the LogLog method. The mean bias for the LogLog method more clearly shows what was noted in Figure 5-4, that the g-function values are overestimated for larger *B/H* values and underestimated for the lower *B/H* values. The LogLog method still has a much smaller bias overall than the Original method.

The greatest percent error in the g-function values occurs around *B/H*=0.05. The average reduction in error for this case (100:10x10 boreholes, *B/H*=0.05) is 7.8%. It is interesting to note that the errors of both methods are nonlinear but follow the same trend of peaking just as the

slope of the g-function curve begins to increase, when the logarithm of the dimensionless time ($ln(t/t_s)$) is approximately -5.

These initial comparisons indicate that a small improvement in the g-functions can be seen by using logarithmic terms for both the *B/H* and g-function values. Further investigation into the effects that replacing the original method will have on the sizing error should be considered.

5.2 Extrapolation of g-functions as *B/H* goes to infinity

The tabulated data in GLHEPro matches well with the graphs published in Eskilson (1987a) and the interpolated values are reasonable. During the development of GLHEPro it was found that the extrapolation when *B/H* is large had *g* values less than the case when *B/H*=infinity, which should never occur. At best, each borehole in the system can only operate as well as a single borehole where there are no borehole interactions to be considered. As shown in Figure 5-5 below, the standard logarithmic extrapolation for *B/H*=1 gets g-values much less than the *B/H* = infinity case.

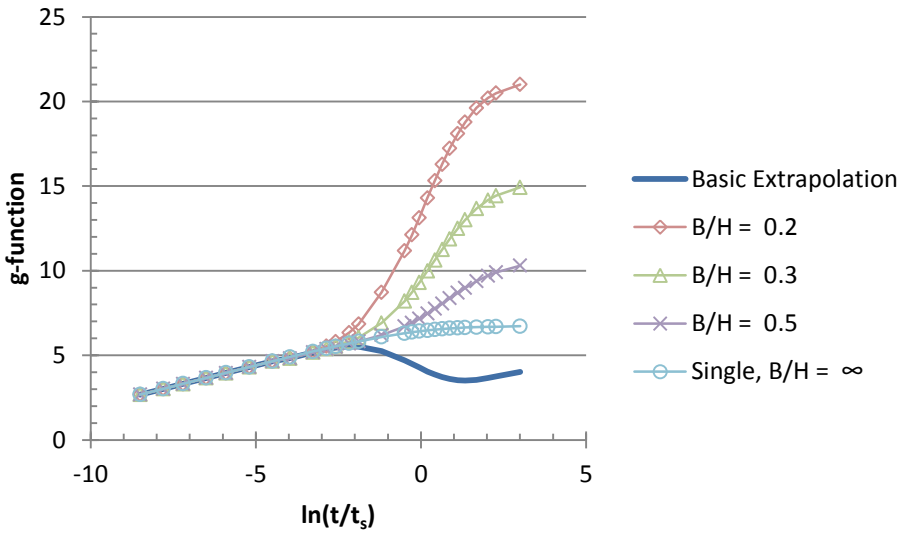

Figure 5-5: Results of basic logarithmic extrapolation at B/H=1 for a 10 x 10 borehole field

While it is unlikely that a real system would have a *B/H* ratio greater than 0.5 it is desirable to correctly treat all cases. In order to fix this extrapolation error, it is necessary to either implement a more accurate extrapolation method or to define infinity such that it is possible to interpolate with the single borehole case. The second option has been implemented.

5.2.1 Methodology

As noted in Section 5.1.1 the g-functions in GLHEPro are tabulated against *B/H* values ranging from 0.05 to 0.5. Eskilson (1987c) provides a series of figures plotting the g-function values for 12 different borehole configurations. Of these 12 plots, 6 include the curves for *B/H*=1. By overlaying plots of the library g-function values and the figures from Eskilson it is possible to estimate the g-function values for these cases when *B/H*=1. Furthermore, this can be done by attempting to interpolate between the g-function values of *B/H*=0.5 and *B/H*=∞ by defining a numerical value for infinity as shown in Equation 5.6. The g-function values for the *B/H*=∞ case are taken from the single borehole case. As detailed in Section 5.1 the method used to interpolate the g-function values is:

$$g = \exp\left(ln(g_1) + \frac{(ln(g_\infty) - ln(g_1))(ln(B/H) - ln(B/H_1))}{ln(B/H_\infty) - ln(B/H_1)}\right) \tag{5.6}$$

Where the terms are defined in Equations 5.1 and 5.2

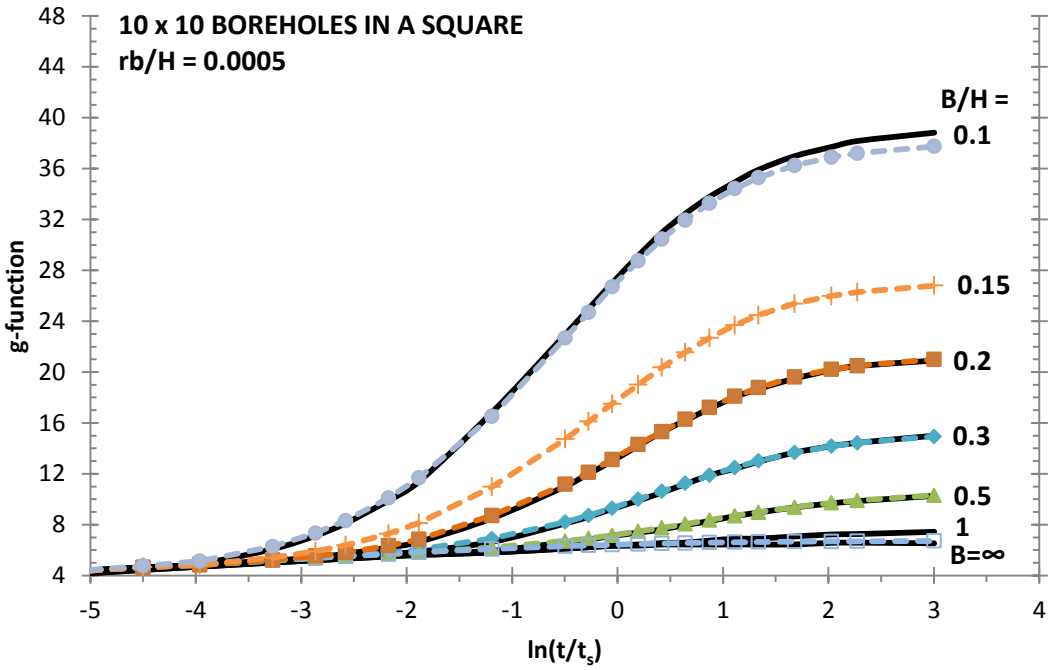

Figure 5-6: Reproduction of g-function values from plotted data (Eskilson 1987c) and tabulated data

Figure 5-6 provides an illustration of the data used for the interpolation. It is a reproduction of Eskilson's plot for the 10 x 10 borehole configuration and the corresponding library g-function values. The solid black curves represent the values plotted by Eskilson and the dashed colorful curves with the various markers show the library data that was calculated by Helström using the methods of Claesson and Eskilson (1987a).

Note that the tabulated data does not always perfectly match Eskilson's curves. There are multiple possible sources for this error. First the solid curves were found by overlaying a Microsoft Excel plot onto a scanned image of the Eskilson (1987c) plot. By using overlaid plots it is possible to get more accurate results than by simply reading values from the original figure. Another possible source of error is that the library data generated by Hellström may have been calculated with a different burial depth than the original values published by Eskilson. During the validation of the FPFLS g-function in Section 3.2 it was found that Hellström likely used a burial

depth of 0 meters[5]. Eskilson did not specify the burial depth, or insulated portion, of the borehole used when calculating his g-functions because it was not deemed important, especially within the range of 1 to 5 meters (Claesson and Eskilson 1987b). The examples published by Eskilson use a depth of 4 or 5 meters.

5.2.2 Results and Conclusions

The numerical value of infinity that was found to provide a reasonable value for interpolation purposes is shown in Table 5-2. The values for each of the six cases were within the range of 1.3±0.05.

Table 5-2: Best fit value of ∞ for *B/H*=1

# Boreholes	Configuration	Value of ∞
100	10 x 10	1.30
64	8 x 8	1.35
50	10 x 5	1.25
36	6 x 6	1.25
32	8 x 4	1.35
18	6 x 3	1.35
	average	1.30

By implementing this improvement and replacing extrapolation with interpolation where the *B/H* value for a single borehole is equal to 1.3, the curve for *B/H* = 1 can be improved as shown in Figure 5-7. In general, the g-function results should never be less than the single borehole case when *B/H* is infinity. So, for cases where the B/H value is greater than 1.3 there will be no interaction between boreholes and the g-function values of the single borehole case should be used. The results of the interpolation with and without this limit are shown in Figure 5-8.

[5] Hellström (2016) stated that both his and Eskilson's g-functions used a burial depth of 5 meters. The difference between the two is due to the different numerical grids used in the g-function generation.

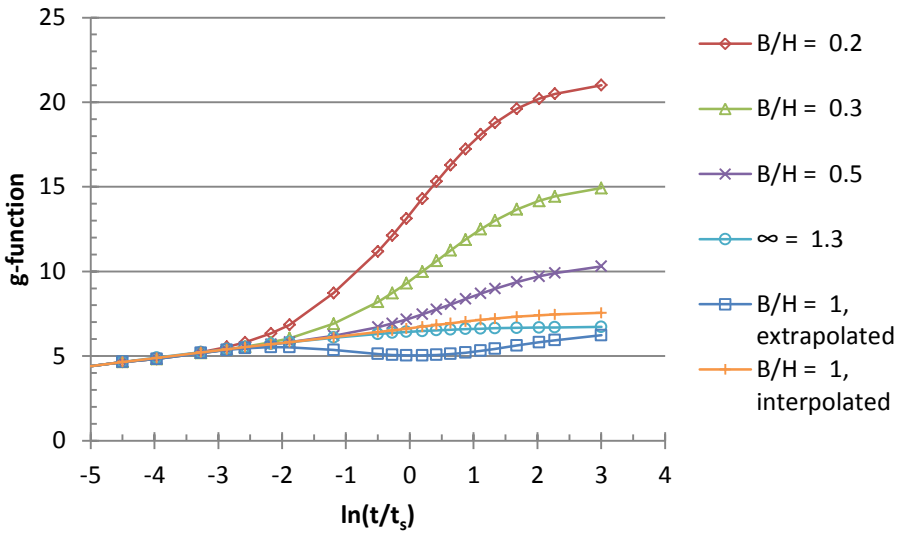

Figure 5-7: g-functions for 10x10 borehole configuration with the *B/H*=1 interpolated values

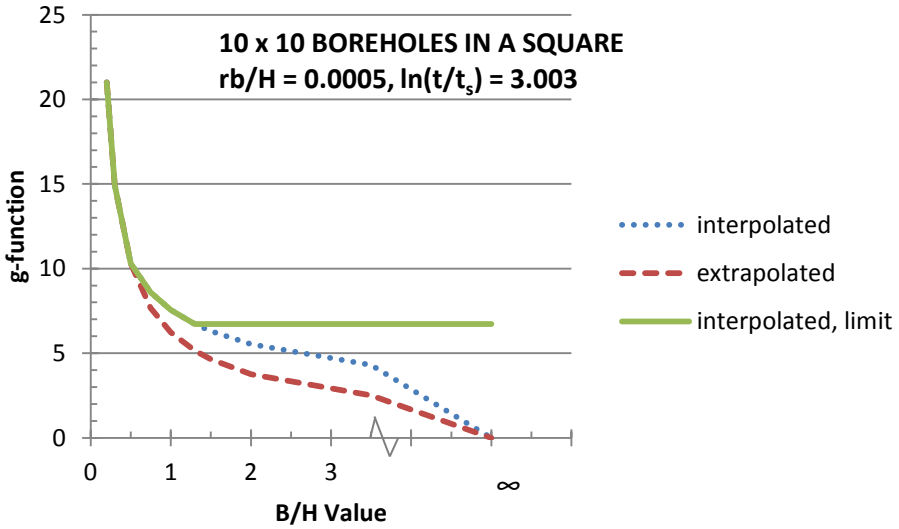

Figure 5-8: g-functions for 10x10 borehole configuration with the r_b/H=0.0005 at $ln(t/t_S)$=3.003

Due to the scale of the published figures it is difficult to fine tune the curves and the resulting g-functions found likely have relatively large errors between $ln(t/t_s)$ values of -5 and -1 where the slope of the g-functions first begins to significantly increase. This issue was also noted with the

method of interpolation in general. Despite these errors there is a significant improvement seen in the g-functions for values of *B/H* between 0.5 and infinity by applying this method to replace the previous extrapolation. Thus the single borehole case with *B/H*=1.3 will be used to interpolate the g-function values for systems with *B/H* greater than 0.5. For systems with *B/H* greater than 1.3 the single borehole g-function values will be used.

Because systems with *B/H* greater than 0.5 are atypical it is expected that there would be little to no improvement seen in the sizing results. For general simulations that fall within this range of *B/H* values the temperature responses should show an improvement similar to that seen in the g-functions.

5.3 Interpolation between LTS and STS

GLHEPro uses interpolated data from a series of g-function data sets provided by Hellström (1991) to get 27 long time step (LTS) g-function values. These g-function values correspond to constant specific values for the logarithm of the dimensionless time from -8.5 to 3.003.

For shorter time steps the short time step method of Yavuzturk and Spitler (1999) with the improvements of Xu and Spitler (2006) is used. This numerical one dimensional finite volume method provides reasonable results for the temperature responses near and within the borehole. Both the long and short time step g-functions are calculated with respect to system specific dimensionless time values with the following equation.

$$\ln(t/t_s) = \ln\left(\frac{t}{t_s}\right) \tag{5.7}$$

$$t_s = \frac{H^2}{9\alpha} \tag{5.8}$$

Where

t is the time [s]

H is the borehole depth [m]

α is the soil thermal diffusivity $[m^2/s]$

Eskilson and Claesson (1987b) give the lower limit on the accuracy of their g-functions to be defined by $\frac{5r_b^2}{\alpha}$; which is set by when the steady state assumption is no longer valid. Combining this lower limit with Equations 5.7 and 5.8 gives the smallest applicable dimensionless time for which long time step g-functions can be used.

$$\ln(t/t_s)_{min} = \ln\left(45\frac{r_b^2}{H^2}\right) \tag{5.9}$$

Where

r_b is the borehole radius [m]

Other terms are defined in Equation 5.8

The g-function methods used in GLHEPro V4.0 do not check to see if the long time step g-functions are applied below the minimum dimensionless time constraint. Another way of identifying when this error occurs is to check if $ln(t/t_s)_{min}$ is greater than -8.5, which is the default lower limit for the long time step method. This is generally not an issue for the simulations within the program as they operate on a monthly time step and should never approach the values that would potentially be affected by this constraint. The problems could be seen in the various other simulations that use the g-functions generated by GLHEPro.

5.3.1 Sample Case: Sandbox

The case for which this problem is considered is the Sandbox experiment completed by Beier et al. (2011). They ran a controlled experiment on a test borehole that consisted of an 18.3 meter (60ft) long U-tube centered inside a 1.8x1.8m (6x6ft) box filled with sand. The borehole wall is

defined by a 12.6cm (4.96in) aluminum pipe and the U-tube is made up of 1 inch nominal SDR11 high density polyethylene pipe. The soil and fluid properties for the ground heat exchanger model are shown in Table 5-3.

Table 5-3: Soil and Fluid Properties for Sandbox GHE

Soil Properties		
Undisturbed Ground Temperature	22	°C
Thermal Conductivity	2.82	W/m.K
Density	1601.8	kg/m^3
Specific Heat Capacity	1400	J/kg.K
Fluid Properties		
System Mass flow rate	0.197	kg/s
Density	993.99	kg/m^3
Volumetric Heat Capacity	4149820	J/K.m^3

The problem in GLHEPro occurs when $ln(t/t_s)_{min}$ is larger than -8.5 (or when $r_b/H \geq 0.00212639$). For the Sandbox case r_b/H=0.064/18.3=0.003497, which is greater than 0.00212639; this results in the following, somewhat disjointed, g-function plot below.

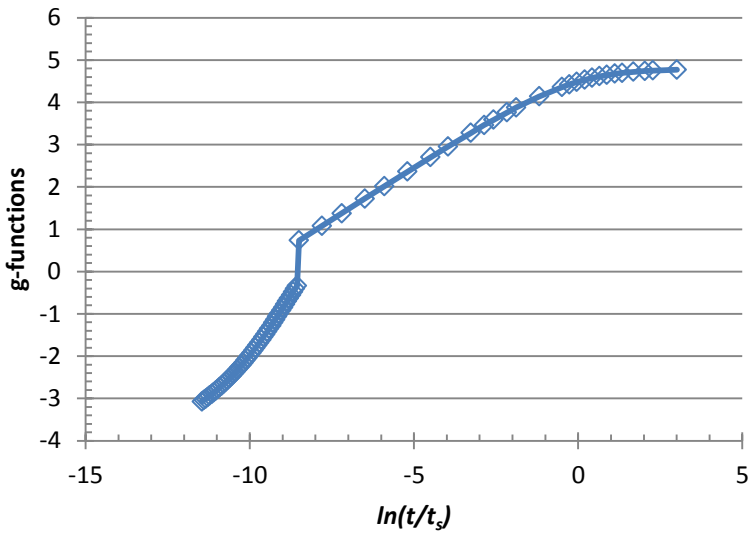

Figure 5-9: G-Functions for the Sandbox Borehole (Beier et al. 2011)

The effects of the short time g-functions are not seen in GLHEPro's monthly simulation though they can clearly be seen in minute by minute simulation as shown in Figure 5-10. The jump in temperature occurs between 1.5 and 2 hours into the simulation.

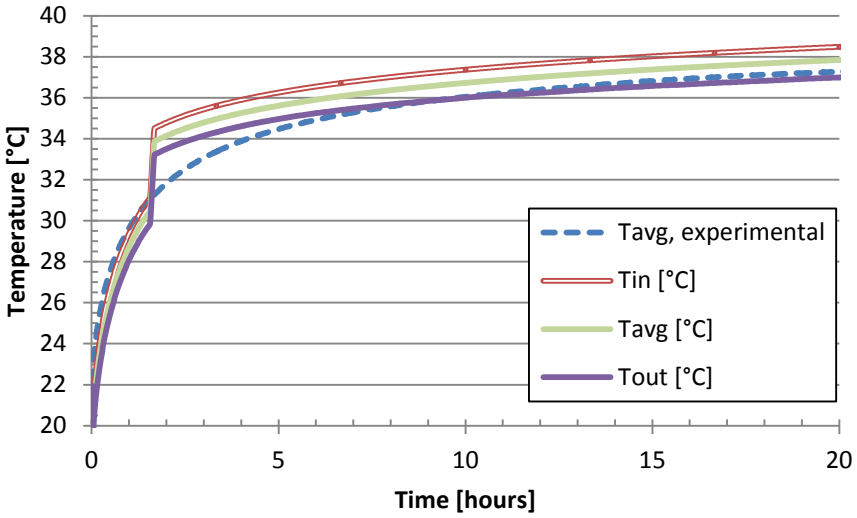

Figure 5-10: Temperature results of minute temperature simulation of the sandbox (Beier et al. 2011), uncorrected g-functions

When compared to the experimental temperatures it is apparent that GLHEPro matches the experimental data well up until the jump in temperature. The $ln(t/t_s)_{min}$ value for this case is about -7.5 (4.5 hours), which is greater than the default minimum $ln(t/t_s)$ value used in GLHEPro for the Long Time step method. A simple method for identifying when this error occurs and implementing a solution is considered in the next section.

5.3.2 Methodology and Results

This improvement can be implemented in GLHEPro by rearranging the calculation of the g-functions to solve for the long time step (LTS) g-functions first. Next, a simple statement checks for cases where the LTS g-functions are used at $ln(t/t_s)$ values less than $ln(t/t_s)_{min}$ and marks them for replacement. When the short time step (STS) g-functions are calculated the method is

extended up to the largest $ln(t/t_s)$ value marked for replacement. If no $ln(t/t_s)$ values are marked for replacement then the STS method terminates at $ln(t/t_s)$=-8.5.

Applying these improvements to the code allows the g-function curve to be shifted as shown in the Figure 5-11. This removes the abrupt step that is seen without this correction.

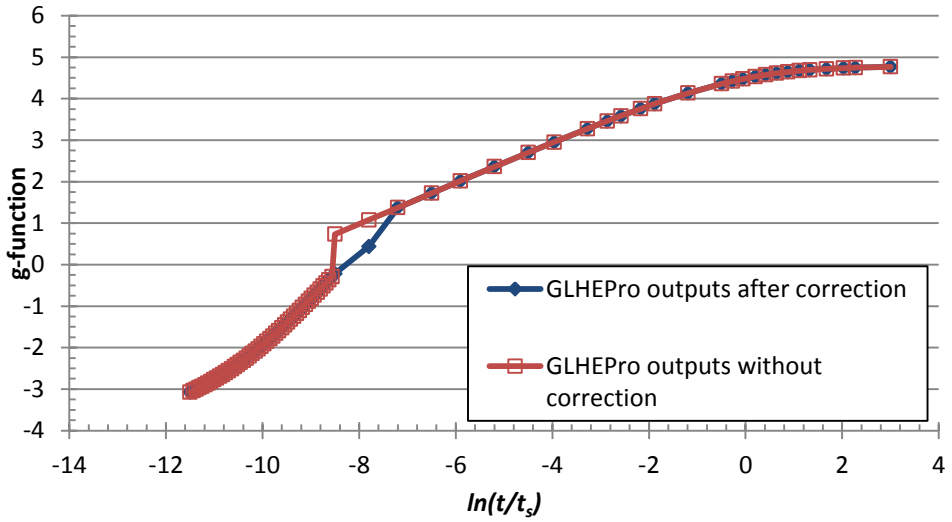

Figure 5-11: Effects of correction on calculated g-functions in GLHEPro for Sandbox case (Beier et al. 2011)

The g-function correction results in the temperature correction shown in Figure 5-12. This is a definite improvement over the previous method. For this case the long time step response still results in temperatures that are higher than the experimental data by about 0.7°C. This could be a result of the model used or uncertainty in the soil or fluid properties.

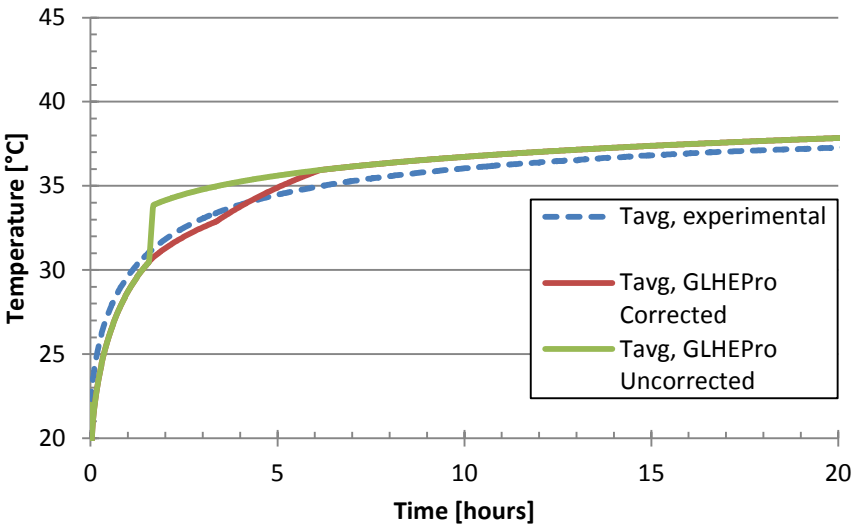

Figure 5-12: Effects of g-function correction on temperature response compared to uncorrected model and experimental data (Beier et al. 2011)

5.4 Conclusions

Three different improvements to the interpolation methods for the library g-function values were proposed. Applying the logarithm to both terms in the interpolation of the library g-functions between *B/H* sets results in a slight underestimation for the smaller *B/H* values and a slight overestimation of the larger *B/H* correlations. Overall the "LogLog" method of interpolation provides better results.

Using the single borehole case as a borefield with effectively infinite spacing allows for better interpolation for GHE systems with large spacing between boreholes. In order to interpolate the g-function values for systems with large spacing between boreholes the B/H value for infinity can be reasonably approximated by using a value of 1.3.

The short time step g-functions are not used in GLHEPro's monthly simulation, but for hourly simulations the transition between the short time step (STS) g-functions and the long time step

(LTS) g-function is not always smooth. Enforcing the lower limit on the LTS method and extending the STS g-function method improves the transition between the two methods.

CHAPTER VI

IMPLEMENTATION OF A GLOBAL AND SEASONAL GROUND TEMPERATURE MODEL

6.1 Introduction

Previous versions of GLHEPro provided a map of the continental United States with isotherms indicating the average annual air temperatures that can be used to estimate the undisturbed ground temperature. While this method provides an easy way to approximate the undisturbed ground temperatures for the continental United States, it is of no help to international users. If actual measures of the ground temperature could not be taken the method suggested for international locations was to base the ground temperature on the average annual air temperature. This method was based on some semi-empirical observations that the ground temperature is typically about ±2.5°F (±1.4°C) warmer than the annual average air temperature, though it was found to vary from -4.6 to +6.1°F among the 13 cases considered (OSU 2016a). The average temperature difference for the 13 cases was 1.85°F.

Both of these methods provide approximations of the undisturbed ground temperature and not necessarily the actual ground temperatures for a given location. For locations in urban areas or other areas where the ground temperature may be disturbed by natural effects or by the workings of man, these approximations will not give the true ground temperature.

A more detailed model of the undisturbed ground temperature has been implemented in GLHEPro V5.0 using the methods of Xing (2014). It is based on a detailed ground heat transfer

model coupled with typical meteorological year weather data. This method not only provides undisturbed ground temperature results for locations in the United States, but also for many global locations. Each of the 4,112 global locations defined by Xing are saved as a record with the coefficients required to get the undisturbed ground temperature at any given depth and time of the year. Nevertheless, this model does not account for local disturbances in the ground temperature (e.g. buildings, pavement, etc.) and field measurements of the ground temperature are preferred.

6.2 Methodology

Two models were developed by Xing (2014); a detailed numerical model and a simple two-harmonic model. The numerical model was developed to accurately model the ground temperature profile by calculating the ground temperatures using a one-dimensional explicit finite volume model with weather files coupled to a full surface heat balance. The weather file provides the air temperature, relative humidity, wind speed, and incident short-wave radiation. The density of vegetation is an input to the model and affects the evapotranspiration. Snow cover is treated as a boundary condition and both freezing and melting of moisture within the soil are considered in the model. Moisture within the soil is assumed to be constant and moisture transport is neglected.

Generally the one-harmonic model is sufficient for engineering applications. In order to better account for precipitation, snow fall, and the freeze/thaw cycle a two-harmonic model is used as shown in equation 6.1.

$$T_s(z,t) = T_{s,avg} - e^{-z\sqrt{\frac{\pi}{\alpha_s t_p}}} T_{s,amp,1} \cos\left(\frac{2\pi}{365}(t - PL_1) - z\sqrt{\frac{\pi}{\alpha_s t_p}}\right) + e^{-z\sqrt{\frac{2\pi}{\alpha_s t_p}}} T_{s,amp,2} \cos\left(\frac{4\pi}{t_p}(t - PL_2) - z\sqrt{\frac{2\pi}{\alpha_s t_p}}\right) \quad (6.1)$$

Where

$T_s(z,t)$ is the undisturbed soil temperature at depth z and time of year t [°C]

z is the soil depth [m]

t is the time of year, starting from January 1st [days]

t_p is the period of soil temperature cycle (out of 365) [days]

α_s is the soil diffusivity [m^2 day^{-1}]

$T_{s,avg}$ is the annual average soil temperature [°C]

$T_{s,amp,n}$ is the n^{th} order surface amplitude, which can be assumed to be half of the difference between the maximum and minimum monthly average temperatures in a year [°C]

PL_n is the n^{th} order phase angle of the annual soil temperature cycle [days]

The annual average soil temperatures, surface amplitude, and phase delay are all estimated by minimizing the sum of the squares of the errors (SSQE) between the numerical model and the two-harmonic model. This was done by calculating the SSQE of the temperatures at four depths (z=0.05, 0.2, 0.5, and 1 meter) for a period of a year. The optimization method used was the Nelder-Mead Simplex method.

The numerical model was validated against an analytical solution (Cengel and Ghajar, 2011; page 251) by comparing the soil temperature response to a constant heat pulse at the surface of the ground. The difference between the analytical solution and the numerical model was less than 0.00015°C (0.00027°F). An experimental validation of 19 locations that compared the ground temperatures at depths of 5cm (2") and 20cm (20") found that the difference between the two

methods decreased as the depth underground increased and did best for warm temperature climates and worst for snowy climates. The two-harmonic model gave RMSEs 0.1-0.8°C (0.2-1.4°F) higher than the numerical model; this is because the two-harmonic model is limited by both its own accuracy and the accuracy of the numerical model on which it is based.

6.3 Implementation

The tabulated coefficients generated by Xing (2014) were uploaded into the resources within GLHEPro and a data structure created to hold each location record. This allows the ground temperature to be calculated for any location using Equation 6.1. Several methods were devised to allow users to select a ground temperature location record. While the tabulated data covers a wide range of global locations it still does not include every location so a designer must consider whether it is better to select the nearest record or the record with the most similar soil and weather conditions.

GLHEPro allows for users to select a record based on region, country and station name or latitude and longitude. Figure 6-1 shows the input dialog for the option to select a record based on region and country. Figure 6-2 shows the input dialog for specifying the latitude and longitude. This option finds the 6 records closest to the specified point and allows the user to select the best location. The final option, shown in Figure 6-3, allows users to specify that a constant ground temperature is to be used. This is useful for when the ground temperature is known and does not match the record for a given location. For every option except the latter, the ground temperature will vary throughout the year along with the typical weather conditions.

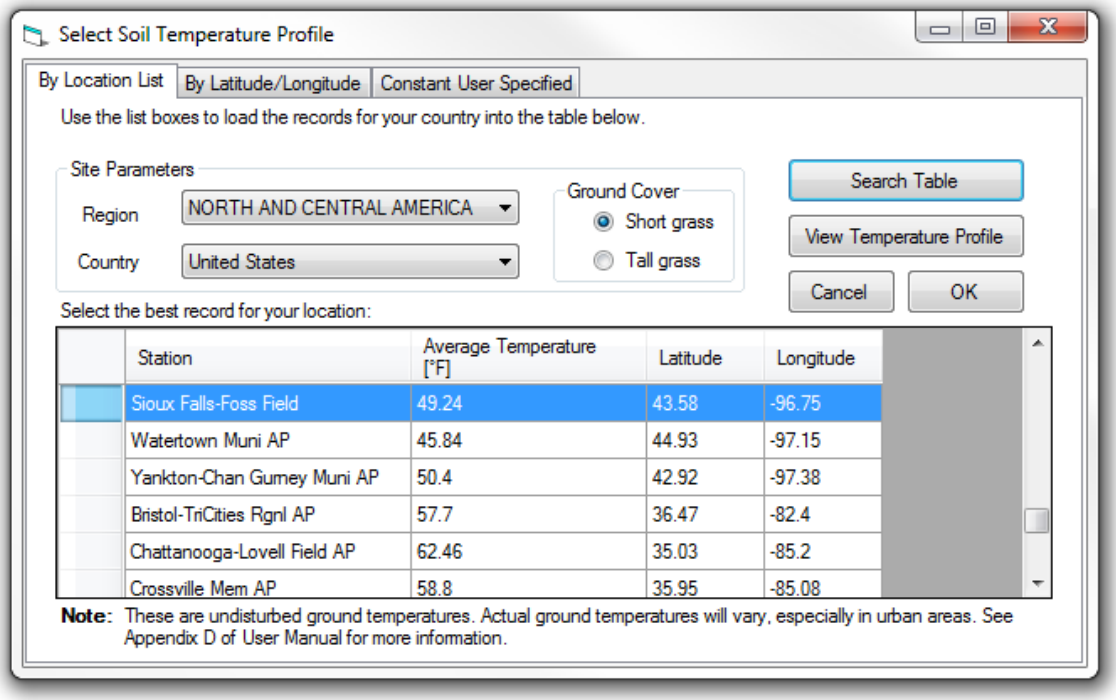

Figure 6-1: Input dialog for selecting the soil temperature profile by Region, Country, and Station

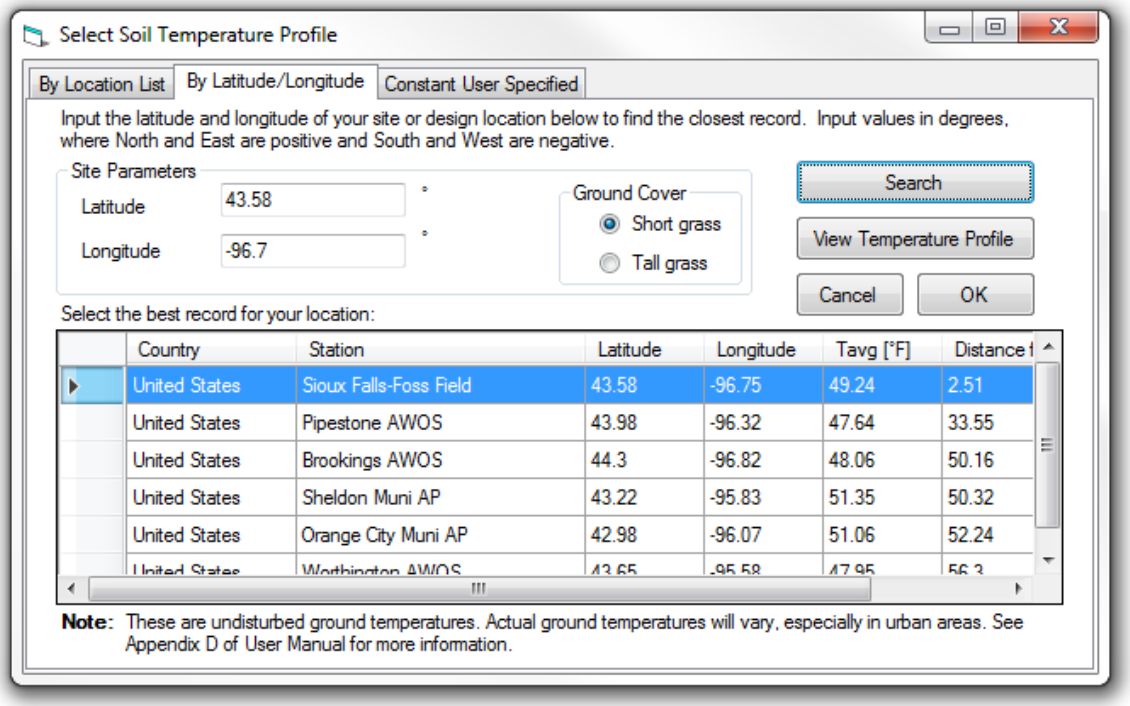

Figure 6-2: Input dialog for selecting the soil temperature profile based on latitude and longitude

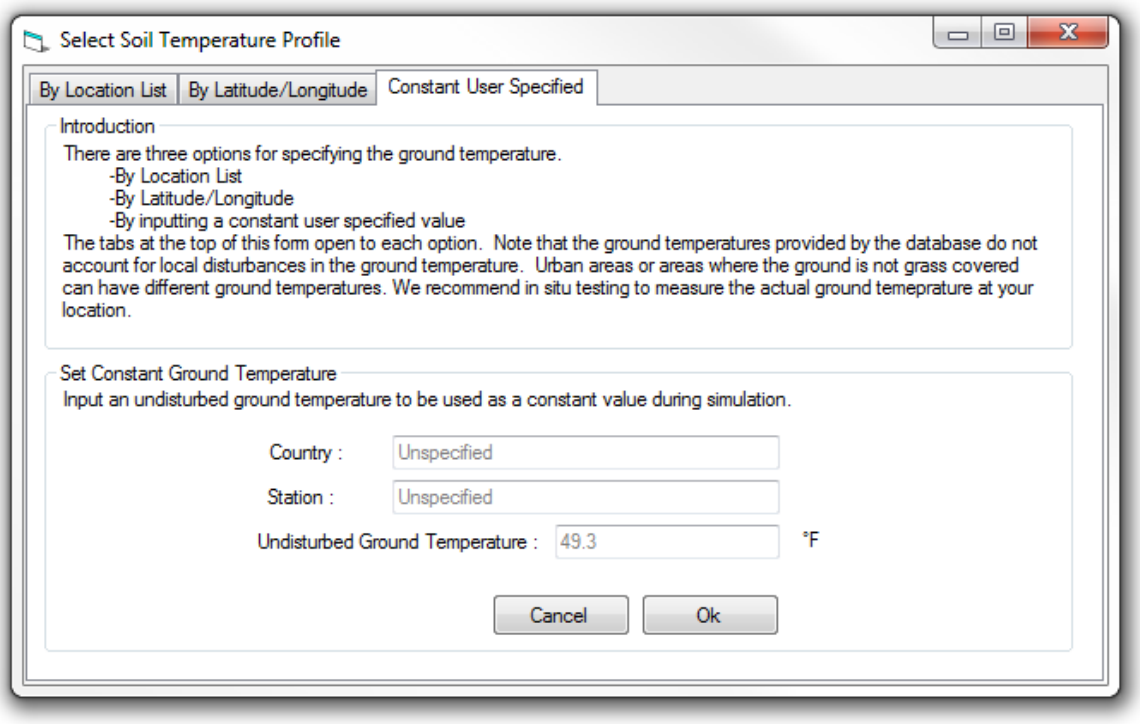

Figure 6-3: Input dialog for setting a constant soil temperature profile

GLHEPro V5.0 can plot depth versus temperature as shown in Figure 6-4. This effectively displays the temperature gradient at the selected location on a specific day of the year. This could be very useful when designing horizontal systems to select the optimum burial depth for the system.

Another plotting option that is available is temperature versus time as shown in Figure 6-5. This figure shows the annual fluctuation in the soil temperatures at a depth of 30 ft (9.1 m). The temperature versus time plot gives the best visualization of the temperatures used when simulating or sizing GLHE systems in GLHEPro V5.0. By default, GLHEPro uses the midpoint of the average borehole depth to calculate the ground temperature for each month or hour as needed. For monthly simulations the average temperature throughout the month is used rather than the temperature for a specific hour in the month.

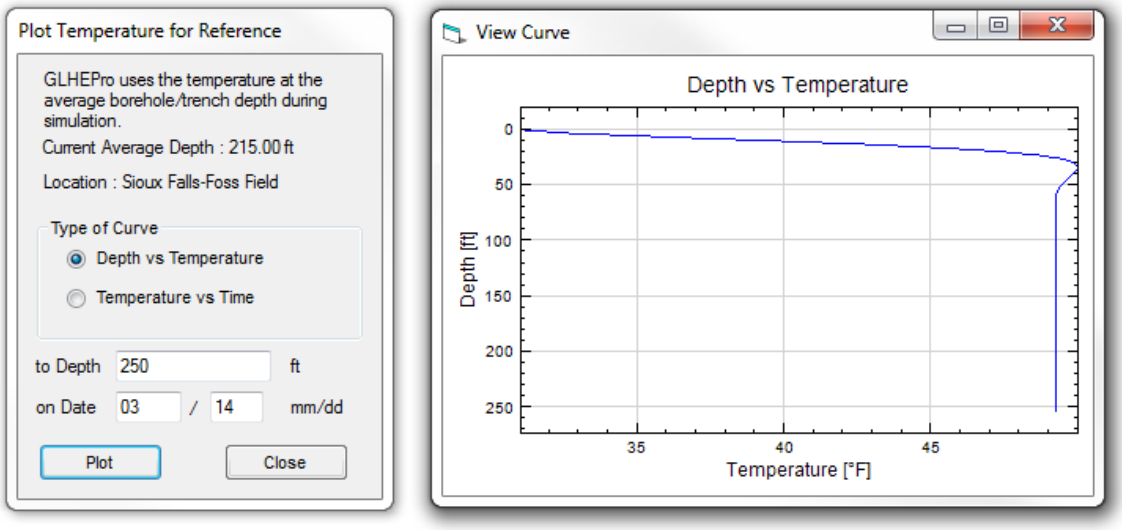

Figure 6-4: Plot of Depth vs Temperature in GLHEPro V5.0

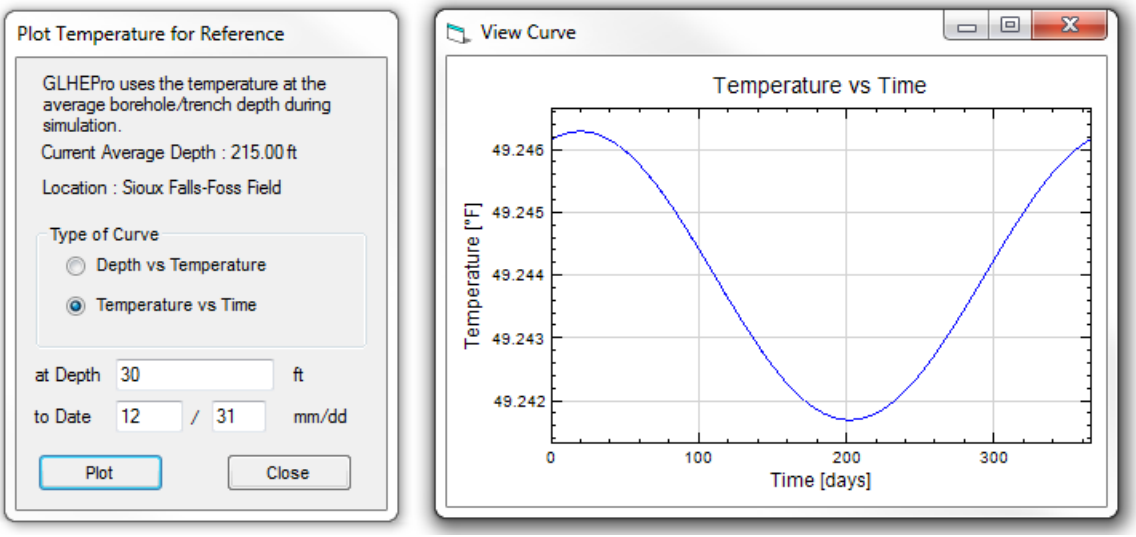

Figure 6-5: Plot of Temperature vs Time in GLHEPro V5.0

6.4 Conclusions

Previous versions of GLHEPro provided limited guidance on the estimation of ground temperatures to users outside of the continental United States. The new method improves ground temperature estimation for international users by offering temperature profiles for locations all

around the globe. Xing's (2014) model is especially important for the implementation of horizontal GHE system because of the time-varying temperatures near the surface. It is a distinct improvement over the previous method recommended in GLHEPro for international users which was based on the average annual air temperature alone.

The two-harmonic model proposed by Xing (2014) is simple enough for engineering analysis but sufficiently detailed for simulation purposes. It accounts for annual weather conditions, ground cover, and moisture within the soil through parameter estimation with a numerical model. Both the numerical and two-harmonic model were validated against a specified surface heat flux solution and found to have reasonable results. It is still recommended that an in-situ thermal response test be completed to get the actual ground temperature (Austin et al. 2000).

CHAPTER VII

SLINKY GLHE IMPLEMENTATION

7.1 Introduction

A Slinky ground loop heat exchanger (GLHE) is a horizontal ground heat exchanger (HGHE) system that is laid out in trenches in a series of overlapping coils as shown in Figure 7-1. The GLHE is named after the Slinky™, a children's toy made up of flattened plastic or metal coiled like a weak spring. The theory behind the design of the slinky GSHP is that it makes it possible to install a larger amount of tubing into a limited area. Horizontal ground heat exchangers typically have a significantly lower installation cost than vertical boreholes because the cost of trenching is usually less expensive than drilling. Models for simulating Slinky GHE are becoming more common and this presents an opportunity to increase the functionality of GLHEPro.

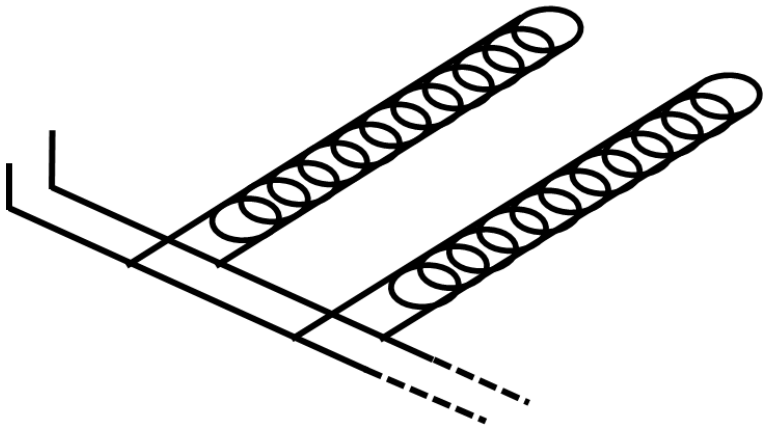

Figure 7-1: Slinky GHE with horizontally oriented rings

7.2 Literature Review

Research has been done by several different groups on the modeling of Slinky GLHE's. The following paragraphs contain a brief review of some the recent Slinky GLHE models. Both numerical and analytical models are considered.

Wu et al. (2010) put together a numerical model of a slinky GLHE using a commercial computational fluid dynamics software package. The model was validated against experimental data and used to compare the slinky GLHE to a straight horizontal GLHE. Their results suggest that a slinky GHE does reject more heat than a straight pipe when compared on the basis of trench length. On the basis of pipe length used, a straight horizontal GHE has better specific heat extraction/rejection. A decline in the coefficient of performance (COP) was seen during the two month operating period of their experimental slinky GHE installation. This is likely due in part to the natural temperature gradient in the ground and to the concentrated effects of the GHE on the local ground temperatures.

Another numerical model for slinky GHEs was created by Fujii et al. (2012) and validated against experimental data. The model was done in a 3D finite-element numerical simulator (FEFLOW) that considers both groundwater and heat transport. Instead of modeling actual slinky coils a rectangular flow path with the same length as the trench, the width equal to the diameter of the slinky loop, and a height to maintain the fluid volume was used. The thermal properties of the rectangular "pipe" had to be adjusted to account for the difference in surface area as the surface area of an actual slinky is much smaller.

Their results show that their numerical model can provide reasonable agreement with experimental data. Also, it is important to account for the surface energy balance when calculating the system outlet temperature.

Congedo et al. (2012) modeled several different types of horizontal ground heat exchangers (HGHE) using a computational fluid dynamics software package (Fluent). The slinky model considered a full section of slinky loops in a vertical orientation, where the plane defined by the slinky loops is perpendicular to the ground surface. The various HGHE models were not validated directly against experimental data; the average hourly ground temperatures at a depth 0.2 meters were validated and showed that the boundary conditions selected were good.

Their comparison showed that the most important factors in the design of HGHE are the ground conductivity and fluid velocity. The slinky model's heat transfer was found to be 5 times higher than a straight pipe system on the basis of trench length. The model they recommended was the helical configuration because it was found to have 5 times the heat transfer of a slinky HGHE.

Another simplified numerical CFD model (Fluent) implemented by Chong et al. (2013) used symmetry to model various arrangements of slinky HGHEs. The model assumed that the surface temperature of the pipe was uniform. They investigated the effects of various design options such as loop spacing, loop diameter, and soil properties on the system thermal response and concluded

that decreasing the loop spacing/pitch is the best method to increase the system heat extraction/rejection. The initial heat extraction was found to be much higher than the final steady state value. Running the HGHE in 12 hour on and off periods was shown to significantly increase the heat transfer of the system.

All of the models discussed above were implemented in a commercial computational fluid dynamics software or 3D finite element simulator. These software packages cannot be packaged with GLHEPro for many reasons and creating new modeling software that could be packaged with GLHEPro is outside the scope of this thesis. These models were also created for research purposes and would not be useful for design purposes because they do not provide sizing functionality. Analytical methods can be more easily implemented for design purposes.

A recent analytical method for modeling a slinky or spiral GHE used a ring source model to get the temperature effects on the ground (Li et al. 2012). The ring source model was created by placing the points of a point source model into rings. Two boundary conditions were considered in their models: constant temperature and adiabatic. The results for the adiabatic case were validated against data collected from a lab based experiment and showed that it was possible to use superposition with a point/ring source model to adequately model the temperature effects of a slinky/spiral HGHE on the ground.

The methods of Li et al. were later expanded to model the entering and exiting fluid temperatures of the slinky GHE system. Xiong et al. (2015) added several improvements to both the g-function calculation and model simulation and experimentally validated the results. Only the g-function calculation method of Xiong et al. (2015) is implemented in GLHEPro V5.0. Improvements include:

- recalculating the equations to use only the Cartesian coordinate system
- simplifying the calculations by assuming that the slinky was buried at a constant depth

- reducing computation time by
    - taking advantage of symmetry in the GHE and only modeling 1/4th of the Slinky's rings to get the g-functions for the full GHE
    - treating rings a more than about 2.5 meters away as point sources and entirely neglecting rings more than about 10 meters away
    - keeping a record of common ring interactions as a function of distance so that the response does not always have to be recalculated

Some of these improvements are discussed in more depth in the following section.

7.3 Methodology

The model implemented in this thesis is that of Xiong et al. (2015; Xiong 2014). Their intention was to develop a method that could be used in a whole-building energy simulation or design tool such as GLHEPro. This was done by using analytical, rather than numerical methods and solving for g-function values rather than the tube wall temperature. G-functions are temperature response functions that account for the temperature response of the GHE system due to loads applied for each time step; these values can be calculated separately from a system temperature simulation.

The original implementation of the methods of Xiong et al. (2015) was done in EnergyPlus and made use of the ground temperature model and system connections. The implementation in GLHEPro V5.0 does not have access to those models and uses alternatives as needed. The ground temperature model of Xing (2014) was used in place of the numerical model implemented in EnergyPlus. The slinky model is based on several assumptions:

- The system is assumed to have uniform heat flux for the entire system at any given time. This approximation is widely accepted for analytical models and makes the calculation

method much simpler but introduces some errors as discussed in Malayappan and Spitler (2013).

- The ground is modeled as a semi-infinite homogeneous medium
- Soil moisture is neglected in the heat transfer calculations
- Thermal storage of the tube or piping is neglected and the interior of the tube is assumed to have the same thermal properties as the ground.

Several simplifying assumptions were made to make defining the systems easier and to reduce computation time.

- The system trenches are assumed to be parallel with equal length and spacing between trenches.
- The size and spacing of the rings in the Slinky GHE are constant.

The calculations are based on the solution of the continuous point source which gives the temperature variation due to a point source with constant heat flux at a given distance from the point and time that the heat has been applied (Marcotte and Pasquier 2009).

$$\Delta T(d,t) = \frac{q}{4\pi k d} erfc\left(\frac{d}{\sqrt{4\alpha t}}\right) \tag{7.1}$$

Where

q is the heat extraction/rejection [W]

α is the ground thermal diffusivity [m^2s^{-1}]

k is the ground thermal conductivity [W m^{-1} K^{-1}]

t is time [s]

u_n is a point on a borehole n, where n=*i* or *j*

d is the distance between the point source and point of interest [m]

$erfc(u)$ is the complementary error function, where $erfc(u) = \frac{2}{\sqrt{\pi}} \int_u^{\infty} e^{-s^2} ds$

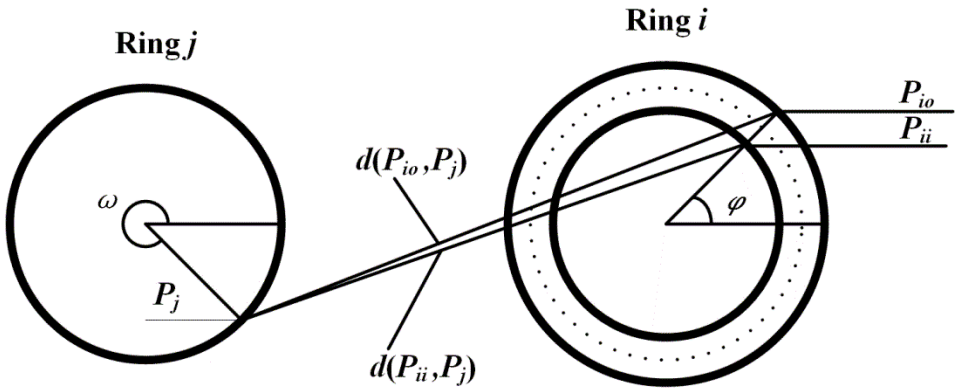

Figure 7-2: Distance between point P_{ii} and P_{io} on ring source *i* and P_j on ring source *j*. [reprinted with permission Xiong 2014]

The point source model can be set up to get the temperature response between points on a pair of rings. Each ring consists of a series of point sources distributed along the centerline of the tube as shown in Figure 7-2 by the dotted line in Ring *i*. This dotted line represents a ring source, essentially a large number of point sources that together form a ring. Rings that are being used as sources are treated as having just the simple centerline and are typically referred to as Ring *j*. The ring for which the temperature perturbation is being calculated is typically called Ring *i* and consists of points on the inner (P_{ii}) and outer (P_{io}) diameters of the tube. When the temperature perturbation is calculated for a ring to itself ($i=j$), the average response of points P_{ii} and P_{io} to the ring source in Ring *i* is found.

The temperature perturbation of a point on one ring to all the points on another can be found by summing up the effects of each point source within the ring *j* on the current point P_i. This can be done by integrating the results of the point sources on Ring *j* as shown in Equation 7.2.

$$\Delta T(P_i,t) = \frac{q_l R}{4\pi k}\int_0^{2\pi} \frac{erfc\left[d\left(P_j,P_i\right)/2\sqrt{\alpha t}\,\right]}{d\left(P_j,P_i\right)}d\omega \tag{7.2}$$

Where

R is the radius of the ring [m]

q_l is the heat rate per tube length [W m^{-1}]

$d\left(P_j,P_i\right)$ is the average distance between point P_j and points P_{ii} and P_{io}

Other terms are defined in equation 7.1

In order to apply the isothermal boundary condition for the ground surface, the method of images is applied as shown in Figure 7-3 for horizontally oriented rings. This is done by subtracting the effects of the fictitious rings within the integral as shown in equation 7.3. The heat flux of the fictitious Ring *j'* is equal and opposite to that of the real Ring *j*, thus the only value that must be different for the response of the fictitious ring is the distance between points.

$$\Delta T(P_i,t) = \frac{q_l R}{4\pi k}\int_0^{2\pi} \frac{erfc\left[d\left(P_j,P_i\right)/2\sqrt{\alpha t}\,\right]}{d\left(P_j,P_i\right)} - \frac{erfc\left[d\left(P_{j'},P_i\right)/2\sqrt{\alpha t}\,\right]}{d\left(P_{j'},P_i\right)}d\omega \tag{7.3}$$

Where

$d\left(P_{j'},P_i\right)$ is the average distance between point $P_{j'}$ and points P_{ii} and P_{io}

Other terms are defined in equation 7.2

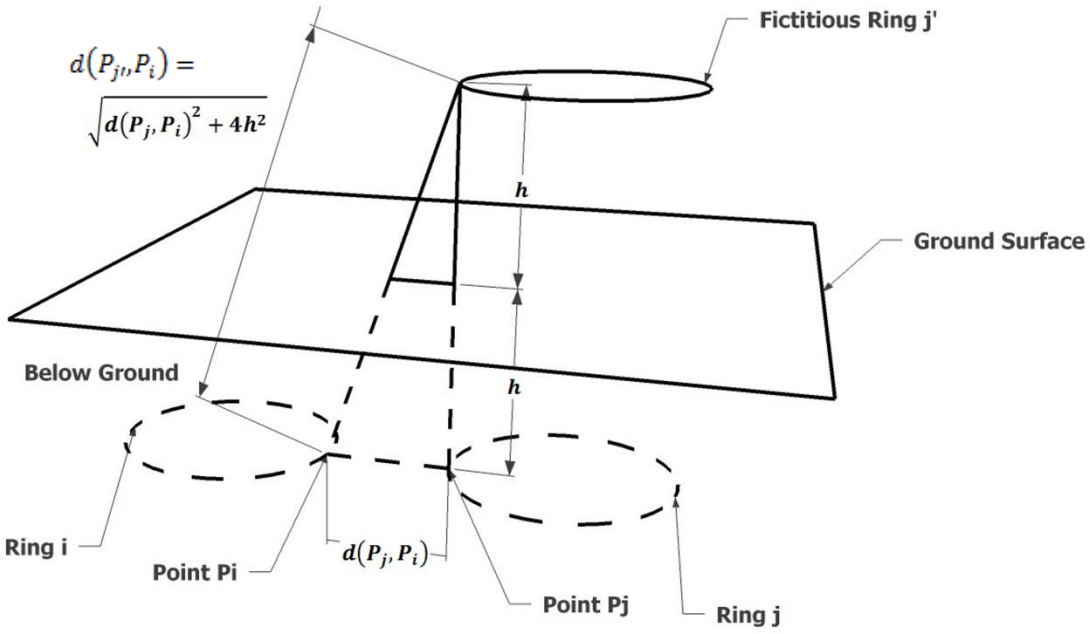

Figure 7-3: Three-dimensional view of fictitious ring source of ring *j* for horizontally oriented rings. [Reprinted with permission, Xiong 2014]

The average temperature perturbation of Ring *i* due to ring source *j* and fictitious ring source *j'* can be found with a double integral.

$$\Delta T_{j-i}(t) = \frac{q_l R}{8\pi^2 k} \int_0^{2\pi} \int_0^{2\pi} \frac{erfc\left[d(P_j,P_i)/2\sqrt{\alpha t}\right]}{d(P_j,P_i)} - \frac{erfc\left[d(P_{j'},P_i)/2\sqrt{\alpha t}\right]}{d(P_{j'},P_i)} d\omega d\phi \qquad (7.4)$$

The mean tube wall temperature variation for the Slinky GHE system can then be found by averaging the temperature effects on each ring due the interactions between all the rings in the GHE system.

$$\Delta \bar{T}(t) = \frac{1}{N_{ring}} \sum_{i=1}^{N_{ring}} \sum_{j=1}^{N_{ring}} \Delta T_{j-i}(t) \qquad (7.5)$$

Where

N_{ring} is the total number of rings or loops in the Slinky GHE

The g-functions can then be calculated by equation 7.6 based on the methods proposed by Claesson and Eskilson (1987). G-functions are dimensionless temperature response functions and are generally calculated in conjunction with a dimensionless time factor (*ln(t/3600)*).

$$g_s(t) = \frac{2\pi k}{q_l}\Delta\bar{T}(t) \tag{7.6}$$

Based on equations 7.4-7.6 the general solution for the temperature response of a slinky GHE would then be:

$$g_s(t) = \sum_{i=1}^{N_{ring}}\sum_{j=1}^{N_{ring}}\frac{R}{4\pi N_{ring}}\int_0^{2\pi}\int_0^{2\pi}\frac{erfc\left[d(P_j,P_i)/2\sqrt{\alpha t}\right]}{d(P_j,P_i)} - \frac{erfc\left[d(P_{j'},P_i)/2\sqrt{\alpha t}\right]}{d(P_{j'},P_i)}d\omega d\phi \tag{7.7}$$

Two specific orientations for the Slinky GHE were developed by Xiong (2014). The horizontal orientation is shown in Figure 7-5 in Section 7.4.1; this is where the rings in the slinky GHE are installed lying horizontally in the trench. The temperature response function for a Slinky GHE with the horizontal ring orientation is:

$$g_s(t) = \sum_{i=1}^{N_{ring}}\sum_{j=1}^{N_{ring}}\frac{R}{4\pi N_{ring}}\int_0^{2\pi}\int_0^{2\pi}\left[\frac{erfc\left(\frac{d(P_j,P_i)}{2\sqrt{\alpha t}}\right)}{d(P_j,P_i)} - \frac{erfc\left(\frac{\sqrt{d(P_j,P_i)^2+4h^2}}{2\sqrt{\alpha t}}\right)}{\sqrt{d(P_j,P_i)^2+4h^2}}\right]d\omega d\phi \tag{7.8}$$

Where

$$d(P_j,P_i) = \frac{d(P_{ii},P_j)+d(P_{io},P_j)}{2} \tag{7.9}$$

$$d(P_{ii}, P_j) = \sqrt{\begin{matrix}\left[x_{0i} + (R-r)\cos(\phi) - x_{0j} - R\cos(\omega)\right]^2 \ldots \\ +\left[y_{0i} + (R-r)\sin(\phi) - y_{0j} - R\sin(\omega)\right]^2\end{matrix}} \quad (7.10)$$

$$d(P_{io}, P_j) = \sqrt{\begin{matrix}\left[x_{0i} + (R+r)\cos(\phi) - x_{0j} - R\cos(\omega)\right]^2 \ldots \\ +\left[y_{0i} + (R+r)\sin(\phi) - y_{0j} - R\sin(\omega)\right]^2\end{matrix}} \quad (7.11)$$

Where

R is the radius of the Ring [m]

r is the radius of the tube [m]

h is the burial depth of the center point of the ring from the ground surface [m]

x_{0n}, y_{0n} are the Cartesian coordinates for the point at the center of ring *n*, where n=*i* or *j*

ϕ and ω are angle coordinates shown in Figure 7-2 [rad]

Other terms are defined in Equations 7.1 and 7.2

The other configuration considered is with vertically oriented rings, where the rings are installed leaning up against the walls of the trench. Figure 7-6 in Section 7.4.1 shows the general layout for a Slinky GHE with vertically oriented rings. The temperature response function, or g-function, for any slinky GHE with a vertical orientation can be calculated by:

$$g_s(t) = \sum_{i=1}^{N_{ring}} \sum_{j=1}^{N_{ring}} \frac{R}{4\pi N_{ring}} \int_0^{2\pi} \int_0^{2\pi} \left[\frac{erfc\left(\frac{d(P_j, P_i)}{2\sqrt{\alpha t}}\right)}{d(P_j, P_i)} - \frac{erfc\left(\frac{d(P_{j'}, P_i)}{2\sqrt{\alpha t}}\right)}{d(P_{j'}, P_i)} \right] d\omega d\phi \quad (7.12)$$

Where

$$d(P_j, P_i) = \frac{d(P_{ii}, P_j) + d(P_{io}, P_j)}{2} \quad (7.13)$$

$$d(P_{j'}, P_i) = \frac{d(P_{ii}, P_{j'}) + d(P_{io}, P_{j'})}{2} \tag{7.14}$$

are the distances between points based on the following equations:

$$d(P_{ii}, P_j) = \sqrt{\begin{matrix}\left[x_{0i} + (R-r)\cos(\phi) - x_{0j} - R\cos(\omega)\right]^2 + \left[y_{0i} - y_{0j}\right]^2 \dots \\ +\left[z_{0i} + (R-r)\sin(\phi) - z_{0j} - R\sin(\omega)\right]^2\end{matrix}} \tag{7.15}$$

$$d(P_{io}, P_j) = \sqrt{\begin{matrix}\left[x_{0i} + (R+r)\cos(\phi) - x_{0j} - R\cos(\omega)\right]^2 + \left[y_{0i} - y_{0j}\right]^2 \dots \\ +\left[z_{0i} + (R+r)\sin(\phi) - z_{0j} - R\sin(\omega)\right]^2\end{matrix}} \tag{7.16}$$

$$d(P_{ii}, P_{j'}) = \sqrt{\begin{matrix}\left[x_{0i} + (R-r)\cos(\phi) - x_{0j} - R\cos(\omega)\right]^2 + \left[y_{0i} - y_{0j}\right]^2 \dots \\ +\left[z_{0i} + (R-r)\sin(\phi) - z_{0j} - 2h - R\sin(\omega)\right]^2\end{matrix}} \tag{7.17}$$

$$d(P_{io}, P_{j'}) = \sqrt{\begin{matrix}\left[x_{0i} + (R+r)\cos(\phi) - x_{0j} - R\cos(\omega)\right]^2 + \left[y_{0i} - y_{0j}\right]^2 \dots \\ +\left[z_{0i} + (R+r)\sin(\phi) - z_{0j} - 2h - R\sin(\omega)\right]^2\end{matrix}} \tag{7.18}$$

Where

x_{0n}, y_{0n}, y_{0n} are the Cartesian coordinates for the point at the center of ring *n*, where n=*i* or *j*

Other terms are defined in Equations 7.8-7.11

For each g-function calculation there are $\left(N_{ring}\right)^2$ calculations of the double integral and for every Slinky GHE 76 g-functions are calculated. This can lead to prohibitively long calculation times to get the g-functions for engineering design purposes. In order to improve the computation speed, three improvements were applied by Xiong (2014) to reduce the number of calculations required.

By taking advantage of symmetry in the Slinky GHE configuration the temperature perturbations of only a quarter of the rings need to be considered to get the average tube wall temperature for the system. Constraints on the configuration definitions make this simplification possible.

As the distance between rings increases the interaction between them decreases, thus rings that are sufficiently far away can be treated as a single point source or neglected entirely. An investigation suggested that rings more than the ring's diameter plus 10 m (33 ft) away could be neglected entirely and rings more than the ring's diameter plus 2.5 m (8.2 ft) away could be treated as point sources.

The final improvement is to make use of the constraints on the system definition once again. Within the Slinky GHE the spacing between rings and the ring diameters are set, constant values. This means that the distance between any two rings or points on rings is likely to be repeated many times; therefore, by saving the temperature perturbations based on the spacing between points a significant number of calculations can be skipped. For example, the temperature response of a ring to itself is the same for all rings in the GHE.

These improvements provide a significant reduction in the computation time. Implementing the method in FORTRAN also provided a boost in computation speed.

7.4 Implementation

The Slinky GHE model was implemented in GLHEPro along with the other horizontal straight pipe GHE option. The majority of the system definitions take place within a single form as shown in the following sections.

7.4.1 Interface in GLHEPro

A series of inputs are necessary to model a Slinky GHE. Figure 7-4 shows the dialog box in GLHEPro V5.0 where these values can be defined. Several of these inputs are shown in Figures 7-5 and 7-6. Required inputs include:

- Active Tube Length per Trench (L_t) is the amount of tubing used to create the slinky rings in each trench. The length of tubing is likely to be a better constraint than the trench length for design purposes.
- Number of Parallel Trenches. Each trench is assumed be parallel with each other and contain the same number of rings.
- The Distance Between trenches (g), or gap, defines the center to center spacing between the trenches.

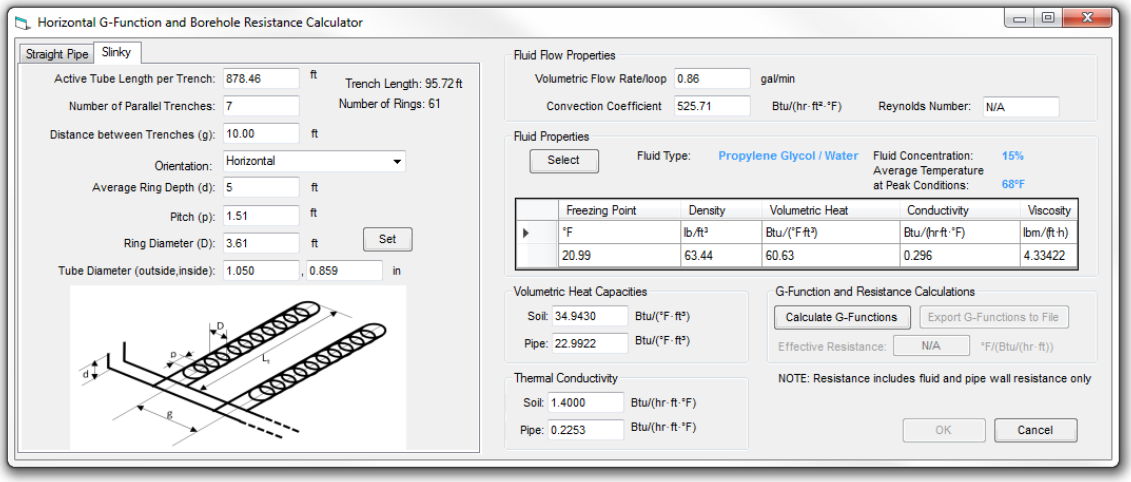

Figure 7-4: Input dialog in GLHEPro for a Slinky GHE

- The Orientation describes the installed orientation of the Slinky rings. The horizontal orientation is shown in Figure 7-5 and the vertical shown in Figure 7-6.

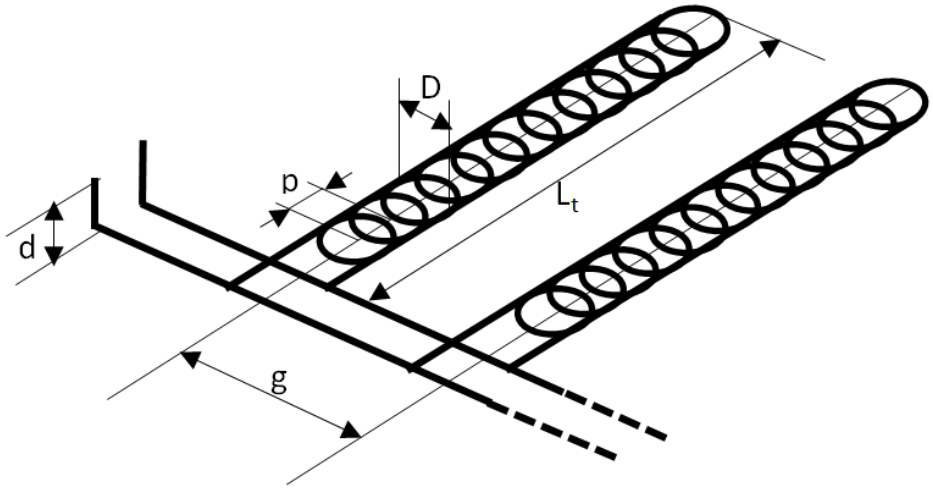

Figure 7-5: Slinky GHE with horizontally oriented rings

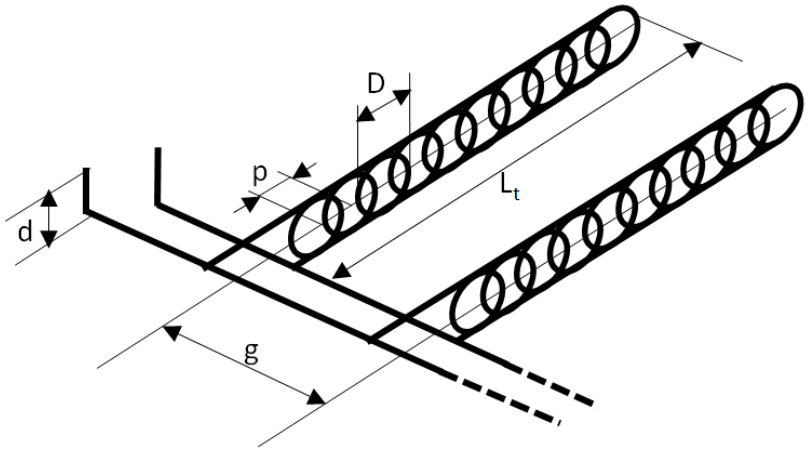

Figure 7-6: Slinky GHE with vertically oriented rings

- The Average Ring Depth (d) defines the average depth at which the rings are buried; this coincides with the depth at which the center of the ring is buried.
- The Pitch (p) is the distance between the centers of neighboring loops or rings within the same row or trench.
- The Ring Diameter (D) is the diameter of the rings or loops within the Slinky GHE
- The Tube Diameter defines the outside and inside tube diameter.

The effective resistance calculated for Slinky GHE in GLHEPro consists only of the tube and fluid convective resistance. GLHEPro will warn the user if systems with more than 100 trenches are selected; large systems may still have a long runtime. The number of rings per trench is limited to 2000; at this point additional rings will provide a negligible change in the system response.

7.4.2 Simulation and Sizing

System temperatures are calculated using the standard methodology applied in GLHEPro as described in Section 1.2.4 except with the time scale, t_s, set to a constant value of 3600 seconds. The ground temperatures used in the temperature calculations are calculated using Xing's methods (2014) described in Chapter VI. This allows for some of the temperature effects due to the seasonal weather change to be accounted for in the simulation.

The method used for sizing a Slinky GHE assumes that the system will maintain a set number of trenches with the given spacing and adjusts the number of rings per trench. This is done by optimizing the required tube length per trench until it converges on a number of rings.

7.5 Sample Results

Using the inputs for the ASHRAE headquarters in Atlanta, Georgia, as defined in Section 3.3.1.3, the sizing results for straight horizontal and horizontal slinky GHE are compared. Table 7-1 gives an overview of the ASHRAE building GSHP system specifications. The straight horizontal configurations have options to use two or four tubes per trench and the slinky GHE allows the rings to be laid flat in the bottom of the trench (horizontal) or laid upright in a narrow trench (vertical).

As shown in Table 7-1, the vertical borehole configuration consisted of 12 boreholes each 427 feet (130 meters) deep. Vertical boreholes do not require a large amount of land to install; this vertical system was installed under the parking lot. The array of vertical boreholes, not including

the horizontal connective piping, was installed under a 25 x 125 ft. (7.6 x 38 m) surface area. Horizontal GHE systems require a larger area of land for installation, which may be a limiting factor on their design.

Table 7-1: Overview of specifications for the sized GSHP system at ASHRAE headquarters in Atlanta, Georgia

Variables	
Borehole configuration	12:2x6
Borehole depth, m (ft.)	130 (427)
U-tube inner diameter, mm (in.)	34.5 (1.36)
U-tube outer diameter, mm (in.)	42.5 (1.66)
Undisturbed Ground Temperature, °C (°F)	20.3 (68.6)
Total System flow rate, L/s (GPM)	9.5 (150)
Sizing duration, years	5
Sizing Temperature limits, °C (°F)	
Maximum HP EWT***, °C (°F)	30 (99.8)
Minimum HP EWT***, °C (°F)	10 (51.2)

The ASHRAE building is on a lot with approximately 98,000 ft^2 (9,100 m^2) including the building footprint as shown in Figure 7-7 taken from Google Maps. If only the parking lots are considered as areas in which a horizontal GHE can be installed then the system size must be limited to approximately 54,000 ft^2 (5,000 m^2), or a 300x100ft (91.4x30.5 m) space. The spacing and number of trenches used in the horizontal GHE definitions shown in Table 7-2 and 7-3 were set in an attempt to allow the system design to fit within the available space.

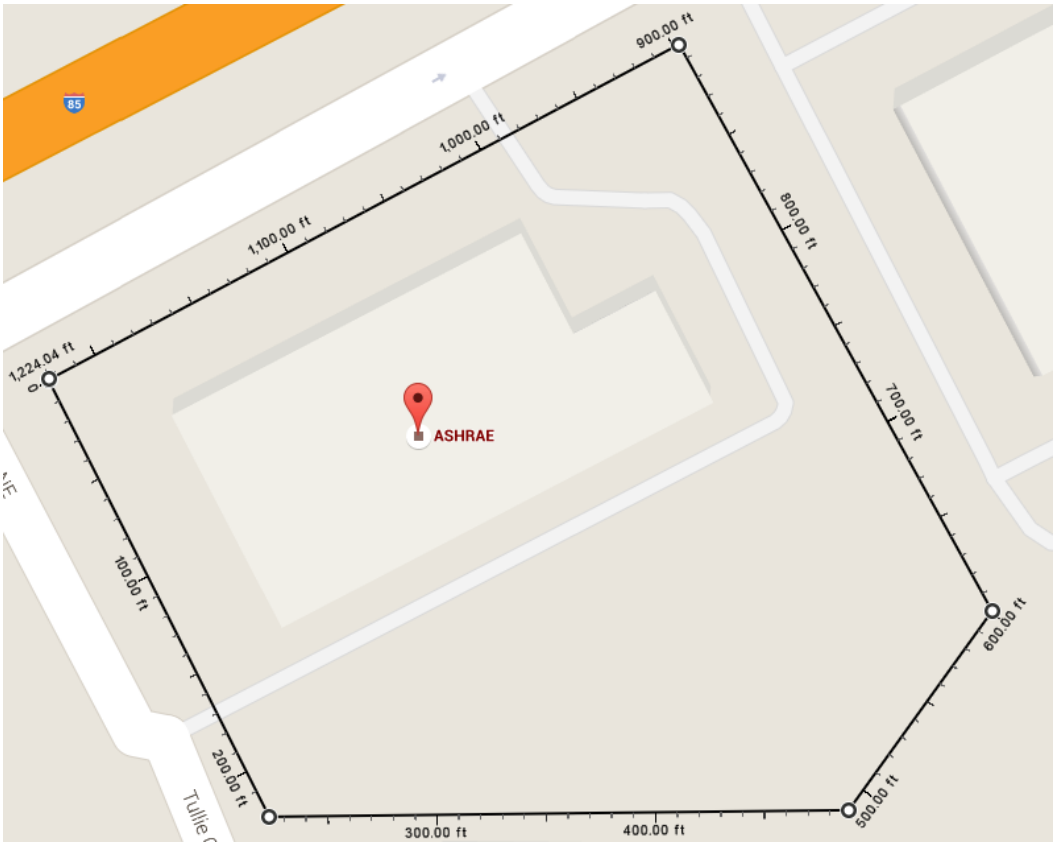

Figure 7-7: Area available at ASHRAE Headquarters in Atlanta, Georgia. (Google 2016)

Table 7-2 gives the inputs for the straight pipe horizontal GHE. This horizontal system was defined to have 24 trenches with the aim of sizing trenches around 200 ft. (61 m) long. The tube spacing (i.e. distance between tubes in the same trench) can be significantly larger in horizontal installations because it is no longer constrained by a maximum borehole diameter. Using a 24 inch (610 mm) tube spacing as opposed to a 0.73 inch (18.5 mm) shank spacing should lead to a horizontal GHE with less active trench length overall than the vertical system has in total active borehole length.

Table 7-2: Sample Horizontal straight pipe GHE definition

Number of Trenches	24
Distance between trenches, m (ft.)	3.0 (10)
Configuration	Single or Double (see results)
Avg. Burial Depth, m (ft.)	1.83 (6.00)
Tube ID, mm (in.)	34.50 (1.36)
Tube OD, mm (in.)	42.16 (1.66)
Tube Spacing, mm (in.)	609.60 (24.00)
Fluid factor	1

Table 7-3 gives the inputs for the slinky GHE. Many of the inputs were selected to be the same as those used for the horizontal straight pipe case. GLHEPro V5.0 offers two configurations for slinky GHE and both are considered in this comparison.

Table 7-3: Sample Horizontal slinky GHE definition

Number of Trenches	24
Distance between trenches, m (ft.)	3.0 (10)
Configuration	Horizontal or Vertical (see results)
Avg. Burial Depth, m (ft.)	1.83 (6.00)
Tube ID, mm (in.)	34.50 (1.36)
Tube OD, mm (in.)	42.16 (1.66)
Ring Diameter, m (ft.)	0.76 (2.50)
Pitch, m (ft.)	0.46 (1.50)
Fluid factor	1
Effective resistance, K·m/W (°F/ (Btu/(hr. ft.)))	0.0809 (0.1400)

The results shown in Table 7-4 were calculated using a constant ground temperature of 68.6°F (20.3°C) as was measured for the undisturbed ground temperature at the site in Atlanta. For this comparison of horizontal GHE, the Slinky GHE requires the least area to handle the load but requires the most tubing. Note that there is only one set of outputs for the Slinky GHE; this is because the sizing results were the same, regardless of the configuration (Horizontal/Vertical) used. This is because the spacing between trenches is large enough that there is very little

interaction between the trenches and the ground temperature was assumed to be a constant value throughout the simulation.

Table 7-4: Horizontal GHE sizing results in Atlanta, Georgia, with a constant undisturbed ground temperature

Configuration	Straight, 2 tubes		Straight, 4 tubes		Slinky	
Sized Trench Length, m (ft.)	38.96	(127.85)	26.29	(86.25)	17.68	(58.00)
Total Trench Length, m (ft.)	935.2	(3068.4)	630.9	(2070.0)	424.3	(1392.0)
Total Tube Length, m (ft.)	1870.5	(6136.8)	2523.7	(8280.0)	2937.6	(9637.9)
GHE surface width, m (ft.)	73.15	(240.00)	73.15	(240.00)	73.15	(240.00)
GHE surface length, m (ft.)	38.97	(127.85)	26.29	(86.25)	17.68	(58.00)
GHE surface Area, m^2 (ft^2)	2851	(30684)	1923	(20700)	1293	(13920)
Effective resistance, K·m/W (°F/(Btu/(hr ft.)))	0.1273	(0.2203)	0.0823	(0.1425)	0.0809	(0.1400)

Figure 7-8 shows the correlation between trench length and tube length for each case considered. As the trench length decreases between the configurations, the tube length increases.

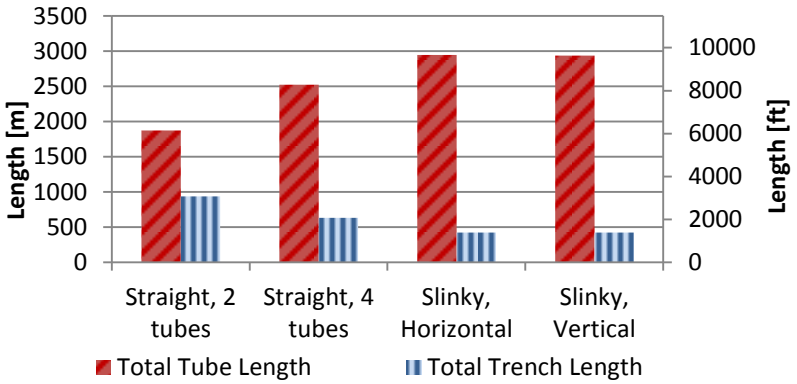

Figure 7-8: Total tube and trench length for each GHE configuration, includes all 24 trenches

If the ground temperature model described in Chapter VI is used, the ground temperature at the average borehole depth will vary throughout the year as shown in Figure 7-9. This variation in the ground temperature reduces the effectiveness of the horizontal GHE systems because the ground temperature variations are usually not beneficial; that is, the peak cooling loads tend to

occur when the ground temperature is warmer and the peak heating loads when the ground temperature is cooler. The average undisturbed ground temperature for this location is 64.0°F compared to the 68.6°F that was experimentally measured.

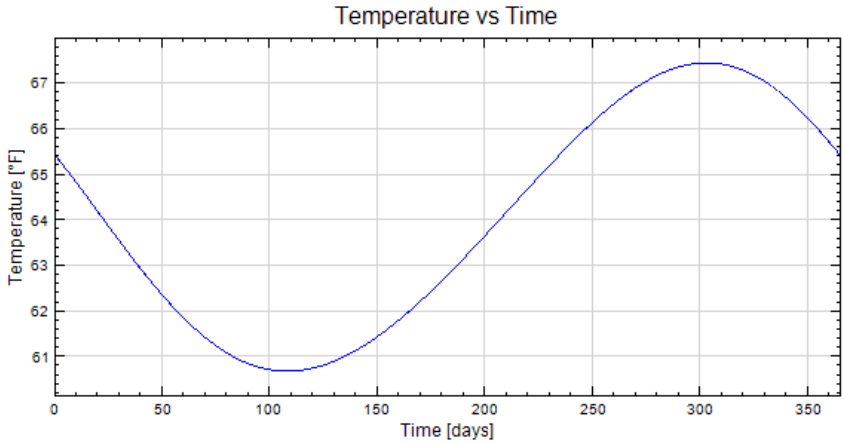

Figure 7-9: Temperature vs. Time plot for Atlanta-Hartsfield-Jackson Intl. Airport at a depth of 6 feet

Accounting for the seasonal variation in the ground temperature leads to longer required trench lengths as shown in Table 7-5. The system size increases by 34%, 26%, and 21% for Straight (2 tube), Straight (4 tube), and Slinky GHE respectively. A large portion of the increase in GHE size is due to a shift in the constraints on the GHE size. With a constant ground temperature the GHE size was set by the minimum temperature entering the heat pump. Using the varying ground temperature causes the GHE size to be constrained by the maximum temperature entering the heat pump instead.

Table 7-5: Horizontal GHE sizing results in Atlanta, Georgia, with varying undisturbed ground temperature

Configuration	Straight, 2 tubes		Straight, 4 tubes		Slinky	
Sized Trench Length, m (ft.)	52.26	(171.45)	33.16	(108.80)	21.34	(70.00)
Total Trench Length, m (ft.)	1254.2	(4114.8)	795.9	(2611.2)	512.1	(1680.0)
Total Tube Length, m (ft.)	2508.4	(8229.6)	3183.6	(10444.8)	3593.4	(11789.3)
System width, m (ft.)	73.15	(240.00)	73.15	(240.00)	73.15	(240.00)
System length, m (ft.)	52.26	(171.45)	33.16	(108.80)	21.34	(70.00)
System Area, m^2 (ft^2)	3823	(41148)	2426	(26112)	1561	(16800)
Effective resistance, K·m/W (°F/(Btu/(hr ft.)))	0.1273	(0.2203)	0.0823	(0.1425)	0.0809	(0.1400)

Now, which of these possible GHE designs could be installed at the ASHRAE building assuming that all of the GHE were to be placed beneath the parking lots? On the basis of total surface area required, all of the considered configurations could fit; but, for the Straight (2 tube) configuration the actual system dimensions are too large to fit beneath the parking lot.

These results should not be directly compared to a vertical GHE size because the spacing of the tubes within the trenches is much larger than can be used in the typical borehole. If a horizontal system with the exact same dimensions and relative configuration as a vertical system was modeled, it is expected that the horizontal GHE would require a longer active length in the GHE due to surface interactions.

Furthermore, the ground temperature model discussed in Chapter VI is used in this example even though it was not originally designed to model the disturbed ground temperatures beneath buildings or parking lots. The ground temperature model was designed to model the ground temperature at undisturbed sites covered with vegetation: either short or tall grass. The actual average ground temperature for this location at a depth of 6 feet is expected to be higher.

The final design for any installation should be based on many factors, not just minimizing the trench or borehole length. As shown in the two sets of results, the ground temperature used to

model the horizontal systems is very important and can have significant effects on the GHE size. Specifying the ground temperature for horizontal systems is even more important than for vertical systems because the seasonal temperature variation cannot be neglected at the burial depths typically used for horizontal systems.

7.6 Conclusions

The Slinky ground heat exchanger (GHE) model of Xiong (2014; Xiong et al. 2015) has been implemented in GLHEPro V5.0. It offers the option to calculate the g-functions (temperature response functions) for Slinky GHE systems with rings installed in a vertical or horizontal orientation. An analogous model for straight horizontal GHE with two or four tubes per trench was also developed using the methodology discussed in Chapter II. A comparison of the horizontal straight pipe model and the horizontal slinky model shows that, while a slinky GHE may require less trench length in total, it requires significantly more tubing per unit length of trench.

The horizontal slinky and horizontal straight pipe GHE model add significant new simulating and sizing options to GLHEPro V5.0. The g-function values for both of these models can be output from the program to allow them to be used in other external simulations in the future.

CHAPTER VIII

CONCLUSIONS AND RECOMMENDATIONS

The GLHEPro design tool has been updated and modified many times over the years. Most additional features are the result of graduate research which produced a thesis or creative component in addition to the work done on the program. This thesis adds to work done on the design tool and corresponds with the release of GLHEPro V5.0. Over the course of the development of GLHEPro V5.0 the following features and improvements were implemented:

- The Free Placement Finite Line Source (FPFLS) model was implemented to allow users to model systems of boreholes with varying lengths and inclinations.
- An option to calculate the effective borehole thermal resistance and account for short circuiting resistance. This can be significant for very long boreholes or boreholes with near laminar flow rates.
- An option to calculate the effective borehole thermal resistance for groundwater-filled single U-tube boreholes.
- A series of improvements to the interpolation of the library g-functions for vertical borehole configurations reduces GHE oversizing between tabulated data points.
- A new ground temperature database based on the methodology of Xing (2014) gives undisturbed ground temperatures for locations around the globe. Previous approximations provided little guidance for locations outside continental United States.

- The option to model a straight horizontal trench has been added using the FPFLS methodology.
- The option to model a horizontal slinky GHE has been added.
- An hourly simulation for vertical standing column wells has been completed.
- A general hourly simulation option for vertical and inclined boreholes was created based on the original GLHESim program. This allows the hourly temperature response for the system to be modeled.
- The option to specify the size of the supplemental device during the hybrid sizing simulation.

More minor additions include

- A new installation program
- An updated User Manual
- Additional Heat Pumps records for the simple heat pump model used in GLHEPro
- A new correlation for the convection in the annulus of a concentric tube
- Completion of the transition from Visual Basic 6.0 to VB.NET

Several of these improvements are discussed in detail in this thesis, others are not. One of the major improvements added to the program was the Free Placement Finite Line Source (FPFLS) model which allows for boreholes placed with irregular spacing in the horizontal plane and borehole inclination from vertical. A validation of the FPFLS method then shows that the resulting system sizes give good results when compared with four instrumented installations and the original methodology used in GLHEPro Version 4.1 and earlier. Then a method for accounting for short circuiting in the borehole thermal resistance calculations is introduced. The thermal borehole resistance and effective resistance can be calculated for grouted and groundwater filled boreholes. Next, the effects of interpolation of the library g-function values

were investigated and a series of improvements suggested and implemented. Finally, an improved model for the undisturbed ground temperature for global locations and a horizontal slinky GHE configuration were added to GLHEPro V5.0 based on existing methodologies. The following specific conclusions were reached:

- The FPFLS method implemented gives designers a convenient method for generating the g-functions for systems with boreholes that are not installed in a grid and have varying depths or inclinations to vertical.
- The sizing comparison showed that the FPFLS method gives reasonable sizing results; the percent difference between the sizing results of library g-functions and the FPFLS g-functions is less than 2% with the FPFLS method tending to size shorter borehole lengths by about 1 m (2 ft.). Both methods oversize the GHE between 2-12% when compared to the experimental borehole lengths.
- Limiting the FPFLS model to 30 boreholes or less guarantees that the simulation and sizing results should be conservative without placing other restrictions on the borehole placement.
- Short circuiting is more significant for GHE with long boreholes or relatively slow flow rates and groundwater filled boreholes. Groundwater filled boreholes also tend to have a lower borehole resistance.
- Interpolation of the library g-functions can be improved by interpolating between the logarithm of both the borehole spacing to depth ratio (B/H) and the g-function values.
- Replacing extrapolation with interpolation for systems with very large spacing between boreholes limits the g-functions to, at best, the single borehole case. This can be done by interpolating with the single borehole case where infinity is approximated by $B/H = 1.3$.
- The ground temperature used for simulating or sizing a system has a large effect on the simulation results for all GHE models considered. The ground temperature model for

horizontal systems is especially important because the surface effects can cause the ground temperature to vary throughout the year.

- Xing's (2014) ground temperature model gives the undisturbed ground temperatures for locations with short or tall grass as the ground cover. For urban or paved locations where the ground temperature is disturbed, the model may not accurately model the ground temperature. This may cause issues during design if not properly considered.

At the defense of this thesis, Göran Hellström attended and answered some of the questions about the assumptions made in the calculation of the g-functions used in GLHEPro and those generated by Eskilson. An active borehole length of 110 meters was used with a burial depth (or insulated depth) of 5 meters (Hellström 2016). The discrepancies between the library g-functions of Hellström and Eskilson are due to changes in the gridding used in the numerical models. The difference between the library g-functions and the finite line source g-functions are due to the approximations and assumptions made by the finite line source methods.

There are a great many improvements that can still be made to the methodology for designing ground source heat exchangers in general and to GLHEPro in particular. The following are recommended for future work:

- The Peak Load Analysis Tool included with GLHEPro Program could be automated and included in the main program code rather than an accompanying spreadsheet. This has been requested by the users. Also, the current method of selecting the peak heating and cooling durations can be difficult for users to understand.
- An effective borehole resistance value that is either updated for each month of simulation based on the average fluid temperature or simply calculated for each heating and cooling mode would provide increased accuracy to the system simulation. For grouted and groundwater filled boreholes the effective borehole resistance varies along with the fluid

temperatures. This is especially important for groundwater filled boreholes because the temperature of the fluid in the annulus drives the natural convection and has a large impact on the resistance.

- A validation for the horizontal model implemented with the FPFLS method should be done when experimental data becomes available. The current model produces reasonable sizing results but an experimental validation might suggest some improvements to the method.
- A horizontal model capable of modeling a single tube should be implemented. This would allow for the sizing and simulation of a wider variety of horizontal GHE.
- The correlations developed for calculating the convective resistance in the annulus of groundwater filled boreholes only treated single U-tube boreholes. If the methodology for calculating the natural convection effects within the annulus of a double U-tube borehole is developed it should be implemented in the program.
- Investigation into the effects of the heat pump model used in GLHEPro with an hourly, as opposed to monthly, simulation time step should be considered. Currently, a simple heat pump model is used in GLHEPro V5.0. With the hourly simulation, it might be beneficial to implement a more detailed heat pump model.
- Implementing the monthly ground temperature of Xing (2014) as an average of the average borehole temperatures along each borehole length rather than the midpoint borehole temperature may improve the ground temperature approximation. The midpoint borehole temperature works well for deep boreholes where the surface effects are small. For short boreholes the surface effects may have a larger effect on the system that may be captured by averaging the temperatures along the borehole length.
- The FPFLS model offers many new configurations for sizing and simulation. Using a more complex sizing method for the FPFLS model would allow more complex systems

to maintain relations between boreholes during sizing. This would be helpful for horizontally drilled boreholes or for sizing both depth and spacing at the same time. A possible method of implementing this may be to use a scaling factor to resize the system rather than adding a constant length to each borehole.

- Currently, GLHEPro does not allow horizontal systems to be simulated with an hourly time step. Adding the option to use an hourly simulation with the horizontal GHE configurations should be considered. The method should also be validated, if possible.
- Allow the FPFLS model to take into account flow rates that vary from borehole to borehole. This will occur for GHE that have boreholes with different depths if no active measures are taken to control the flows.
- Currently, GLHEPro V5.0 assumes that the system operates at a constant flow rate. Variable speed drives are readily available so allowing the hourly simulation to use variable fluid flow would offer users new options.
- Optimize the calculation method of the Free Placement Finite Line Source (FPFLS) g-functions to improve the computation time. Xiong (2014) implemented a series of improvements to his g-function calculations for slinky GHE. Similar methods may be applicable for the FPFLS model.

REFERENCES

ASHRAE. 2015. The Living Lab: access to ASHRAE Living Laboratory Trend Data. http://images.ashrae.biz/renovation/ Accessed 9/25/2015.

ANSYS. 2009. ANSYS FLUENT 12.0: User's Guide. http://users.ugent.be/~mvbelleg/flug-12-0.pdf Accessed 2/16/2016.

Austin, W., C. Yavuzturk, and J.D. Spitler. 2000. Development Of An In-Situ System For Measuring Ground Thermal Properties. *ASHRAE Transactions.* 106(1):365-379.

Bandos, T., Á. Montero, E. Fernández, J. Santander, J. Isidro, J. Pérez, P. Córdoba, and J. Urchueguía. 2009. Finite line-source model for borehole heat exchangers: effect of vertical temperature variations. *Geothermics*. 38:263-270.

Beier, R.A. 2011. Vertical temperature profile in ground heat exchanger during in-situ test. *Renewable Energy*. 36(5):1578-1587.

Beier, R.A., and M.D. Smith. 2002. Borehole thermal resistance from line-source model of in-situ tests. *ASHRAE Transactions*. 108(2):212-219.

Beier, R.A. M.D. Smith, and J.D. Spitler. 2011. Reference data sets for vertical borehole ground heat exchanger models and thermal response test analysis. *Geothermics*. 40:79-85.

Bennet, J., J. Claesson, and G. Hellström. 1987. Multipole Method to Compute the Conductive Heat Flows to and Between Pipes in a Composite Cylinder. Notes on Heat Transfer (3). Department of Building Technology and Mathematical Physics, Lund Institute of Technology, Sweden.

Carslaw, H. S. and J. C. Jaeger. 1959. *Conduction of Heat in Solids*. Second Edition. Oxford: Clarendon Press.

Çengel, Y.A. and A.J. Ghajar. 2011. *Heat and Mass Transfer*. 4th ed. McGraw-Hill. Page 251,489.

Chong, C.S.A., G. Gan, A. Verhoef, R.G. Garcia, and P.L. Vidale. 2013. Simulation of thermal performance of horizontal slinky-loop heat exchangers for ground source heat pumps. *Applied Energy*. 104:603-610.

Cimmino M. and M. Bernier. 2014. A semi-analytical method to generate g-functions for geothermal bore fields. *International Journal of Heat and Mass Transfer*. 70: 641-650.

Claesson, J. and P. Eskilson. 1987. Conductive Heat Extraction by a Deep Borehole: Analytical Studies. Dept. of Mathematical Physics, Lund Institute of Technology, Sweden.

Claesson, J. and P. Eskilson. 1987a. Conductive Heat Extraction by Thermally Interacting Deep Boreholes. Dept. of Mathematical Physics, Lund Institute of Technology, Sweden.

Claesson, J. and P. Eskilson. 1987b. Thermal Analysis of Heat Extraction Boreholes: Conductive Heat Extraction by a Deep Borehole: Thermal Analyses and Dimensioning Rules. Doctoral Thesis. Dept. of Mathematical Physics, Lund University, Sweden.

Claesson, J. and S. Javed. 2011. An analytical method to calculate borehole fluid temperatures for time-scales from minutes to decades. *ASHRAE Transactions*. 117(2): 279-288.

Claesson, J. and G. Hellström. 2011. Multipole method to calculate borehole thermal resistances in a borehole heat exchanger. *HVAC&R Research*, 17(6):895-911.

Congedo, P.M., G. Conlangelo, and G. Starace. 2012. CFD simulations of horizontal ground heat exchangers: A comparison among different configurations. *Applied Thermal Engineering*. 33-34:24-32.

Cui, P., H. Yang, and Z. Fang. 2006. Heat transfer analysis of ground heat exchangers with inclined boreholes. *Applied Thermal Engineering*. 26: 1169-1175.

Cullin, J.R. 2008. Improvements in Design Procedures for Ground Source and Hybrid Ground Source Heat Pump Systems. MS Thesis. Oklahoma State University. Stillwater, OK.

Cullin, J.R. and J.D. Spitler. 2011. A computationally efficient hybrid time step methodology for simulation of ground heat exchangers. *Geothermics*. 40(2):144-56.

Cullin, J.R. 2014. Advancements in the simulation of ground source heat pump systems. Ph.D. Thesis. Oklahoma State University. Stillwater, Oklahoma.

Cullin, J. R., J. D. Spitler, C. Montagud, F. Ruiz-Calvo, S. J. Rees, S. S. Naicker, P. Konečný and L. E. Southard. 2015. Validation of vertical ground heat exchanger design methodologies, *Science and Technology for the Built Environment*. 21:2, 137-149.

Cullin, J.R., C. Montagud, F. Ruiz-Calvo, and J.D. Spitler. 2014. Experimental validation of ground heat exchanger design methodologies using real monitored data. *ASHRAE Transactions.* 120(2):357-639.

Eklöf, C. and S. Gehlin. 1996. TED - a mobile equipment for thermal response test. Master's Thesis. Lulca University of Technology, Sweden.

Eskilson, P. 1987a. Thermal Analysis of Heat Extraction Boreholes. Doctoral Thesis. Lund University, Sweden.

Eskilson, P. 1987b. PC-programs for Dimensioning of Heat Extraction Boreholes. Departments of Building Technology and Mathematical Physics, Lund Institute of Technology, Sweden.

Eskilson, P. 1987c. Temperature Response Function g for 12 Borehole Configurations. Notes on Heat Transfer 5-1987. Departments of Mathematical Physics and Building Technology, Lund University, Sweden.

Ewbank and Assocaites. 2008. In-situ Thermal Conductivity Report, Direct Measurement of Thermal Conductivity Test Results: ASHRAE Headquarters Renovated Facility.

Fisher, D.E., S.J. Rees, S.K. Padhmanabhan, and A. Murugappan. 2006. Implementation and validation of ground-source heat pump system models in an integrated building and system simulation environment. *HVAC&R Research.* 12(3A):693–710.

Fourier, J. 1878. *The analytical theory of heat.* Trans. Alexander Freeman, M.A. Cambridge: The University Press.

Fujii, H., K. Nishi, Y. Komaniwa, and N. Chou. 2012. Numerical modeling of slinky-coil horizontal ground heat exchangers. *Geothermics*. 41: 55-62.

Gaia Geothermal. 2014. Ground Loop Design™ Premier 2014 User's Guide. Celsia LLC.

Gentry, J.E., J.D. Spitler, D.E. Fisher, and X. Xu. 2006. Simulation of Hybrid Ground Source Heat Pump Systems and Experimental Validation. Proceedings of the *7th International Conference on System Simulation in Buildings.* Liège. December 11-13, 2006.

Geothermal International. 2009. De Montfort University, Leicester. Geothermal Pipe Work Layout, drawing no. 103 rev. AB. Provided by Simon Rees, September 24, 2015.

Google. 2016. Google Maps: Map data. Accessed 3/22/2016. https://www.google.com/maps/place/ASHRAE/@33.8341056,-84.3294285,19z/data=!4m2!3m1!1s0x88f506233606925b:0x3608df8501dd7ccc?hl=en

Hellström, G. 1991. *Ground Heat Storage: Thermal Analyses of Duct Storage Systems*. Department of Mathematical Physics, University of Lund, Sweden.

Hellström, G. 2016. Personal e-mail sent from Dr. Göran Hellström to Dr. Jeffrey Spitler. Subject: Re: Grundmann Thesis: Improved Design Methods for Ground Heat Exchangers. <gh.neoenergy@gmail.com> Sent April 5, 2016.

Hellström, G., and B. Sanner. 1994. Software for dimensioning of deep boreholes for heat extraction. Proceedings of *Calorstock 1994*, Espoo/Helsinki, Finland, pp. 195–202.

Hern, S.A. 2004. Design of an Experimental Facility for Hybrid Ground Source Heat Pump Systems. Master's Thesis. Oklahoma State University. Stillwater, OK.

Incropera, F.P. and D.P. DeWitt. 2002. *Introduction to Heat Transfer*. 4th ed. John Wiley & Sons, Inc. p. 459, 469, 470.

Ingersoll, L. R. and H. J. Plass. 1948. *Theory of Ground Pipe Heat Source for the Heat Pump*. Heating Piping and Air Conditioning 20:119-122.

Ingersoll, L.R., O.J. Zobel, and A.C. Ingersoll. 1948. Heat Conduction With Engineering and Geological Applications. New York/Toronto/London: McGraw-Hill Book Company, Inc.

Javed, S. and J.D. Spitler. 2016. Calculation of borehole thermal resistance. In S.J. Rees *Advances in ground-source heat pump systems*. London: Woodhead Publishing. In press.

Kavanaugh, S.P. 2010. Ground Source Heat Pump System Designer GshpCalc Version 5.0: An Instruction Guide for Using a Design Tool for Vertical Ground-Coupled, Groundwater and Surface Water Heat Pump Systems. Downloaded from www.geokiss.com.

Kavanaugh, S.P. and K. Rafferty. 2014. *Geothermal Heating and Cooling: Design of Ground-Source Heat Pump Systems*. American Society of Heating, Refrigerating and Air-Conditioning Engineers, Inc.

Kavanaugh, S.P. and K. Rafferty. 1997. *Ground-Source Heat Pumps: Design of Geothermal Systems for Commercial and Institutional Buildings*. American Society of Heating, Refrigerating and Air-Conditioning Engineers, Inc.

Lamarche, L. 2011. Analytical g-functions for inclined boreholes in ground-source heat pump systems. *Geothermics*. 40: 241-249.

Lamarche, L. and B. Beauchamp. 2007. A new contribution to the finite line-source model for geothermal boreholes. *Energy and Buildings.* 39: 188-189.

Li, H., K. Nagano, and Y. Lai. 2012. A new model and solutions for a spiral heat exchanger and its experimental validation. *International Journal of Heat and Mass Transfer*. 55:4404-4414.

Liu, X., and G. Hellstrom. 2006. Enhancements of an integrated simulation tool for ground-source heat pump system design and energy analysis. Proceedings of the *10th International Conference on Thermal Energy Storage*. Richard Stockton College of New Jersey, 2006.

Malayappan, V. 2012. Implementation of a Finite Line Source Solution for Sizing Borehole Heat Exchangers. M.S. Creative Component Report, Oklahoma State University, Stillwater, Oklahoma.

Malayappan, V., J.D. Spitler. 2013. Limitation of Using Uniform Heat Flux Assumptions in Sizing Vertical Borehole Heat Exchanger Fields. Proceedings of *Clima 2013*. Prague. June 16-19.

Manickam, A. 1996. Enhancements to a Windows based program for Design of Ground Loop Heat Exchangers. M.S. Creative Component. Oklahoma State University, Stillwater, OK.

Manickam, A. M. Dharapuram, R.D. Delahoussaye, and J.D. Spitler. 1996. *GLHEPRO for Windows: The Professional Ground Loop Heat Exchanger Design Software: Users Guide*

Version 2.06. School of Mechanical and Aerospace Engineering, Oklahoma State University, Stillwater, OK.

Marcotte, D. and P. Pasquier. 2008. On the estimation of thermal resistance in borehole thermal conductivity test. *Renewable Energy.* 33:2407–2415.

Marcotte, D. and P. Pasquier. 2009. The effect of borehole inclination of fluid and ground temperature for GLHE systems. *Geothermics*. 38:392-398.

Marshall, C.L. and J.D. Spitler. 1994. *GLHEPRO: The Professional Ground Loop Heat Exchanger Design Software: Users Guide*. School of Mechanical and Aerospace Engineering, Oklahoma State University, Stillwater, OK.

MathWorks. 2016. Matlab Software.MathWorks, Inc. http://www.mathworks.com/products/matlab/ Accessed January 21, 2016.

Mogensen, P. 1983. Fluid to Duct Wall Heat Transfer in Duct System Heat Storages. *International Conference on Subsurface Heat Storage in Theory and Practice*. Stockholm, Sweden, Swedish Council for Building Research, June 6-8.

Mokashi, S. et al. 2004. *GLHEPRO 3.0 for Windows: The Professional Ground Loop Heat Exchanger Design Software: Users Guide.* School of Mechanical and Aerospace Engineering, Oklahoma State University, Stillwater, OK.

Montagud, C., J.M. Corberán, Á. Montero and J.F. Urchueguía. 2011. Analysis of the energy performance of a ground source heat pump system after five years of operation. *Energy and Buildings.* 43:3618-3626.

Naicker, S.S., and S.J. Rees. 2011. Monitoring and Performance Analysis of Large Non-domestic Ground Source Heat Pump Installation. *CIBSE Technical Symposium*. De Montfort University, Leicester UK, September 6-7, 2011.

Oklahoma State University (OSU). Division of Engineering Technology, and National Rural Electric Cooperative Association (NRECA). 1988. *Closed-loop/ground-Source Heat Pump Systems: Installation Guide.* Stillwater, Okla: Distributed by International Ground Source Heat Pump Association.

Oklahoma State University (OSU). 2004. *GLHEPRO 3.0 for Windows: The Professional Ground Loop Heat Exchanger Design Software: Users Guide.* School of Mechanical and Aerospace Engineering, Oklahoma State University, Stillwater, OK.

Oklahoma State University (OSU). 2007. *GLHEPRO 4.0 for Windows: The Professional Ground Loop Heat Exchanger Design Software: Users Guide*. School of Mechanical and Aerospace Engineering, Oklahoma State University, Stillwater, OK.

Oklahoma State University (OSU). 2016a. *GLHEPRO 4.1 for Windows: The Professional Ground Loop Heat Exchanger Design Software: Users Guide*. School of Mechanical and Aerospace Engineering, Oklahoma State University, Stillwater, OK.

Oklahoma State University (OSU). 2016b. *GLHEPRO 5.0 for Windows: The Professional Ground Loop Heat Exchanger Design Software: Users Guide*. School of Mechanical and Aerospace Engineering, Oklahoma State University, Stillwater, OK.

Paul, N.D. 1996. The effect of grout thermal conductivity on vertical geothermal heat exchanger design and performance. MS Thesis, South Dakota State University, Brookings, SD.

Rees, S. 2015. Personal e-mail sent from Dr. Simon Rees to Dr. Jeffrey Spitler. Subject: Hugh Aston Building bore field. <S.J.Rees@leeds.ac.uk> Sent September 24, 2015.

Remund, C.P. 1999. Borehole Thermal Resistance: Laboratory and Field Studies. *ASHRAE Transactions.* 105(1):439-445.

Ruiz-Calvo, F., and C. Montagud. 2014. Reference data sets for validating GSHP system models and analyzing performance parameters based on a five-year operation period. *Geothermics*. 51, 417-428.

Sanner, B., G. Hellström, J. Spitler and S. Gehlin. 2005. Thermal Response Test – Current Status and World-Wide Application. Proceedings of the *World Geothermal Congress 2005*. Antalya, Turkey. April 24-29, 2005.

Southard, L. 2013. MAE 5863 Project: Validation of the EnergyPlus Ground Loop Heat Exchanger Model. Oklahoma State University Class Project Presentation.

Spitler, J.D. 2000. GLHEPRO -- A Design Tool For Commercial Building Ground Loop Heat Exchangers. Proceedings of the *Fourth International Heat Pumps in Cold Climates Conference*. Aylmer, Québec. August 17-18, 2000.

Spitler, J.D. and M. Bernier. 2016. Vertical borehole ground heat exchanger design methods. In S.J. Rees *Advances in ground-source heat pump systems*. London: Woodhead Publishing. *In press.*

Spitler, J.D., and J. Cullin. 2008. Misconceptions Regarding Design of Ground-source Heat Pump Systems. Proceedings of the *World Renewable Energy Congress*. Glasgow, Scotland. July 20-25.

Spitler, J.D. and S.E.A. Gehlin. 2015. Thermal response testing for ground source heat pump systems-An historical review. *Renewable and Sustainable Energy Reviews*. 50:1125-1137.

Spitler, J.D., S. Javed and R. Kalskin Ramstad. 2016. Natural Convection in Groundwater-filled Boreholes used as Ground Heat Exchangers. *Applied Energy*. 164: 352-365.

Stewart, J. 2003. *Calculus*. 5th ed. Brooks/Cole. Pg. 560.

Thomson, W. 1880. Heat. Being the Article Contributed to the Encylopædia Britannica. Edinburgh: Adam and Charles Black.

Thomson, W. 1884. Compendium of the Fourier Mathematics for the Conduction of Heat in Solids, and the Mathematically Allied Physical Subjects of Diffusion of Fluids, and Transmission of Electric Signals through Submarine Cables. Article 72. Mathematical and Physical Papers, Volume II. Cambridge, University Press**:** 41-60.

University of Wisconsin Madison. 2013. A TRaNsient Systems Simulation Program. Accessed 3/19/2016. http://sel.me.wisc.edu/trnsys/index.html

Urchueguía, J.F., M. Zacarés, J.M. Corberán, Á. Montero, J. Martos, and H. Witte. 2008. Comparison between the energy performance of a ground coupled water to water heat pump system and an air to water heat pump system for heating and cooling in typical conditions of the European Mediterranean coast. *Energy Conversion and Management.* 49: 2917-2923.

Vaughn, M.R. 2014. Lessons Learned From ASHRAE HQ Renovation. *ASHRAE Journal.* 56(4): 14-30.

Whitehead, S. 1927. Determining Temperature Distribution - A Contribution to the Evaluation of the Flow of Heat in Isotropic Media. *The Electrician*. (August 19):225-226.

Witte, H.J.L., G.J. Van Gelder and J.D. Spitler. 2002. In situ measurement of ground thermal conductivity: a Dutch perspective. *ASHRAE Transactions*. 108(1):263-272.

Wu, Y., G. Gan, A. Verhoef, P.L. Vidale, and R.G. Gonzalez. 2010. Experimental measurement and numerical simulation of horizontal-coupled slinky ground source heat exchangers. *Applied Thermal Engineering*. 30:2574-2583.

Xing, L. 2014. Estimations of Undisturbed Ground Temperatures Using Numerical and Analytical Modeling. PhD Thesis. Oklahoma State University. Stillwater, OK.

Xiong, Z. 2014. Development and Validation of a Slinky™ Ground Heat Exchanger Model. Maste's Thesis. Oklahoma State University. Stillwater, OK.

Xiong, Z., D.E. Fisher, and J.D. Spitler. 2015. Development and validation of a Slinky™ ground heat exchanger model. *Applied Energy*. 141: 57-69

Xu, X., and J.D. Spitler. 2006. Modeling of Vertical Ground Loop Heat Exchangers with Variable Convective Resistance and Thermal Mass of the Fluid. Proceedings of the *10th International Conference on Thermal Energy Storage-Ecostock.* Pomona, NJ. 2006.

Yavuzturk, C., and J.D. Spitler. 1999. A Short Time Step Response Factor Model for Vertical Ground Loop Heat Exchangers. *ASHRAE Transactions*. 105(2): 475-485.

Yeung, D. 1996. Enhancements to a ground loop heat exchanger design program. Master's Thesis. Oklahoma State University. Stillwater, OK.

Young, T.R. 2004. Development, Verification, and Design Analysis of the Borehole Fluid Thermal Mass Model for Approximating Short Term Borehole Thermal Response. Master's Thesis. Oklahoma State University. Stillwater OK.

APPENDICES

APPENDIX A: FROM FOURIER'S POINT SOURCE TO INGERSOLL'S LINE SOURCE (1878-1948)

As noted in Chapter II there has been some confusion as to who originally developed the line source method. Some researchers point to a paper by Ingersoll and Plass (1948) and state that Lord Kelvin (Sir William Thomson) (1880) was the first to develop the line source. Others (Spitler and Bernier 2016) dispute this, stating that Kelvin makes no mention of an infinite line source model and merely gives a series of Fourier's solutions (1878).

An investigation into the derivation of the equation presented in the paper by Ingersoll and Plass (1948) suggests that, while both Fourier and Kelvin present an equation that can be used to derive the infinite line source, neither Fourier nor Kelvin actually derived an equation for the infinite line source as presented by Ingersoll and Plass.

Derivation of the Infinite Line Source

Kelvin[6] (Thomson 1884, p. 44) gave the equation for the instantaneous simple point-source in an infinite homogeneous solid as

$$v = \frac{Q\epsilon^{\frac{-r^2}{4\kappa t}}}{8\pi^{\frac{3}{2}}(\kappa t)^{\frac{3}{2}}} \qquad (A.1)$$

[6] This specific equation can be found in Article LXXII, Expression I, equation 10, page 58 of 515 of the PDF available for free download through Google Books.

$$x^2 + y^2 + z^2 = r^2 \tag{A.2}$$

$$\int_{-\infty}^{\infty}\int_{-\infty}^{\infty}\int_{-\infty}^{\infty} v dx dy dz = 4\pi \int_{0}^{\infty} v r^2 dr = Q \tag{A.3}$$

Where

v is the temperature response [°C]

Q is the heat per unit time over a given area [W m^{-2}]

κ is the thermal diffusivity of the ground [$m^2 s^{-1}$]

t is the time since the load at the heat source was applied [s]

r is the distance from the heat source to the point of interest [m]

x, y, z defines the point of interest assuming the heat source is at the origin

Fourier[7] (1878, p. 382) gave a similar equation for the case with free movement of heat in an infinite solid from a single point, or very small prismatic element, located at the origin with diffusion of heat in all directions. Note that a prismatic element is one with sides made of parallelograms and with two identical and parallel ends.

$$v = \left(\frac{1}{2\sqrt{\pi k t}}\right)^3 e^{\frac{-[x^2+y^2+z^2]}{4kt}} \int_{-\infty}^{\infty} dz \int_{-\infty}^{\infty} d\beta \int_{-\infty}^{\infty} f(z, \beta, \gamma) d\gamma \tag{A.4}$$

Where

v is the temperature response at a point P [°C]

k is the thermal diffusivity of the ground [$m^2 s^{-1}$]

[7] The specific equation referenced can be found in Chapter IX, Section II, Article 384, page 411/523 of the PDF available for free download through Google Books.

t is the time since the load at the heat source was applied [s]

x, y, z defines the point of interest *P*

$f(z, \beta, \gamma)$ represents the distribution of heat in the solid

z, β, γ defines the dimensions of the small prismatic heated element at the origin

$\int_{-\infty}^{\infty} dz \int_{-\infty}^{\infty} d\beta \int_{-\infty}^{\infty} f(z, \beta, \gamma) d\gamma$ is given to be the whole quantity of heat, *B*, which is contained in the solid (prismatic element)

From either of these equations, the point source equation given by Ingersoll et al. (1948) in equation 9.41d can be found.

$$T = \left(\frac{1}{2\sqrt{\pi\alpha t}}\right)^3 \int_{-\infty}^{\infty} \int_{-\infty}^{\infty} \int_{-\infty}^{\infty} e^{\frac{-[x^2+y^2+z^2]}{4\alpha t}} f(\lambda, \mu, \nu) d\lambda d\mu d\nu \qquad (A.5)$$

Where

T is the temperature response at a point *P* [°C]

α is the thermal diffusivity of the ground [m^2s^{-1}]

$f(\lambda, \mu, \nu)$ is the distribution of heat in the solid

λ, μ, ν are the dimensions of the small prismatic heated element at the origin

Note that there is a change of variable between the works of Fourier, Kelvin, and Ingersoll et al. Table A-1 shows the nomenclature that differs between the different publications.

Table A-1: Nomenclature use by Fourier, Kelvin, and Ingersoll et al. (1948)

Value	Fourier (1878)	Kelvin (Thomson 1884)	Ingersoll (1948)
Temperature	v	v	T
Thermal Diffusivity	k	κ	α
Heat distribution in the solid	$f(z,\beta,\gamma)$	$f(z,\beta,\gamma)$	$f(\lambda,\mu,\nu)$
Dimensions of the heated prismatic element	z,β,γ	z,β,γ	λ,μ,ν
Base of the natural logarithm	e	ϵ	e

Next say that $\eta = \frac{1}{2\sqrt{\alpha t}}$ and $x^2 + y^2 = r^2$. This gives:

$$T = \left(\frac{\eta}{\sqrt{\pi}}\right)^3 \int_{-\infty}^{\infty}\int_{-\infty}^{\infty}\int_{-\infty}^{\infty} e^{-r^2\eta^2} e^{-z^2\eta^2} f(\lambda,\mu,\nu) d\lambda d\mu d\nu \qquad (A.6)$$

To convert this into an infinite line source in an infinite medium it must be resolved down into a line instead of a volume. This equation is given in Ingersoll and Plass (1948, p146) as equation 9.8a.

$$T = S\left(\frac{\eta}{\sqrt{\pi}}\right)^3 e^{-r^2\eta^2} \int_{-\infty}^{\infty} e^{-z^2\eta^2} dz \qquad (A.7)$$

Where

S is the strength of the line source

The next step substitutes η back out and allows for the initial time at which the heat was applied to be nonzero by introducing τ. This equation is given in Ingersoll et al. (1948, p146) as equation 9.8b.

$$T = \frac{S'}{4\pi\alpha}\int_0^t \frac{e^{-\frac{r^2}{4\alpha(t-\tau)}}}{t-\tau} d\tau \qquad (A.8)$$

Where

S' is the strength of the line source per unit length

τ is the initial time [s]

The final substitution is that of β (Ingersoll et al. 1948).

$$\beta = \frac{r}{2\sqrt{\alpha(t-\tau)}} \qquad (A.9)$$

This is the equation for the infinite line source found in Ingersoll and Plass (1948) that is often attributed to Kelvin. The equation corresponds to equation 9.8d in the Ingersoll et al. (1948) text.

$$T = \frac{S'}{2\pi\alpha}\int_{r\eta}^{\infty}\frac{e^{-\beta^2}}{\beta}d\beta = \frac{S'}{2\pi\alpha}I(r\eta) = \frac{Q'}{2\pi k}I(r\eta) \qquad (A.10)$$

Where

Q' is the number of heat units released per unit of time per unit length of the line source.

$S' = \frac{Q'}{c\rho}$ is the strength of the line source per unit length

Conclusions

While Kelvin did present the instantaneous point source model in his publications, the same model can be found in Fourier's work. Neither Kelvin nor Fourier explicitly presents an infinite line source model and the point source model from which Ingersoll et al. (1948) derives his line source solution can definitely be attributed to Fourier as the original source. Kelvin presents his solution as a point source more clearly than Fourier which is likely why he tends to receive credit over Fourier.

APPENDIX B: INPUTS FOR EXAMPLES IN CHAPTER IV

Complete system definition for example used in Chapter IV. U.S. Customary or Imperial units are used for all inputs. Inputs are based on the default input file (.gli) supplied with GLHEPro V5.0 beta. Note that this is not a complete input file for GLHEPro V5.0 and contains only the inputs required for the comparison.

```
;Ver 5.0
;Borehole Profile and Monthly Loadings Table
;=========================================
Units IN (IP : 1; SI : 2)                = 1
Units OUT (IP : 1; SI : 2)                    = 1
;COMMON VERTICAL BH VARIABLES
Main Configuration of Borehole = SINGLE CONFIGURATION
Sub Configuration of Borehole            = 1 : single
Depth of the borehole                    = 420
Bore hole spacing                        = 15
Radius of the borehole                   = 2.165
Borehole thermal resistance              = 0.3683
U-TUBE
Pipe Type/Size Selection                 : 11
U-Tube Inside Diameter                   = 0.859055118110236
U-Tube Outside Diameter                  = 1.05
Shank Spacing Selection                  : B
Shank Spacing                            = 0.742913385826772
Pipe Conductivity                        = 0.225
; PROPERTIES
Soil type currently entered              = Average Rock
Thermal conductivity of the ground       = 1.4
Ground Volumetric heat capacity          = 34.943
Undisturbed ground temperature           = 49.3
Soil record currently entered            = United States, Sioux Falls-Foss Field
Ground Cover selected                    = Short Grass
Average Annual ground temperature        = 49.2
Fluid type currently entered             =15% Propylene Glycol / Water
Fluid Conductivity                       = 0.29629314755078
Fluid Volumetric heat capacity           = 60.6278923881161
Fluid Viscosity                          = 4.33422471777599
Density of the fluid                     = 63.436559978193
Mass flow rate of the fluid              = 6.023
```

Grout Conductivity = 0.42998266897747
Grout Volumetric heat capacity = 58.1664303950538
Convection Coefficient = 525.71327475
Convection Coefficient at Inside InnerPipe = 244.4523
Convection Coefficient at Outside InnerPipe = 12.1099
Fluid Factor = 1
g-function number = 0
;
;
;Antifreeze and Numerical Model Related Variables
Average Temperature for thermophysical properties calculation = 68.0000
Volumetric Heat Capacity of Pipe = 22.9920
Volumetric Heat Capacity of Pipe of double U-tube = 23.0071
Volumetric Heat Capacity of Inner Pipe = 22.9922
Volumetric Heat Capacity of Outer Pipe = 22.9922
Volumetric Heat Capacity of Horizontal Pipe = 22.9922
Freezing point of the fluid = 20.991
Boolean to check if the fluid was chosen from library = False
Fluid type represented in numbers = 1
Concentration of fluid in the mixture = 15.00
;
;Monthly Loadings
;==========
;
GLHE Loads

;Month	Total Heating	Total Cooling	Peak Heating	Peak Cooling
January	0.00	0.00	0.00	0.00
February	0.00	0.00	0.00	0.00
March	0.00	0.00	0.00	0.00
April	0.00	0.00	0.00	0.00
May	0.00	0.00	0.00	0.00
June	0.00	0.00	0.00	0.00
July	0.00	0.00	0.00	0.00
August	0.00	0.00	0.00	0.00
September	0.00	0.00	0.00	0.00
October	0.00	0.00	0.00	0.00
November	0.00	0.00	0.00	0.00
December	0.00	0.00	0.00	0.00

;
;
HeatPump Loads

;Month	Total Heating	Total Cooling	Peak Heating	Peak Cooling
January	8843106.75	0.00	22724.85	0.00
February	6629549.17	0.00	21155.27	0.00
March	4142474.45	0.00	13955.65	0.00
April	2256345.82	0.00	10441.15	0.00
May	0.00	233424.50	0.00	3787.48

June 0.00 1271192.76 0.00 6960.77
July 0.00 1902233.93 0.00 7199.62
August 0.00 1633118.45 0.00 8598.59
September 254818.62 2968.56 3514.50 784.79
October 1973342.93 716.55 11055.33 375.34
November 4990357.11 0.00 18186.71 0.00
December 7685640.62 0.00 21598.85 0.00
;
;
Peak_Heating Hours = 9
Peak_Cooling Hours = 4
;
;
First month you want data for = 1
Last month you want data for = 120
Maximum entering fluid temperature = 90
Minimum entering fluid temperature = 25
;
;
;Heat pump curve fit equations and coefficients:
Heatpump selected = ClimateMaster : TS024_ECM_MOTOR@6GPM_610CFM
;
;Cooling: Heat of Rejection = QC[a+b(EFT)+c(EFT^2)]
; Power = QC[d+e(EFT)+f(EFT^2)]
a = 1.0924400000
b = 0.0003143610
c = 0.0001144560
d = 0.0955068000
e = 0.0003059820
f = 0.0001123770
;
;Heating: Heat of Absorption = QH[a+b(EFT)+c(EFT^2)]
; Power = QH[d+e(EFT)+f(EFT^2)]
u = 0.7054590000
v = 0.0054469600
w = -0.0000772000
x = 0.3099770000
y = -0.0067573500
z = 0.0000978000
;
Default
Default file for User Manual.
;

VITA

Rachel Marie Grundmann

Candidate for the Degree of

Master of Science

Thesis: IMPROVED DESIGN METHODS FOR GROUND HEAT EXCHANGERS

Major Field: Mechanical Engineering

Biographical:

Education:

Completed the requirements for the Master of Science in Mechanical Engineering at Oklahoma State University, Stillwater, Oklahoma in May, 2016.

Completed the requirements for the Bachelor of Science in Mechanical Engineering at Oklahoma State University, Stillwater, Oklahoma in December, 2013.

Experience:

Research Assistant at Oklahoma State University and GLHEPro Technical Support and Programmer from May 2013 to May 2016.

Professional Memberships:

ASHRAE Student Member